(33)

Aircraft Engine Performance Improvements Using Multistage Compressors with Actively Controlled Stall Lines

by
Kevin Robert Tow
S.B. Aeronautics and Astronautics
Massachusetts Institute of Technology
(1989)

Submitted in Partial Fulfillment of the
Requirements for the degree of
MASTER of SCIENCE in MECHANICAL ENGINEERING
at the
Massachusetts Institute of Technology
February 1994

Signature of Author_____
Department of Mechanical Engineering
January 14, 1994

Certified by_____
Alan H. Epstein
Professor of Aeronautics and Astronautics

Certified by_____
David C n Wilson
Professor of Mechanical gineering

Accepted by_____
ain Sonin
Chairman, G ate Office
Department of Mechanical Engineering

Aircraft Engine Performance Improvements Using Multistage Compressors with Actively Controlled Stall Lines

Abstract

Recent experiments have demonstrated that a compressor stall line may be suppressed by active control schemes. The instability suppression results in a higher stall line by reducing the stalling flow coefficient of the compressor stage characteristic. This study examined potential applications of this technology to aircraft engines having multistaged axial-flow compressors. The primary focus of the analysis was to implement active stability control as a retrofit or upgrade to an existing engine configuration. Specifically, the effect of active control providing assumed levels of 5% and 20% additional stability margin on a baseline low bypass ratio, afterburning turbofan engine has been evaluated. The additional stall margin was applied in two ways: first, compressor component efficiency was optimized at the expense of stability margin; second, both fan and high pressure compressor pressure ratios were increased. In both cases, overall stall margin otherwise sacrificed was provided by active control.

On a component level, optimizing the core compressor variable stators improved efficiency by .5% to 1.0% for rotor speeds in the typical range of operation. The corresponding decrease in stall margin ranged from -4.0% to -5.0%.

On an engine system level, the effect of higher pressure ratio operation depended on the engine power setting and flight condition. When active control provided 5% additional stall margin, significant performance benefits (particularly cruise specific fuel consumption (SFC)) were achieved. Along a 35,000 ft/.85 MN cruise operating line, for example, a 5% higher core operating line improved SFC by -.74% to -.82%. Installed SFC would improve further because the accompanying increase in engine inlet flow at these conditions would decrease the aircraft spillage drag.

At high power, a design point cycle study indicated that higher cycle pressure ratios caused both performance benefits and penalties. The penalties may only be eliminated if additional engine configuration changes are also made. Improving SFC at constant thrust or improving thrust at constant SFC, for example, would require lower levels of design bypass ratio.

At high power operation throughout the flight envelope, the effect of higher pressure ratios depended on the region of the flight envelope and whether the fan or compressor was actively controlled. For the engine studied, three distinct regions of operation occurred. At intermediate rated power (IRP), as core compressor pressure ratio was raised 5%, the effect on thrust in each region was: -1.5% to -2.5% (fan stall margin limited region, characterized by low Mach number/ high altitude operation); 0.0% to -.5% (turbine inlet temperature limited region); and -2.0% to -7.7% (compressor discharge temperature limited region, characterized by high Mach number operation). At maximum afterburner operation, the effect on thrust was: -.6% to -1.55% (fan stall limited region); +.1% to +.8% (T41 limited region); and -1.2% to -4.3 % (compressor discharge temperature limited).

At high power, increased fan pressure ratios affected the fan stall limited region only. IRP thrust in this region improved up to 8.0%; maximum afterburner thrust increased up to 5.4%.

For the engine configuration studied, available stall margin above 5% could not be used by raising either the fan or compressor pressure ratios due to the presence of other cycle limits. Further increases in fan pressure ratio were restricted by minimum bypass ratio and/or minimum exhaust nozzle area constraints. Further increases in core compressor pressure ratios also resulted in significant thrust losses due to extended regions where operation was limited by compressor discharge temperature.

For active control stall margin contributions above 5%, preliminary design applications would achieve larger benefits than existing configurations. During the developmental phase, the design may be tailored to maximize the benefits of the available stall margin.

Thesis Supervisor: Alan H. Epstein
Title: Professor of Aeronautics and Astronautics

Thesis Reader: David Gordon Wilson
Title: Professor of Mechanical Engineering

Acknowledgments

This project has been a learning and rewarding experience- one filled with both high points and low points. I'd like to take this opportunity to acknowledge those individuals who made the high points possible and the low points temporary.

Thanks to Alan Epstein, my thesis supervisor, for his technical guidance during this project. He deserves much of the credit for formulating the topic of this research.

Thanks to Dick Davis, Principal Engineer, General Electric Aircraft Engines, for his boundless enthusiasm and constructive advice. Those who know him will undoubtedly notice his influence on this work.

Thanks to David Gordon Wilson for serving as my thesis reader and for providing encouragement and constructive feedback during this analysis.

I gratefully acknowledge the support of the General Electric Company for sponsoring this research. Thanks to Glen Allen, Fred Pineo, Ken Zagray, Peter Hull, and Lee Weider for their patience and tolerance as I negotiated my way through the Advanced Courses. In addition, special thanks to all those who were willing to listen to, and to answer my many questions: Mike French, Ron Giffen, Dave Fink, Fred Ehrich, Brian Acampa, Chuck Christopherson, Sandy Moltz, Jim Geiger, John Moulton, Todd Spezzaferro, Mark Prell, Bob Vandermolen, Dan Gilmore, Stu Bassler, Harold Brown, W. Hosny, and Bob Howell.

A warm thanks to my family whose contribution of support and encouragement cannot be overestimated- Mom, Dad, Cheryl, Lena, and Darrick.

A special thanks to my grandparents: Mr. Chin Wah Bow, Mr. Tso Wai Lam, and Mrs. Sun Ho Chin- from whom I learned so much through the unspoken word and to whom I respectfully dedicate this work.

Table of Contents

Abstract 2
Acknowledgments 4
Table of Contents 5
List of Figures 8
List of Tables 11
Nomenclature 12

1. Introduction 14

2. Background 18
    2.1 Introduction 18
    2.2 Compressor Instability Phenomena 18
    2.3 Stability Audit 22
    2.4 Advanced Control Technologies 24
        2.4.1 Stall Avoidance 24
        2.4.2 Active Control of Stall Line Position 25

3. Analytical Modelling 30
    3.1 Compressor Model 30
        3.1.1 Definitions 34
    3.2 Cycle Design Point Model 34
        3.2.1 Baseline Model 34
        3.2.2 Cycle Model Degrees of freedom 36
        3.2.3 Definitions 39
    3.3 Cycle Off Design Point Model 40
        3.3.1 Control Modes 40
        3.3.2 Cycle Mechanics 41
        3.3.3 Cycle Model Inputs 45

4. Compressor Component Analysis 47
4.1 Introduction 47
4.2 Background 48
4.3 Stall Margin Gain for a Lower Stalling Flow Coefficient 49
4.4 Optimizing Core Compressor Variable Stators 55
4.5 Comparisons to other Compressor Designs 57
4.6 Discussion and Conclusions 57

5. Cycle Design Point Analysis 61
5.1 Introduction 61
5.2 Method 61
5.3 Higher Pressure Ratio Operation 65
5.4 Design Trades 65
5.5 Conclusions 68

6. Cycle Off Design Analysis: Higher Pressure Ratio Operation 71
6.1 Introduction 71
6.2 Figures of Merit 73
6.2.1 Aircraft Mission Profiles 73
6.2.2 Cycle Design Limits 76
6.3 Method for Achieving Higher Pressure Ratio Operation 78
6.4 Results 80
6.4.1 Higher Pressure Ratio Operation Core Compressor 81
6.4.2 Higher Pressure Ratio Operation Fan 93
6.5 Conclusions 106

7. The Effect of Compressor Efficiancy Improvements on Cycle Off Design Performance 108
7.1 Introduction 108
7.2 Method 109
7.3 Results 111
7.3.1 Cycle Sensitivity Factors 111
7.3.2 Optimizing Core Variable Stators 114
7.4 Conclusions 116

8. Recommendations for Future Research 119
8.1 Introduction 119
8.2 Additional Benefits of Applying Active Control on Existing Configurations 120
8.2.1 Reduced Rotor Speeds 120
8.2.2 Lower LPT Temperature 120
8.2.3 Transient Performance 121
8.3 Benefits of using Active Control on Developmental Engines at the Preliminary Design Level 121
8.3.1 Designing New Compressors to Maximize Efficiency 121
8.3.2 Designing New Compressors to Minimize Weight 121
8.3.3 Active Control as an Alternative to Variable Stators 123

9. Summary of Conclusions 124
9.1 Introduction 124
9.2 Compressor Optimization Results 124
9.3 Design Point Cycle Analysis Results 125
9.4 Off Design Cycle Results of Higher Pressure Ratios 125
9.4.1 Higher Core Compressor Pressure Ratio 126
9.4.2 Higher Fan Pressure Ratio 126
9.5 Off Design Cycle Results with Improved Compressor Efficiency 127

10. References 129

Appendix A: The Effect of Higher Cycle Pressure Ratios on Exhaust Temperature and Pressure 133

List of Figures

Figure 2-1	Typical Compressor Map	20
Figure 2-2	Compressor Map with a Stall Line Knee	20
Figure 2-3	Stability Audit	23
Figure 2-4	Active Control of Surge in a Centrifugal Compressor	29
Figure 2-5	Stage Characteristic: Active Control of Rotating Stall in a 3 Stage Compressor	29
Figure 3-1	Fan Performance Map	32
Figure 3-2	High Pressure Compressor Performance Map	33
Figure 3-3	Stall Margin Definitions	35
Figure 3-4	Mixed Flow Turbofan: Engine Flow Path Station Designations	38
Figure 3-5	Turbine Temperature Technology Progress	42
Figure 3-6	Block Diagram of Cycle Deck Calculation Procedure	44
Figure 4-1	Calculation of Flow Coefficient and Pressure Coefficient	50
Figure 4-2A	New Stall Line after Extrapolation of the Stage Characteristics	51
Figure 4-2B	Extrapolated Stall Line at 90% Speed	52
Figure 4-2C	Extrapolated Stall Line at 70% Speed	52
Figure 4-3	Typical Variable Stator vs Corrected Speed Howell Diagram	54
Figure 4-4	Core Compressor Howell Diagram	56
Figure 4-5	Potential Efficiency Gains for Different Compressors	58
Figure 5-1	Ideal Gross Thrust Function	64
Figure 5-2	Typical Specific Fuel Consumption vs. Specific Thrust Carpet Plot	66
Figure 5-3	SFC vs Specific Thrust at Various Levels of Pressure Ratio and Bypass Ratio	67
Figure 5-4	Cycle Design Trades: Improved SFC at constant Thrust and Improved Thrust at constant SFC	69

Figure 6-1	Flight Envelope	75
Figure 6-2	Summary of Engine System Design Limits	77
Figure 6-3	Raising HPC Operating Line using HPT and LPT Nozzle Areas	77
Figure 6-4	Turbine Temperature Profile vs Inlet Temperature: Higher Core Compressor Pressure Ratios	82
Figure 6-5	Thrust Impact at IRP due to Raising Core Operating Line 5%	84
Figure 6-6A	Turbine Discharge Temperature Profile: T56 vs T2 for a 5% High Core Operating Line at IRP	86
Figure 6-6B	Turbine Discharge Temperature Profile: BPR vs T2 for a 5% High Core Operating Line at IRP	87
Figure 6-7	T3 Limited Operation Covers a Larger Portion of the Flight Envelope as Core Pressure Ratio is Raised	89
Figure 6-8	Raising Core Pressure Ratio by 5%: Part Power Benefit at SLS	92
Figure 6-9	Raising Core Pressure Ratio by 5%: Part Power Benefit at 35,000 ft/ .85 MN	92
Figure 6-10	Raising Fan Pressure Ratio: T41 vs T2 Profile at IRP	94
Figure 6-11	Raising Fan Pressure Ratio by 5%: Change in Exhaust Temperature	95
Figure 6-12	Raising Fan Pressure Ratio by 5%: Thrust Contour Plot	97
Figure 6-13	Raising Fan Pressure Ratio by 20%: Thrust Contour Plot	98
Figure 6-14	Raising Fan pressure Ratio: T41 vs T2 profile during Afterburning Operation (with BPR limit)	100
Figure 6-15	Raising Fan Pressure Ratio: Thrust Contour Plot with Region that is BPR Limiting	101
Figure 6-16	Region of Envelope in which Minimum BPR Eventually Supersedes Minimum Fan Stall Margin as the Limiting Cycle Constraint	102

Figure 7-1 SLS Operating Line: SFC vs FN with Optimized Core Variable Stators 117
Figure 7-2 35,000 ft/.85 MN Operating Line: SFC vs FN with Optimized Core Variable Stators 117

Figure A1-1 Temperature vs Entropy Diagram Indicating Excess Cycle Exhaust Pressure and Temperature..... 134
Figure A1-2 Turbine Exhaust Temperature and Pressure After an Increase in Compressor Pressure Ratio at Constant T41 and BPR 134
Figure A1-3 The Lower Turbine Inlet Entropy Tends to Lower the Turbine Exhaust Pressure 137
Figure A1-4 The Higher Turbine Inlet Pressure Tends to Increase the Exhaust Pressure 137
Figure A1-5 Exhaust Pressure will Increase or Decrease Depending on the Magnitude of the Increase in Compressor Pressure Ratio 139

List of Tables

Table 3-1	Comparison of the Features of Design Point Cycle Programs and Off Design Cycle Decks	37
Table 6-1	Part Power Performance Improvements for a 5% Higher Core Operating Line	93
Table 6-2	Performance Improvements at 35,000 ft/.85 MN/IRP	105
Table 6-3	Performance Improvements at 30,000 ft/.80 MN/Max AB	105
Table 7-1	Engine Performance Sensitivities to Component Efficiency Improvements: SLS/STD/IRP	113
Table 7-2	Engine Performance Sensitivities to Component Efficiency Improvements: SLS/STD/Max AB	113
Table 7-3	Engine Performance Sensitivities to Component Efficiency Improvements: 35,000 ft/ .85 MN/ 80% IRP thrust	113
Table 7-4A	Key High Power Mission Points with Optimized Core Variable Stators	115
Table 7-4B	Key Part Power Mission Points with Optimized Core Variable Stators	115
Table 9-1	The Results of Active Control on Both the Fan and Core Compressors	128

Nomenclature

a9	Speed of sound at the nozzle exit plane	ft/sec
A41	High Pressure Turbine Nozzle Throat Area	in^2
A49	Low Pressure Turbine Nozzle Throat Area	in^2
AB	Afterburner	-
ADECS	Adaptive Engine Control Systems	-
ALT	Altitude	ft
BPR	Bypass Ratio	-
EPR	Engine Pressure Ratio	-
FG	Gross engine thrust	lbf
FN	Net engine thrust	lbf
H	Enthalpy	BTU
HIDEC	Highly Integrated Digital Electronic Control	-
h	Specific enthalpy	BTU/lbm
HPC	High Pressure Compressor	-
HPT	High Pressure Turbine	-
IGV	Inlet Guide Vane	-
IRP	Intermediate Rated Power	-
LPT	Low Pressure Turbine	-
MN	Aircraft Flight Mach number	-
MN9	Mach number at nozzle exit plane	-
N	Rotor Speed	rpm
N2	Rotor Speed of the fan	rpm
N25	Rotor Speed of the compressor	rpm
P21Q2	Fan pressure ratio	-
P3Q25	Core pressure ratio	-
P41	High Pressure Turbine inlet pressure	psia
P49	Low Pressure Turbine inlet pressure	psia
P8	Nozzle throat total pressure	psia
P9	Total pressure at nozzle exit plane	psia
PCN25R	Core compressor corrected speed	%
PCN2R	Fan corrected speed	%
PR	Pressure Ratio	-
PS16	Bypass duct static pressure prior to mixing	psia
PS56	Core stream static pressure prior to mixing	psia
PS9	Static pressure at nozzle exit plane	psia
S	Entropy	BTU/°R
S3	Compressor exit entropy	BTU/°R
S4	Turbine inlet entropy	BTU/°R
SFC	Specific fuel consumption	lbm/(lbf hr)

SL	Sea Level	-
SLS	Sea Level Static flight condition	-
SM	Stall Margin	%
SR	Specific Range	
STD	Standard Day Inlet Conditions	-
T2	Engine inlet temperature	^oR
T3	Core compressor discharge temperature	^oR
T41	High Pressure Turbine inlet temperature	^oR
T49	Low Pressure Turbine inlet temperature	^oR
T8	Nozzle throat total temperature	^oR
T9	Total temperature at nozzle exit plane	^oR
TS9	Static temperature at nozzle exit plane	^oR
U	Rotor wheel speed	ft/sec
V9	Flow velocity at nozzle exit plane	ft/sec
Vk	Flight Velocity	knots
W2	engine inlet physical flow	lbm/sec
W25	core compressor physical flow	lbm/sec
W25R	Core compressor corrected flow	lbm/sec
W2R	Engine inlet corrected flow	lbm/sec
W41	High Pressure Turbine inlet flow	lbm/sec
W49	Low Pressure Turbine inlet flow	lbm/sec
W8	Nozzle throat physical flow	lbm/sec
W9	Nozzle exit physical flow	lbm/sec
WFM	Main combustor fuel flow	lbm/hr
Φ	Flow coefficient	-
Ψ	Work Coefficient	-
Ψ'	Pressure Coefficient ($\Delta h/U^2$)	-
η_p	Polytropic efficiency	-
γ	Ratio of specific heats	-
R	Gas constant	
η_{fan}	Fan adiabatic efficiency	-
η_{core}	Comp. adiabatic efficiency	-
η_{HPT}	HPT efficiency	-
η_{LPT}	LPT efficiency	-
η_{prop}	Propulsive efficiency	-
η_{therm}	Thermal efficiency	-
η_{over}	Overall cycle efficiency	-

Chapter 1: Introduction

Active control is a general term which describes the use of feedback logic to achieve a desired operating condition. Sensors monitor the magnitude of an appropriately selected physical parameter. As required, signals are sent to an actuator which drives the system to the desired operating condition. An example in turbofan engines is using fuel flow to control fan speed. A sensor monitors the rotor speed; as the speed deviates from the desired value, more or less fuel is added.

With the development of high response electronics, the application of advanced control schemes toward actively suppressing stall was initiated by Epstein, et. al. in the 1980's (reference 1-1). For compressors with actively controlled stall lines, sensors monitor the unsteady flow oscillations characteristic of an impending stall- precursors which would otherwise increase in magnitude and cause surge or rotating stall (reference 1-1, 1-2). Actuators modify the dynamic response of the unsteady flow by applying perturbations which dampen the oscillations and suppress its growth. Among the actuators studied include throttle valves, bleed valves, fuel flow modulation, and high frequency inlet guide vane manipulation. Selection of appropriate actuator/sensor combinations are discussed in reference 1-3.

This study is motivated by the need to quantify how gains in compressor stall margin may be exploited in an engine system. Because of the existence of other design

constraints such as peak pressures and temperatures, the full benefits of increased stall margin are not readily apparent. In addition, there are subtle, but important, advantages and disadvantages to the various approaches to applying the added stall margin in the design process.

The primary focus of the analysis was to implement active stability control as a retrofit or upgrade to an existing engine configuration. For this study, a level of additional stall margin provided by active control has been assumed. To cover a range of benefits that may eventually be realized, 5% and 20% stall margin gains have been examined. The study made no assumption regarding the specific method of active control utilized-whether it be inlet guide vane manipulation, flow injection, etc. In addition, potential compressor efficiency losses and/or gains due to the control actuators were assumed negligible.

Chapter 2 further elaborates upon previous advanced stall control applications on aircraft engines. Included are stall avoidance methodologies which use advanced control schemes to improve detection and avoidance of aerodynamic instabilities. Active stall control incorporates a different philosophy: the aerodynamic instability line is not only avoided, but also suppressed. The result is an extended region of safe operation.

Chapter 3 outlines the analytical models used in this study. For the compressor, the application of component performance maps is reviewed. For the engine cycle, the cycle design point program and the more elaborate thermodynamic cycle deck are introduced. The differences between these cycle models are summarized.

This thesis investigated how active control offers performance benefits on two levels. First, on a component level, **Chapter 4** examines potential improvements in compressor aerodynamic performance. With active control schemes, the required overall stall margin is provided by two sources: "conventional stall margin" provided by current compressor design techniques; and "control stall margin" provided by actively suppressing stall initiation. Because control stall margin is available, the aerodynamicist may design to

lower conventional stall margin goals and improve pressure rise, flow, and/or efficiency. The stall margin otherwise sacrificed is provided by active control. Hence, compressor efficiency is improved while maintaining the same net stall line. This component level analysis focused on tuning variable stator settings to improve efficiency while lowering the conventional stall margin.

On an engine system level, both cycle design point and cycle off design studies were conducted to assess the impact of using active control to raise fan and compressor pressure ratios. The design point analysis, discussed in **Chapter 5**, was made to identify the various cycle trends which occur with the higher pressure ratio operation. The off design analysis models a baseline, low bypass ratio afterburning turbofan to quantify the engine performance changes due to both higher compressor pressure ratios (**Chapter 6**) and efficiencies (**Chapter 7**). In doing so, engine performance improvements throughout the flight envelope and at both high power and part power conditions have been quantified.

A consequence of this research was that several additional applications of actively controlled compressors were identified. However, addressing these additional topics was beyond the scope of this study. These topics are suggested as areas of future research in **Chapter 8.**

Chapter 9 summarizes the conclusions of this study. In short, the largest improvements in high power afterburning thrust were achieved when active control permitted higher pressure ratios across both the fan and core compressor. Further, significant subsonic cruise fuel consumption benefits were realized. However, the use of active control to tune variable stators for best efficiency can only be justified if done in conjunction with the higher pressure ratio application. By itself, the performance improvement of optimizing the variable stators on a baseline engine design were not enough to warrant the use of active control.

The presence of other cycle limits (such as turbine temperatures, compressor temperatures and bypass ratio) prevented the best optimization of the additional stall margin on the baseline engine configuration. Greater performance benefits would be realized if active control is implemented during the preliminary design phase of the engine.

Chapter 2: Background

2.1 Introduction

Currently, compressor operating lines are positioned to maximize performance while satisfying cycle design constraints. One important limit is stall margin; i.e., the maximum allowable operating pressure ratio relative to the stall pressure ratio. This chapter reviews the phenomena of compressor stall and the traditional means used to avoid this situation. In addition, various applications of advanced control methods are discussed. A summary of recent analytical and experimental active control studies is also included.

2.2 Compressor Instability Phenomena

A compressor in aerodynamic instability may manifest itself in two ways: surge stall which is characterized by one dimensional, axisymmetric, axial oscillations; and rotating stall which is a localized instability characterized by circumferential flow oscillations. Both forms are unacceptable in terms of aerothermal performance and structural integrity. Stall will manifest itself as either surge or rotating stall based on the coupled dynamics of the compressor/combustor system (reference 2-1).

Although several analytical models have been developed to predict the stalling point, commonly used methods are the empirical correlations developed by Lieblein

(reference 2-2) and Koch (reference 2-3). The former method correlates the stall point of a stage to a limiting diffusion factor (D Factor). The D Factor is a function of the aerodynamic velocity triangles and the stage solidity and is related to the blade boundary layer thickness. The latter method applies two dimensional diffuser correlations to determine the stalling static pressure rise capability of compressor stages. Both methods predict that stall occurs due to a limiting stage. The potential stabilizing influence of adjacent stages (reference 2-4) is not modelled directly. Other models attempt to account for this effect by modelling the overall compression system dynamics to determine when stall occurs (reference 2-5, 2-6). Even with these different models, however, extensive stall line testing is required to verify new compressor designs.

For multistage compressors, the overall stall line shown in Figure 2-1 is influenced by how the enthalpy rise is distributed, or stacked, across the stages. Applying the stage limiting stall criteria conceptually demonstrates how stage matching affects stall line position in a multistage compressor. The overall stall line is limited by the stage(s) having the least stall margin (reference 2-7). In general, at high rotor speeds, the rear stages are stall limiting; at low speeds, the front stages are limiting. Hence, optimizing the stall line at high speeds negatively impacts low speed stall margin, and vice versa. As a result, depending on how the aerodynamicist ultimately designs the work distribution among the individual stages, the stall line may exhibit a knee, or pinch point. This characteristic is indicated on a compressor map by the abrupt change in the slope of the stall line (see Figure 2-2).

To maximize the stable operating region, several traditional compressor design options are available. These options include judicious selection of the aerodynamic design point (reference 2-9); low aspect ratio blades and high solidity designs (references 2-10, 2-11, 2-12) ; low tip clearances; casing treatment; optimized velocity triangles ; and stage matching (references 2-4, 2-7).

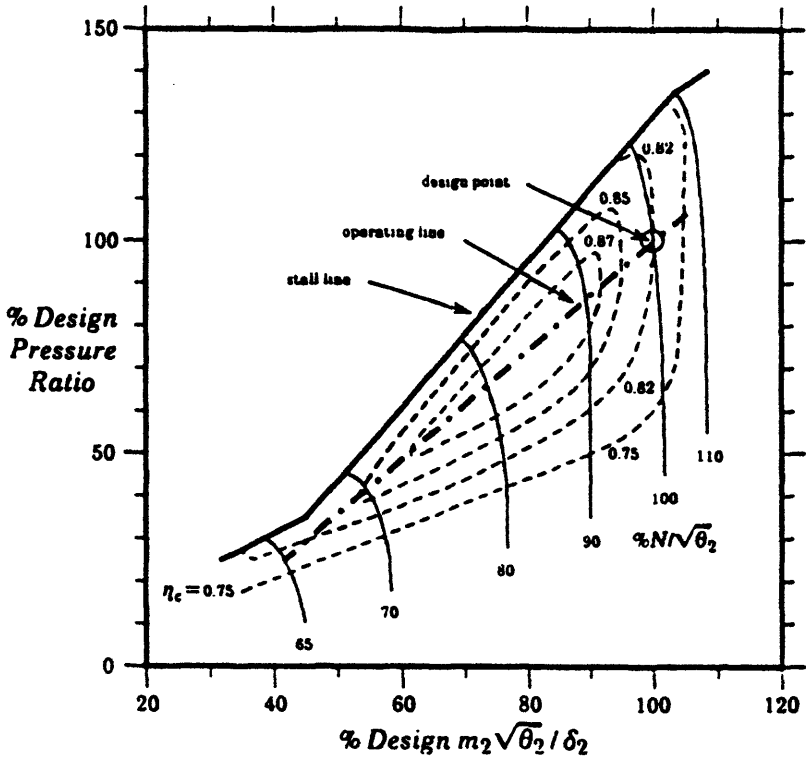

Figure 2-1: Typical Compressor Map (reference 3-3)

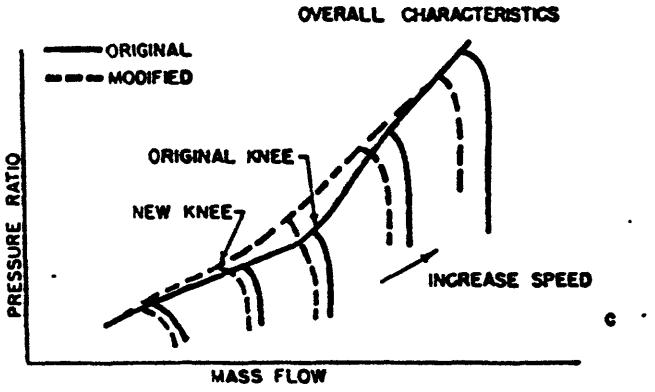

Figure 2-2: Compressor Map with a Stall Line Knee (reference 2-7)

The compressor design point is often at pressure ratios well above the intended range of operation (reference 2-7). This design trade is characteristic of highly loaded stage designs in which a high priority is placed on minimizing the number of stages and the weight of the compressor. To achieve the required stall margin if the design point is placed in the region of operation, the loading on each stage would have to be reduced. Hence, to operate at the same required overall cycle pressure ratio, more stages would be required.

Unlike industrial gas turbine applications, an aircraft engine compressor must maximize performance over a range of operating speeds. Because of the increase in pressure ratio with succeeding stages, the stage inlet density is higher than the inlet density of the preceding stage. In reference 2-7, Stone further elaborates on the cause of stage mismatching in a multistage compressor. Stone describes a simple model which indicates that rear stages tend to be stall limiting above design speed and front stages tend to be stall limiting below design speed.

To avoid the stall line knee (Figure 2-2), three different approaches have historically been used. First, interstage bleed valves were often required to unload the front stages and prevent premature stalls. Second, dual spool designs improved stall margin by unloading stall limiting front stages by running them to a slower rotor speed. Finally, variable stators were used to allow the compressor to achieve the higher stall line without the performance penalty associated with bleeding air or the mechanical complexity of the dual rotor configuration. The variable stators essentially modify the velocity triangles at low power to alleviate the stage mismatch dilemma.

The use of variable stators provides more off design stall margin and potentially greater efficiency than compressors without any variable geometry. However, although efficiency is improved relative to the fixed geometry compressor, the maximum potential efficiency is often not realized; the variable stator angles are defined to satisfy stall margin requirements and not to optimize efficiency. This topic is further explored in Chapter 4.

2.3 Stability Audit

Once the stall line has been established, the maximum operating pressure is dictated by stall margin requirements. The magnitude of this limit is determined analytically by superposition of the various elements which degrade stability. Among the various factors include:

- engine deterioration- for example, as component efficiencies decrease, operating lines rise to hold performance.
- engine-to-engine manufacturing variation-stall lines and operating lines are representative of statistically average compressor performance;
- transient operation- acceleration of the compressor rotor requires unbalanced torque between the compressor and the turbine;
- tip clearances - leakage across the tip from the blade pressure side to suction side generates blockage and increased end wall loading.
- inlet distortion- non uniform pressure and velocity profiles cause extreme local incidence angles.

As indicated by Figure 2-3, these factors influence the operating line, the stall line, or both. To assure stall free operation, the stall margin stack is based on worst case scenarios. Hence, the stack includes the effects of statistical uncertainty as well as maximum inlet distortion levels.

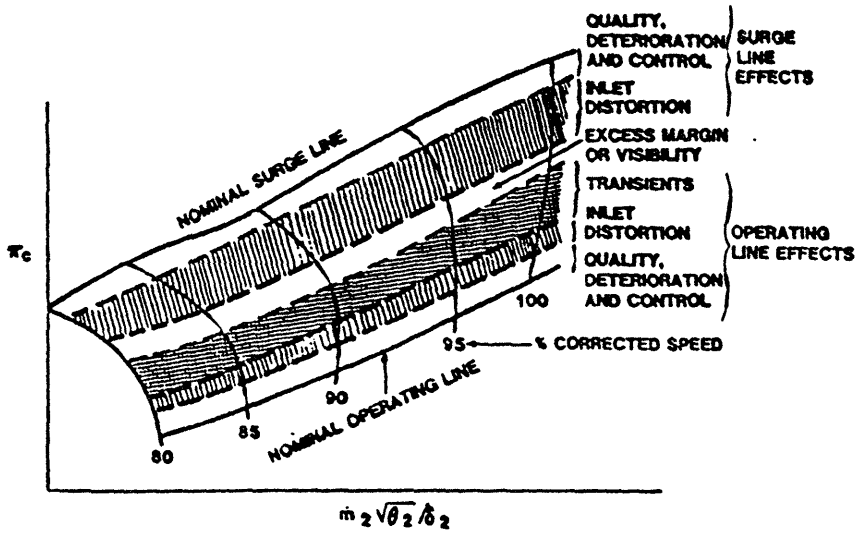

Figure 2-3: Stability Audit (reference 3-1)

Distortion effects often contribute significantly to the stall margin requirement, especially for high performance military fighters. High angle of attack operation and other intricate flight maneuvers cause inlet flow separation which results in non-uniform inlet flow. The spatial differences (circumferential and/ or radial distortion) in velocity and pressure cause sections of the blading within a stage to operate at lower flow coefficients and hence points along the stage characteristic closer to stall. To minimize inlet distortion, proper engine/aircraft integration requires that the inlet be sized to avoid or minimize inlet flow separation during these maneuvers. As such, the minimum inlet size is often not dictated by the maximum engine airflow condition, but instead by the size resulting in the maximum acceptable level of flow distortion. Thus, the distortion tolerance of the engine has a direct effect on the size and weight of the aircraft.

2.4 Advanced Control Technologies

2.4.1 Stall Avoidance

The use of advanced control systems on aircraft engines has been investigated as a means to remove unnecessary conservatism from the stability stack. Several approaches have been studied to apply controls technology to improve engine performance.

Previous efforts have focused on exploiting situations in which less compressor stall margin was required. These stall avoidance methods use sophisticated control logic to add flexibility to the engine control schedules. During non-stall limiting scenarios, real-time control inputs tune baseline schedules which had been designed for worst case stall situations. For example, one phase of the Highly Integrated Digital Electronic Control (HIDEC) program tested an Adaptive Engine Control Systems (ADECS) on an F-15 aircraft (reference 2-13). The control system actuated the variable area exhaust nozzle to increase fan pressure ratio when excess stall margin was available due to the absence of inlet distortion. The up trim was based on inlet distortion correlated as a function of aircraft angle of attack, sideslip angle, Mach number and corrected fan flow. Flight testing

resulted in a maximum increase in intermediate rated thrust of +12% (25,000 ft/.6 MN). Other improvements to performance included the rate of climb, the time to climb, and the flight acceleration.

Follow up studies included performance seeking control algorithms which optimized control schedules to achieve optimum values of thrust, fuel burn, or turbine temperature based on actual engine operating conditions (reference 2-14, 2-15, 2-16). Flight testing resulted in up to 15% increases in thrust; reducing low pressure turbine inlet temperature by 100 ^{o}R at high altitudes; and reducing fuel consumption up to 2%.

Another approach applied a stall detection control scheme to avoid an instability (reference 2-17). The compressor on a J85 engine was trimmed to higher pressure ratios having lower levels of stall margin. An array of pressure transducers sensing for unsteady pressure signals characteristic of rotating stall actuated interstage bleed valves prior to an impending stall. The interstage bleed valves opened to prevent throttling into the stall region. Engine testing successfully demonstrated the concept although the stall control system did not anticipate and prevent stall completely.

2.4.2 Active Control of Stall Line Position

The methods described above use control sophistication to optimize control schedules. The added flexibility regains the performance otherwise sacrificed during non-stall limiting scenarios. The concept of active stall control, however, increases the stall margin inherent to the system by suppressing the transition from stable to unstable operation. Hence, the stall line of a given compressor is effectively raised and more margin is available for all flight conditions including those currently stall limited. Thus, for several reasons, the potential benefits of active control include and exceed the benefits of the approaches described above.

First, compressors not controlled by variable area throttles may also be optimized. The HIDEC program described above, for example, increased fan pressure

rise using a variable exhaust nozzle. Active control, however, would extend this benefit to fixed exhaust area fans and compressors.

Second, performance benefits would not depend on specific destabilizing elements being absent. This characteristic becomes more important for next generation military fighters which emphasize low observable features. The stealth characteristics of the complex inlets cause levels of distortion which exist over the entire flight envelope even during benign flight maneuvers.

Third, active control offers the advantage of being appropriate during the preliminary design of the engine and/or aircraft. Because the stall margin inherent to the system is increased, the additional margin may be incorporated into the baseline engine design. Potential applications to reduce weight include using fewer stages to achieve the same overall pressure rise and smaller engine inlets if the compressor can accommodate higher levels of inlet distortion.

The concept of active control was first initiated by Epstein, et al in the 1980's (reference 1-1). Since then, several experiments have successfully demonstrated the concept of active control. Surge suppression on centrifugal compressors resulted in a 25% reduction in the stalling flow coefficient (Figure 2-4) and 10% additional shaft power (reference 2-18). Rotating stall was delayed to a flow coefficient 20% lower than the baseline in a single stage low speed axial compressor (2700 rpm, .245 tip Mach number; reference 2-19). The experiment manipulated high frequency inlet guide vanes to suppress rotating stall.

More recent research has applied control technology to a 3 stage, low speed compressor (2400 RPM, 660 mm tip diameter; reference 2-20). By using a circumferential array of hot wires to sense axial velocity disturbances and inlet guide vanes to damp the 1st and 2nd spatial modes, the stalling flow coefficient was reduced by 8%. As shown by the stage characteristic from the experiment, stall was suppressed until the stage characteristic had a positive slope of .9 (Figure 2-5).

Hosny, et al (reference 2-5) conducted an analytical study investigating active stabilization in multistage axial compressors using stator angle settings as the control actuator. The study modelled an 8 stage compressor design with IGV and third, fourth and fifth stage interstage bleed capabilities. Performance above the baseline stall line was calculated by extrapolating the stage characteristics. For this study, each stage was modelled as a discrete volume to form a matrix of equations which represented overall compression system behavior. Among the conclusions include:

- at 100% speed, a .3% maximum increase in overall stall margin was calculated.
- at 87% speed, a 2% maximum increase in overall stall margin was calculated.
- at 87% speed and a mismatched stage loading distribution (due to interstage bleed), significant stall margin improvements are achieved.

Past engine system studies include reference 2-21 and 2-22. In reference 2-21, Brown, et al calculated the decrease in take off gross weight based on an assumed stall margin improvement and aircraft design sensitivity factors. In reference 2-22, Seymour assessed the benefits of a 20% stall margin (defined as [(PRstall/PR)(W/Wstall)-1]) improvement for an afterburning turbofan engine at discrete design point locations (design bypass ratio =1.0). Potential aircraft range and weight savings due to operation in the region above the existing stall line were quantified by extrapolating the shape of the speed lines. The potential benefits of a 20% reduction in stall margin include an 11.2% increase in mission radius and a 5.3% increase in net thrust at 36089 ft and .90 Mach number.

In addition to these engine system studies, active control has potential benefits to the aircraft system. Currently, for high performance military applications, the engine inlet is sized to achieve levels of inlet distortion which are acceptable to the engine. As a result, the inlet area is larger than needed in terms of maximum airflow requirements. Furthermore, at cruise, the larger inlet area requires more airflow to be bypassed, or "spilled", around the engine. Hence, aircraft cruise performance is compromised due to

the higher levels of spillage drag. Previous aircraft systems studies predict substantial aircraft range improvements if this design compromise becomes less stringent (reference 2-23). For this application, the stall margin otherwise sacrificed by the higher inlet distortion index would be provided by active control (reference 2-24).

Issues addressed in this thesis build upon these earlier efforts. This study extends the analysis to engine performance improvements throughout the flight envelope including comparisons at both high power and part power conditions. In addition, engine cycle limits are identified which limit the benefits of active control on a baseline engine configuration. These cycle limits explain the fundamental cause for both the benefits and penalties of applying active control. In doing so, the study qualitatively identifies the aircraft applications for which active control is an attractive design option. Furthermore, this study identifies additional design changes which must accompany the use of active control in order to maximize the benefits of additional stall margin on an engine system.

For this analysis, a low bypass ratio, afterburning turbofan was selected as the baseline engine configuration- a configuration typical of high performance military fighter applications. These aircraft require challenging levels of stall margin due to the high levels of inlet distortion present during fighter aircraft operation. Hence, active control is potentially a suitable design alternative for this engine application.

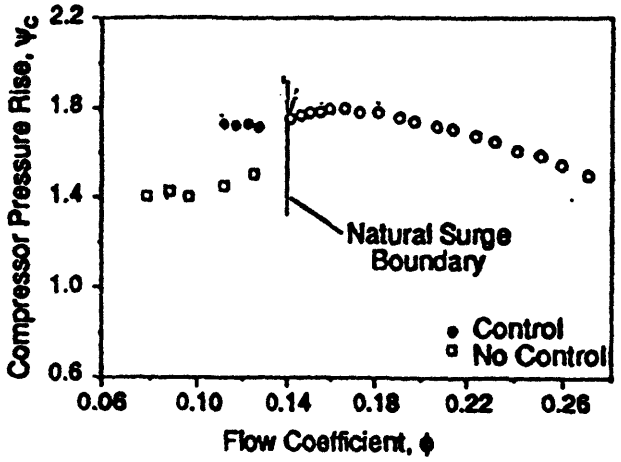

Figure 2-4: Active Control of Surge in a Centrifugal Compressor (reference 1-2)

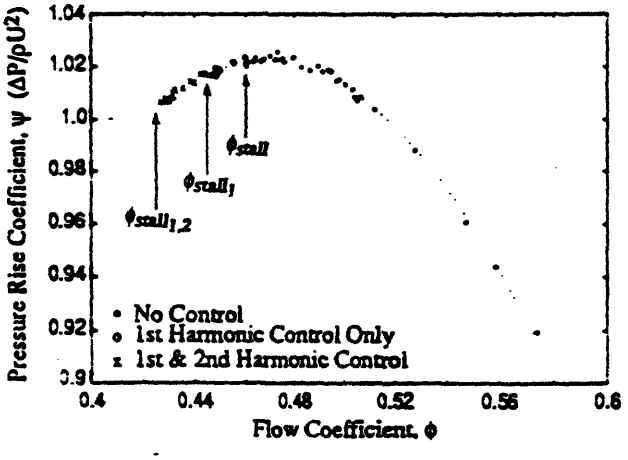

Figure 2-5: Stage Characteristic: Active Control of Rotating Stall in a 3 Stage Compressor (reference 2-20)

Chapter 3: Analytical Models

This section describes the analytical tools which were used in this study. Both the mechanics of the models and the necessary assumptions are described for the compressor and engine. Three analytical tools are described:

- Compressor component performance modelling;
- Cycle design point modelling used to identify cycle trends. Design point models are commonly used during the preliminary design phase of engine cycles. Performance sensitivities based on a single operating condition are assessed. For this model, the engine hardware configuration has not been defined in the design process; hence, the designer may specify the flow areas needed to achieve the desired thermodynamic properties.
- Cycle off design modelling used to quantify engine performance for a specified baseline engine configuration. The model quantifies performance at a variety of important flight conditions and power settings.

3.1 Compressor Modeling

The fan used in this study was a multistage design with inlet guide vanes (IGV) and variable stators. The high pressure compressor was also a multistage design with IGV and variable stators. Fan and compressor aerodynamic performance were modelled

using component maps. The component maps modelled the relationship of pressure ratio, adiabatic efficiency, flow and rotor speed. The performance maps used in this study represent analytical predictions for compressor performance. Although the designs are not based on specific test data, they are derived from previous designs upon which a large experience base exists.

The baseline fan and compressor map values, in nondimensional form, are shown in Figures 3-1 and 3-2 , respectively. Pressure ratio is expressed as a function of corrected flow with lines of constant corrected speed and adiabatic efficiency superimposed on the plot. By convention, corrected parameters are used to generalize the data over a range of different inlet conditions. The stall line shown is indicative of clean inlet conditions.

Compressor component performance maps are based on a reference operating condition. The reference flight condition is generally sea level static conditions since most compressor verification testing is done at this condition. However, to predict performance at other altitudes and Mach numbers, pertinent adjustments to the baseline map performance must be made. One effect which is commonly modelled is the change in the flow Reynolds number. Modifiers to flow, efficiency, and/or pressure ratio are applied to account for different boundary layer behavior.

In addition to a reference flight condition, the map data is indicative of a reference stator variable geometry schedule. An additional adjustment is made, when appropriate, for operation at off nominal variable geometry schedules. These modifiers are determined analytically using stage stack analyses and/or experimentally from test data. For this study, the effects of varying the variable geometry schedules are taken from sensitivity factors from compressors with similar aerodynamic characteristics as the compressor used in this study.

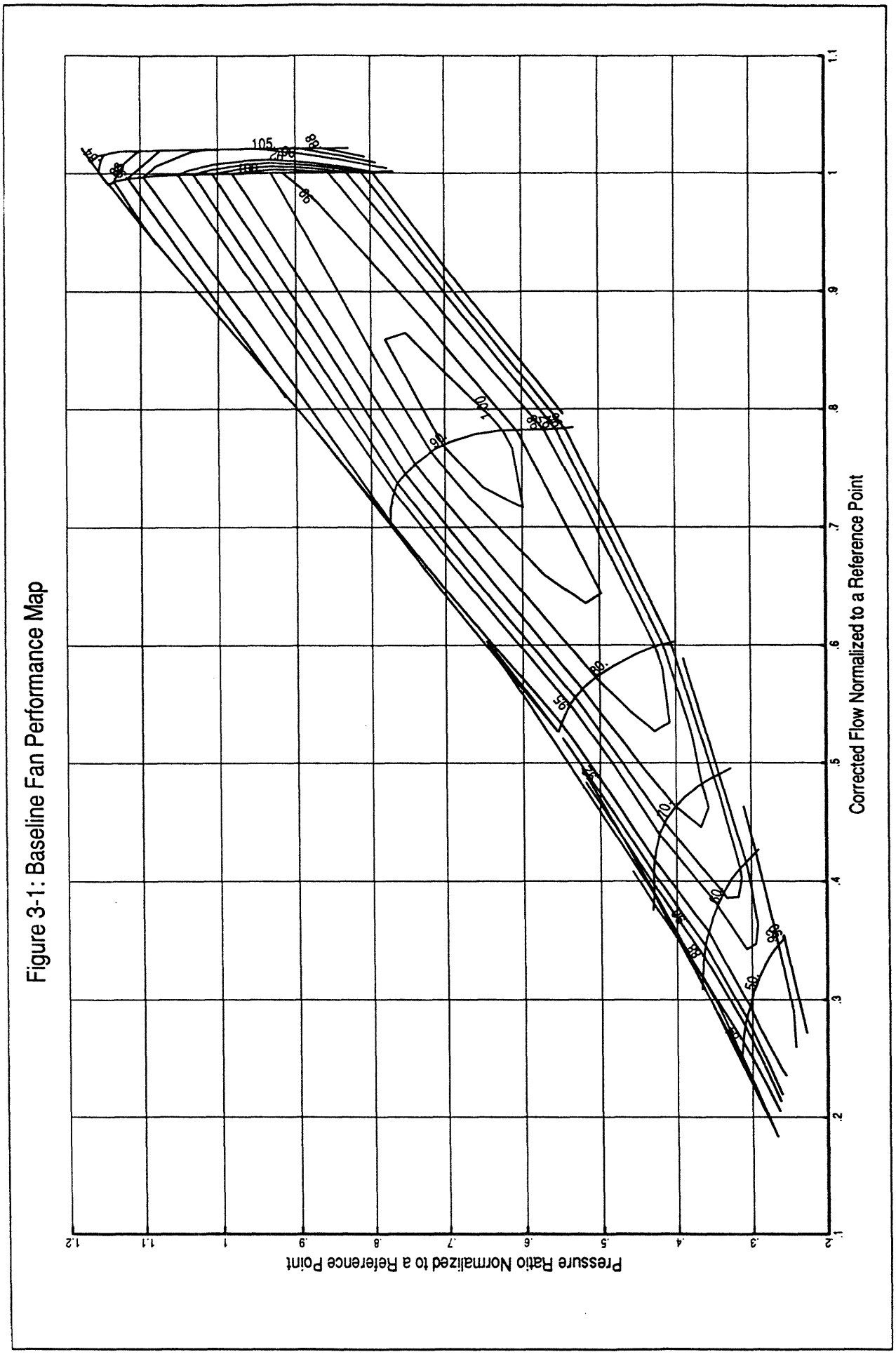

Figure 3-1: Baseline Fan Performance Map

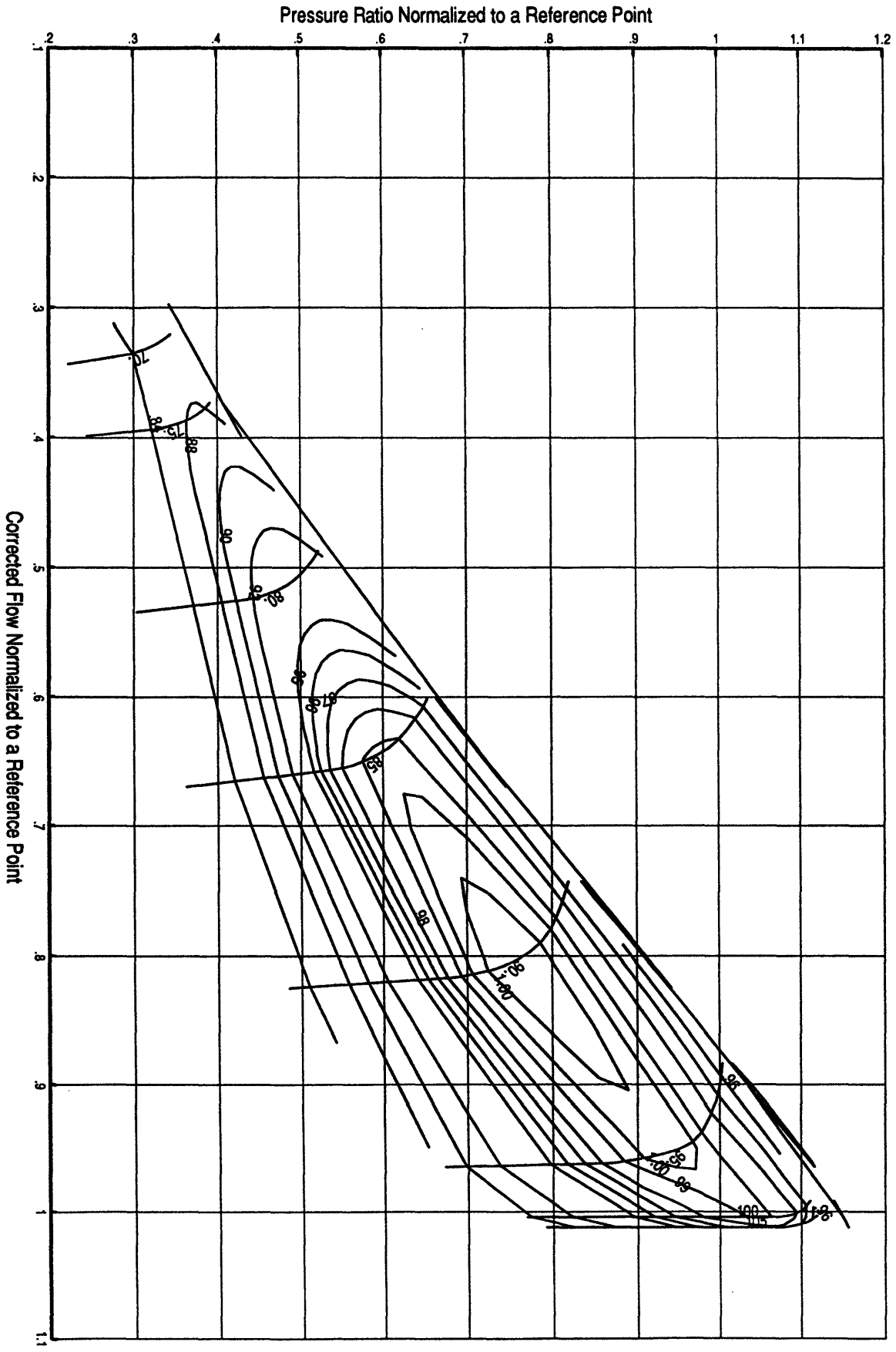

Figure 3-2: Baseline Core Compressor Performance Map

3.1.1 Definitions

Several definitions for stall margin are used in industry. In this analysis, the compressor stall margin is defined at constant flow;i.e.,

(3-1) $$SM|_{\text{corrected flow}}=[\ PR|_{sl}/PR|_{ol}\ -1]\ *\ 100$$

where $PR|_{sl}$= stall line pressure ratio

$PR|_{ol}$= operating line pressure ratio

This definition was selected because the effect of distortion on stall margin (distortion indices) are specified at constant flow (reference 3-1).

Another definition commonly used is stall margin at constant speed which includes the change in compressor flow between the operating point and the stall point (eq 3-2). The differences between these definitions are shown graphically in Figure 3-3.

(3-2) $$SM|_{\text{corrected speed}}=[(PR|_{sl}/PR|_{ol})(W|_{ol}/W|_{sl})-1]*100$$

where $PR|_{sl}$= stall line pressure ratio

$PR|_{ol}$=operating line pressure ratio

$W|_{ol}$ = the operating line flow

$W|_{sl}$= the stall line flow

3.2 Design Point Program

3.2.1 Baseline selection

A baseline engine configuration was selected to establish reference levels of engine performance. The selected baseline cycle is a low bypass ratio, mixed flow, afterburning turbofan (Figure 3-4). This configuration was selected because it is typical of high performance military fighter applications. The selection was motivated by the fact that high performance military fighters frequently are designed to stall margin limits due to high levels of inlet distortion. Hence, active control is potentially a suitable candidate for this application.

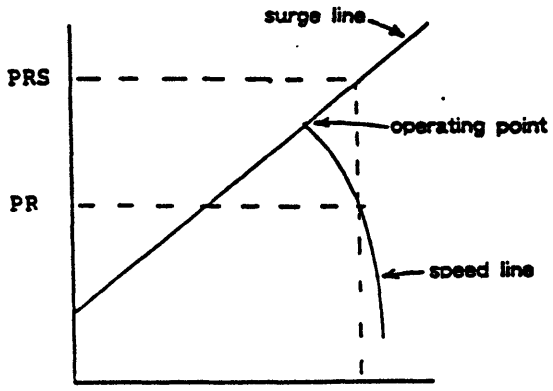

(Eq 3-1)

$SM|_{corrected\ flow} = [PRS/PR - 1]*100$

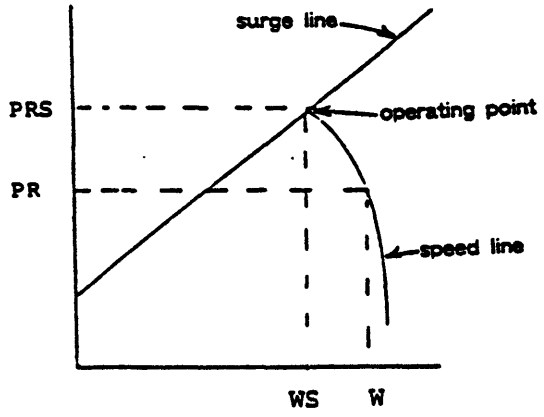

(Eq 3-2)

$SM|_{corrected\ speed} = [(PRS/PR)(W/WS)-1]*100$

Figure 3-3: Stall Margin Definitions (reference 2-22)

When appropriate, conclusions have been generalized to encompass other engine configurations. In explaining the phenomena based on thermodynamic fundamentals, guidelines have been established for applying active control benefits to different aircraft applications.

Initial parametric studies were conducted on an engine design point program (reference 3-2). Design point programs, commonly used during the preliminary design phase of an engine, provide a flexible tool to determine cycle performance sensitivities (reference 3-3). The usefulness of the design point analysis lies in the fact that several thermodynamic properties may be held constant while pertubating a single thermodynamic input property.

Unlike more elaborate cycle decks, design point programs model "rubber engines"; i.e., configurations in which the hardware geometry- turbine nozzle areas, mixing plane areas, and exhaust nozzle area- have not been defined in the design process. Hence, design point programs isolate the effect of changing a single thermodynamic property and eliminate the secondary thermodynamic effects associated with the cycle rebalancing to match specified duct areas. Table 3-1 summarizes the primary differences between the design point program and the more sophisticated off design cycle deck.

3.2.2 Cycle model degrees of freedom

The required number of thermodynamic inputs to the design point program is specified by dimensional analysis. Dimensional analysis expresses a system of equations as unique functions of the minimum number of independent variables. For a cycle with fixed geometry (that is, all duct areas are defined), the turbofan engine has one degree of freedom during dry operation and two degrees of freedom during afterburning operation. Hence, during dry operation, specifying a single independent variable (for example, main combustor fuel flow) defines all other thermodynamic properties in the cycle.

A variable exhaust nozzle area (A8) configuration requires an additional degree of freedom. This area may be scheduled explicitly. Alternatively, because of the interdependence of the cycle properties, the area may be indirectly specified by defining, for example, a target turbine temperature corresponding to that exhaust area.

Table 3-1: Comparison of the Features of Design Point Cycle Programs and Off Design Cycle Decks

	Design Point Program	Cycle Deck
Purpose:	• Performance sensitivities calculated as a single thermodynamic property is modified.	• Performance sensitivity calculations include secondary effects as the cycle rebalances.
	• Does not easily represent a single engine configuration at different flight conditions.	• Can easily represent a single engine configuration throughout the flight envelope and at various power settings.
Features:	• 5 thermodynamic inputs are required for a mixed flow afterburning turbofan with variable exhaust nozzle (dry operation).	• 2 thermodynamic inputs are required (dry operation).
	• Does not include component maps for off design performance.	• Includes component maps for off design performance.

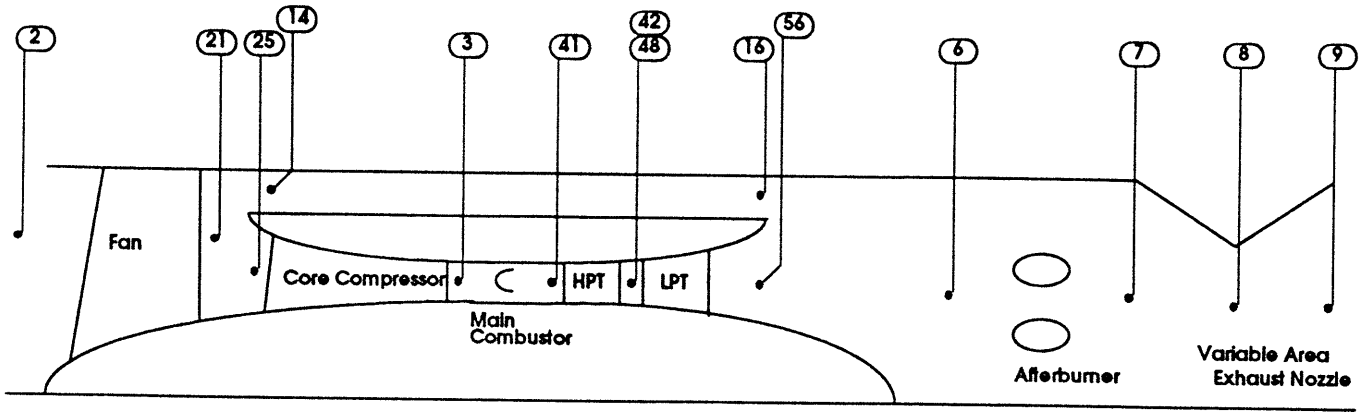

Engine Flowpath Station Designations

Station No.	Description
2	Engine Inlet
21	Fan Exit
25	Core Compressor Inlet
3	Core Compressor Exit
41	HPT Inlet
42	HPT Exit
48	LPT Inlet
14	Bypass Duct Inlet
16	Bypass Duct Exit
56	Core Stream Exit
6	Afterburner Inlet
7	Nozzle Inlet
8	Nozzle Throat
9	Engine Exhaust Plane

P&W F100 (reference 3-6)

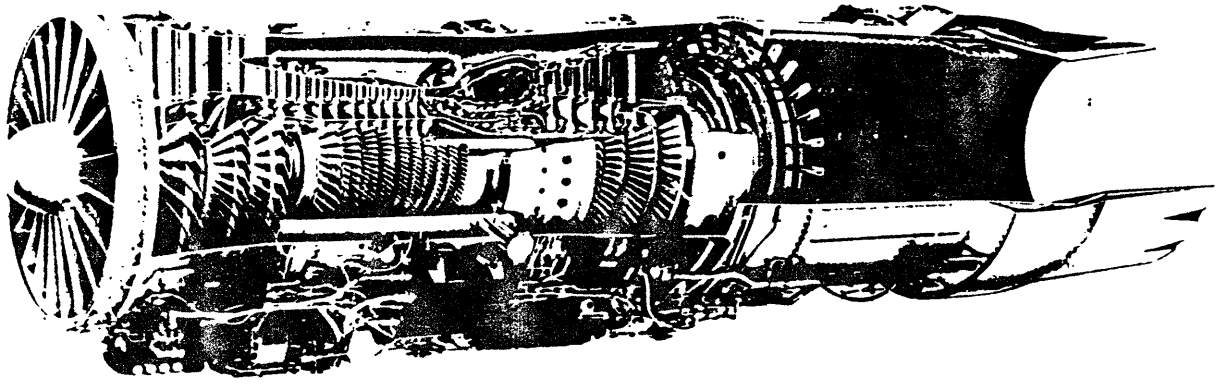

Figure 3-4: Mixed Flow Turbofan: Engine Flow Path Station Designations

During the preliminary design of an engine cycle, additional degrees of freedom exist because the duct areas have yet to be defined. For the mixed flow turbofan (Figure 3-4), the cycle designer must specify 5 areas: 2 turbine nozzle areas, the area of the bypass duct, the area of the core stream at the mixing plane, and the exhaust nozzle area. Again, because of the interdependence of the cycle properties, specifying the thermodynamic properties is equivalent to defining the areas. By convention cycle properties such as compressor pressure ratios are defined because they have more engineering aerothermal meaning and offer better insight into the mechanics of the cycle.

3.2.3 Definitions

Specific Fuel Consumption (SFC) is a measure of how efficiently the engine burns fuel. The parameter is defined as the ratio of total fuel flow (main combustor and afterburner) divided by net engine thrust. Because it is desirable for fuel flow to be low for a given level of thrust, a lower SFC means better performance.

(3-3) SFC=WFT/FN

where WFT is fuel flow

FN is engine net thrust

The specific thrust (FN/W2) is the engine net thrust divided by the engine inlet flow. This parameter is often used during the preliminary design phase of the engine.

The overall efficiency of the gas turbine cycle is the product of the cycle's overall thermal efficiency and the propulsive efficiency. These two efficiencies have diverging influences: propulsive efficiency increases with decreasing exhaust velocity (v9) ; thermal efficiency increases with higher compressor exit temperature (T3) (reference 3-4, 3-5, 3-6).

- overall efficiency

(3-4) $$\eta_{overall}=\eta_{th,o}\eta_{prop}$$

where η_{prop}= propulsive efficiency
$\eta_{th,o}$=overall thermal efficiency

- propulsive efficiency

(3-5) $$\eta_{prop} = \frac{\text{useful work supplied to aircraft}}{\Delta\text{kinetic energy of the propellant}}$$

$$= \frac{(FN)(V_{fl})}{W9(V9)^2/(2g)-W1(V_{fl})^2/(2g)}$$

where FN is the net thrust
V_{fl} is the flight velocity
W1 is the engine inlet flow
W9 is the engine exhaust flow
V9 is the engine exhaust velocity

- thermal efficiency

(3-6) $$\eta_{th,o} = Wnet/Qin$$

$$= \frac{W9(V9)^2/(2g)-W1(V_{fl})^2/(2g)}{(WFT)(FHV)}$$

where Wnet is the net work
Qin is the heat input
WFT is the combustor fuel flow
FHV is the fuel heating value

3.3 Engine Cycle Deck for Off Design Analysis

3.3.1 Cycle Control Modes

The cycle deck calculates the thermodynamic cycle properties at off design conditions. Unlike the design point analysis described above, however, the engine hardware configuration has been defined; hence, fewer degrees of freedom exist. For the baseline afterburning turbofan with variable exhaust nozzle, the control system specifies two parameters during dry operation and three parameters during augmented operation.

For this study, idealized control modes have been adopted. The first mode defined the engine inlet flow as a function of engine inlet conditions. This mode was assumed to have already been optimized for the baseline configuration.

The second control mode was turbine inlet temperature (T41). For this study, a maximum turbine temperature representative of the current state of the art was selected (Figure 3-5). At high power, the cycle deck solved this maximum temperature unless other cycle properties became limiting. In this study, two factors which caused T41 to operate below its maximum level were fan stall margin and compressor discharge temperature (T3).

In actual engine control systems, T41 is not measured directly because instrumentation cannot survive in the severe temperature environment at that flow path station. Hence, turbine temperature is indirectly specified by a different thermodynamic property. These actual control modes are tailored to satisfy fan stall margin, T41, T3, and other limits as appropriate.

3.3.2 Cycle Mechanics

The component modelling within the cycle deck address nonstandard, non ideal operating conditions. For example, the compressors and turbines have maps to define the component performance. As described in Section 3.1, the cycle model modifies the turbomachinery components map values for nonstandard conditions which include the effects of Reynolds number, humidity, tip clearances, and deviations from the nominal variable stator schedule.

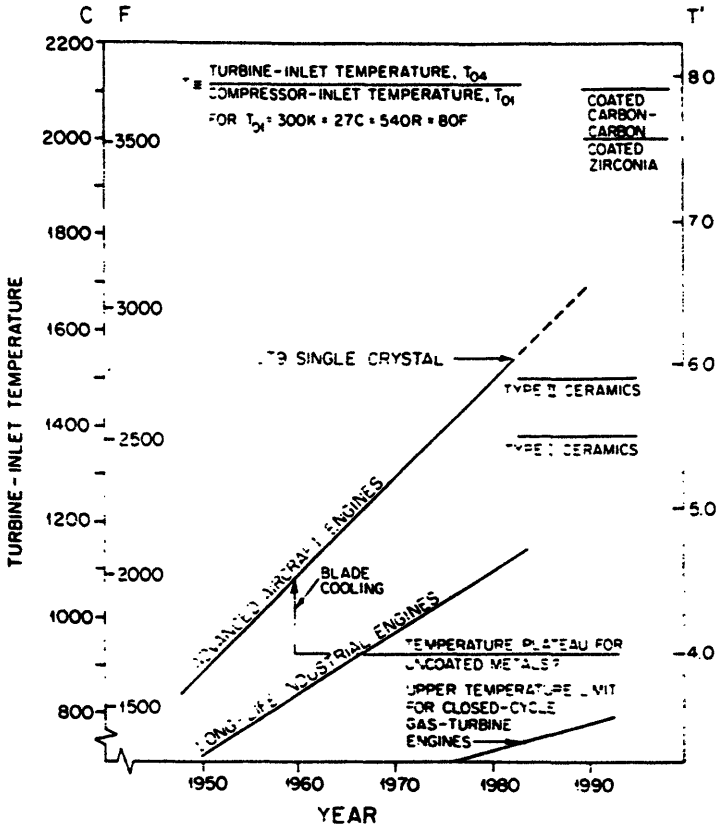

Figure 3-5: Turbine Temperature Technology Progress (reference 2-11)

Empirically based modifiers are also applied to model the combustion process and flow through the various ducts. These factors include:

- combustor heat loss- energy convected from the gas generator to the bypass duct;
- stratification- the non-uniform radial profile of temperature and pressure exiting the fan;
- mixing of the bypass and core streams- conservation of momentum and energy calculation as the bypass air is reintroduced into the primary flow path.
- cooling and leakage flows- including overboard leakage, internal bore cooling, and turbine nozzle and blade cooling;
- pressure losses- due to friction, diffusion, and heat addition.
- installation effects-compressor bleed flow and horsepower extraction to power aircraft accessories.
- exhaust nozzle aerodynamics - modelling of overexpanded and underexpanded operation.

Figure 3-6 is a block diagram of the cycle deck calculation procedure. Mathematically, the cycle solution is achieved by solving a system of equations formed by combining the control inputs with boundary conditions dictated by first principles. Because the governing equations cannot be expressed in closed form, the solution is obtained by iteration. To expedite the calculation process, the cycle deck applies the Simultaneous Linear Algebraic Method (reference 3-8).

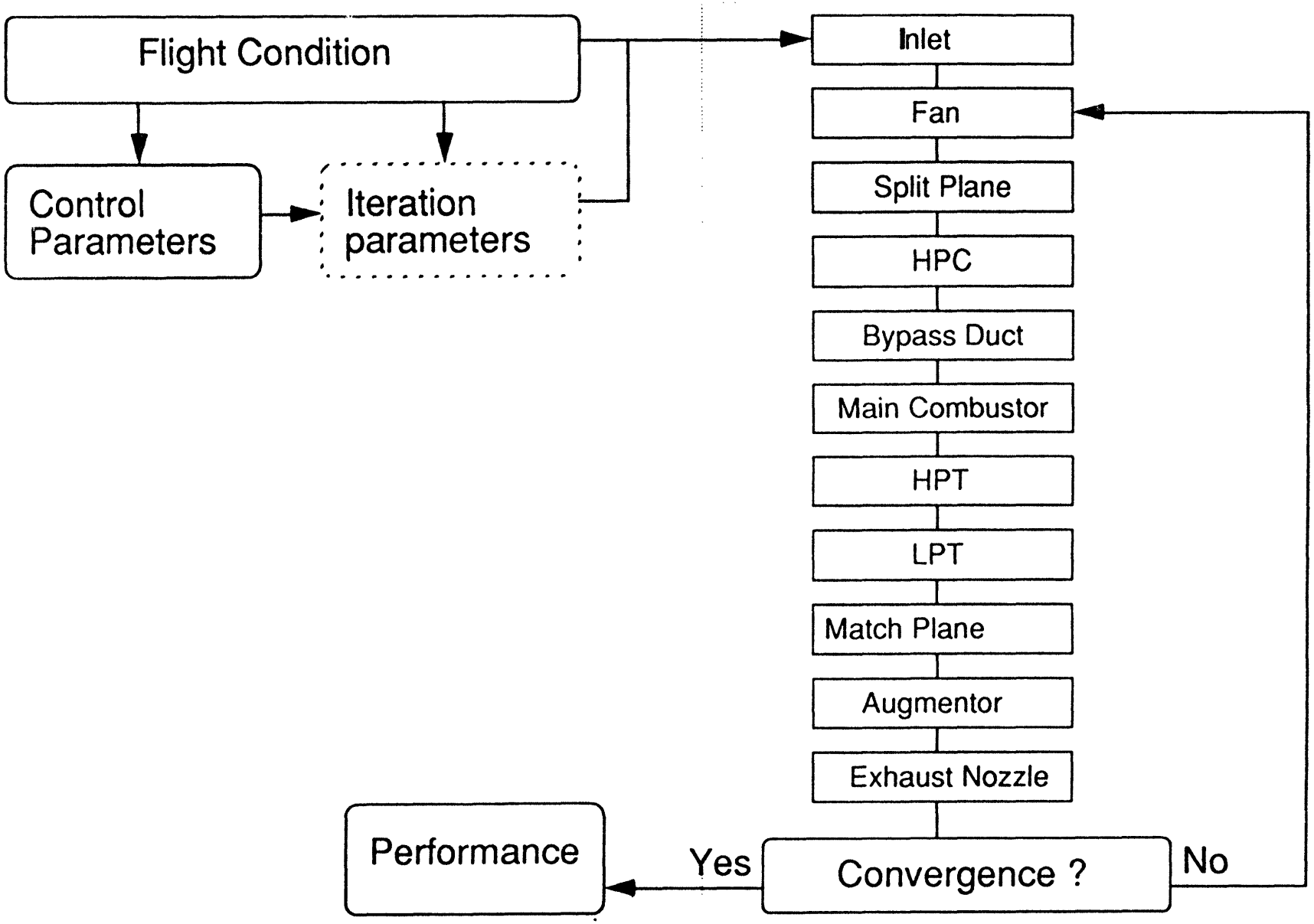

Figure 3-6: Block Diagram of Cycle Deck Calculation Procedure

The boundary conditions assure that the conservation of mass and the conservation of energy are maintained through the engine. The following elaborates on the boundary conditions and the criteria for converged solutions.

High Pressure Compressor (HPC) inlet flow: The inlet flow to the HPC is calculated independently two ways: the flow that is calculated from the component map; and the flow that is passed from the upstream station. The boundary condition is satisfied when both solutions agree within an acceptable tolerance.

Turbine flow functions: Conservation of mass at the high pressure turbine (HPT) and the low pressure turbine (LPT) rotor inlets are similarly satisfied by comparing the map value to the flow passed from the upstream station.

Nozzle Throat: Conservation of mass at the throat is determined in a slightly different manner. Upstream conditions provide one value of flow. The other value is associated with the static quantities at the throat. These static quantities depend on whether or not the throat is choked and are related to properties at the discharge plane.

Match plane static pressure balance: For unchoked bypass duct operation, the model iterates until the bypass duct discharge static pressure (PS16) equals the core duct exit static pressure (PS56).

3.3.3 Cycle Model Inputs

Altitude, Mach number, and ambient temperature define the engine's operating point in the flight envelope. However, to completely define the engine operating condition, the effects of engine/aircraft integration must be modelled. These installation effects include engine bleed flow, engine horsepower extraction, and inlet ram recovery.

The aircraft uses engine bleed flow and engine rotor work to power its onboard accessories. For this study, the bleed flow is modelled by a constant 3.5% (of the core flow) extracted from the high pressure compressor. The gearbox extracts a constant 100 horsepower from the high pressure rotor.

Ram recovery models the total pressure loss in the inlet as a function of flight speed. The cycle model defines the pressure recovery as a function of Mach number per the standard MIL-E- 5008C.

Chapter 4: Optimizing Compressor Component Performance

4.1 Introduction

Compressor aerodynamic design involves compromises among pressure rise, flow, efficiency and overall stall margin. Hence, optimized levels of efficiency, flow and/or pressure rise may be sacrificed in order to achieve satisfactory levels of stall margin. However, with active control schemes, the required overall stall margin is provided by two sources: "conventional stall margin" provided by current compressor design techniques; and "control stall margin" provided by actively suppressing stall initiation. Because control stall margin is available, the design is not subject to the compromises traditionally needed to meet stall margin goals; as a result, the designer can optimize the compressor for pressure rise, flow and/or efficiency.

For the same net stall margin ($SM|_{total}$), the presence of the stall margin provided by active control allows the conventional stall margin ($SM|_{conv}$) to decrease by one of two methods. First, for the same aerodynamic stall line ($PR|_{sl,conv}$ = constant), the operating line pressure ratio ($PR|_{ol}$) is increased while the conventional stall margin is decreased ($SM|_{conv}$; eq 4-1). Stall margin otherwise sacrificed is provided by active control and the same net stall margin is maintained (eq 4-2). Second, for the same operating line ($PR|_{ol}$= constant), the conventional stall line occurs at lower pressure ratio

($PR|_{sl,conv}$ is lower) which allows a decrease in conventional stall margin. Again, active control provides the stall margin otherwise sacrificed.

(4-1) $$SM|_{conv} = \left(\frac{PR|_{sl,\,conv}}{PR|_{ol}} - 1\right) * 100$$

(4-2) $$SM|_{total} = SM|_{conv} + SM|_{ac}$$

where $PR|_{sl,conv}$ is the conventional stall pressure ratio established by traditional techniques.
$PR|_{ol}$ is the operating line pressure ratio
$SM|_{conv}$ is the conventional stall margin provided by traditional techniques.
$SM|_{ac}$ is the stall margin provided by active control
$SM|_{total}$ is the net stall margin

This chapter focuses on the latter method: a lower conventional stall line pressure ratio is acceptable when used with active control. The benefit is an improvement in component efficiency. These efficiency benefits are later applied to the engine in Chapter 7 to quantify the impact of improved compressor efficiency on system level performance.

Chapters 5 and 6 analyze the impact of the other method: maintaining the same conventional stall pressure ratio and instead raising the operating pressure ratio.

4.2 Background

As discussed in Chapter 2, variable stators are a common solution for improving the stall line during low speed operation on multistage compressors. For example, reference 4-1 details a design in which the desired operating line intersected the stall line at low speeds. Inlet guide vanes and 4 stages of variable stators were required to make the compressor viable. Further, as stated in Chapter 2, variable stators are designed to provide adequate stability margin and not necessarily to maximize efficiency.

The following analysis explores how active control can improve compressor performance. First, the magnitude of potential stall margin gains has been estimated based on experimentally demonstrated results of actively controlled compressors. Second,

the use of actively controlled compressors to eliminate efficiency compromises has been evaluated. The variable stators have been defined to maximize efficiency; stall margin otherwise sacrificed would be provided by active control.

4.3 Stall margin gain for a lower stalling flow coefficient

Active control experiments demonstrated a reduction in the stalling flow coefficient by 8% to a characteristic slope ($d\Psi'/d\Phi$) of .9 on a 3 stage axial flow compressor (reference 2-20). Studies by Hendricks, et al (reference 4-2) indicate that stall may be suppressed to a characteristic slope of up to 4 on high speed multistage machines.

These magnitudes have been applied to the fan and compressor in this study to quantify the stall margin gain (stall margin at constant corrected flow, eq. 3-1). The method for converting pressure ratio and corrected flow into compressor stage characteristics (Ψ' vs Φ) is shown in Figures 4-1. The method assumes perfect gas properties, standard day inlet conditions, and no inlet swirl.

First, the performance maps (pressure ratio vs flow) were converted to its compressor characteristic equivalent (Ψ' vs Φ). Second, the characteristics at different speeds were extrapolated to a positive slope to determine the new stalling pressure and flow coefficients. The extrapolation was conducted assuming symmetric stage characteristics (reference 4-3). Finally, knowing the new pressure and flow coefficients, the new stall pressure ratio was calculated and plotted on the component map (Figure 4-2A).

Figure 4-1: Calculation of Flow Coefficient and Pressure Coefficient

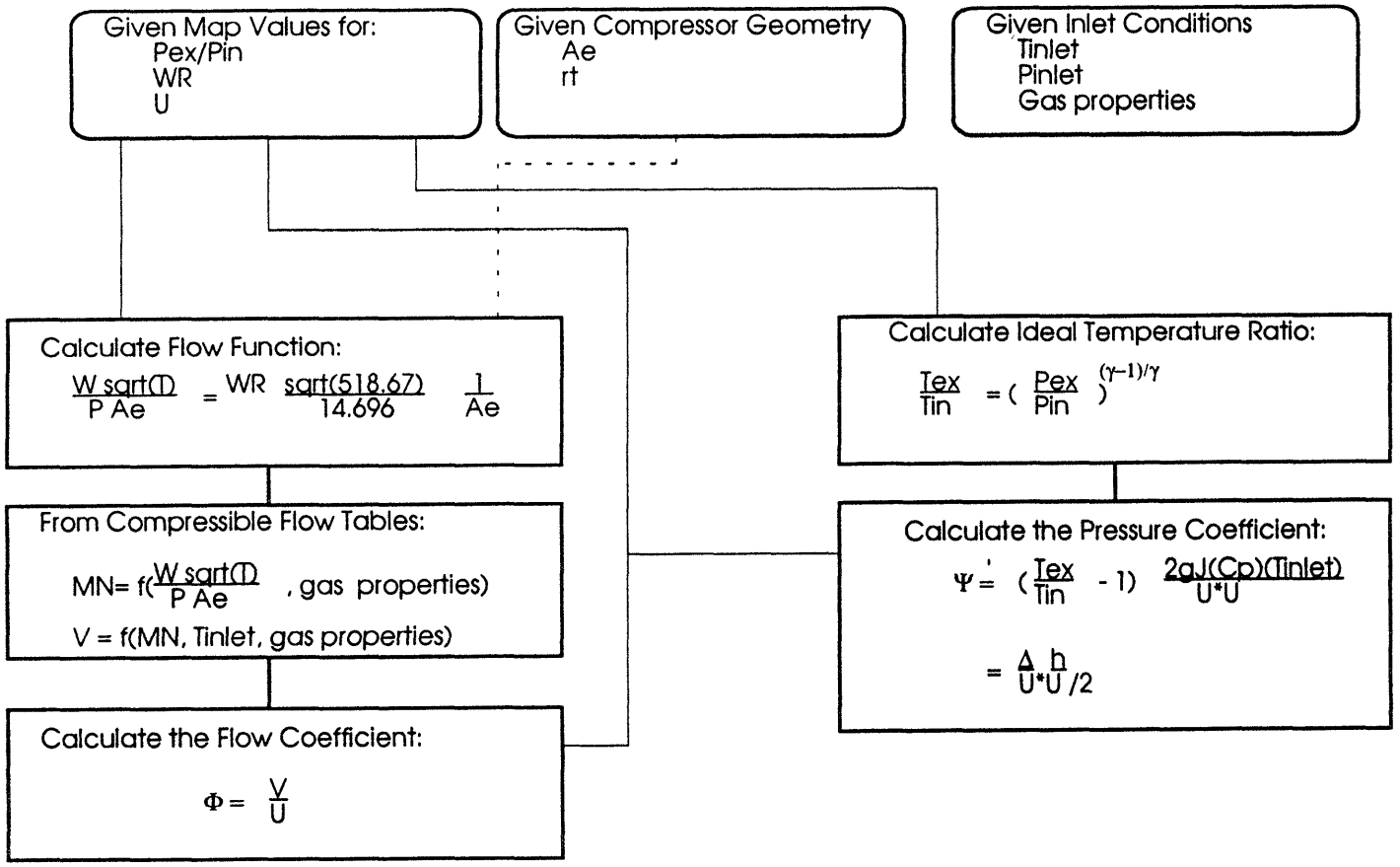

where Pex/Pin is the exit to inlet total pressure ratio.
Tex/Tin is the exit to inlet total temperature ratio.

WR is the map corrected flow.
U is the wheel speed.
Ae is the reference effective area.
rt is the reference radius for U.
V is the axial flow velocity.
MN is the flow Mach number.

h is the specific enthalpy.
Cp is the specific heat capacity.
J is Joules constant.
g is the gravitational constant.
γ is the ratio of specific heats.

Figure 4-2A: New Stall Line after Extrapolation of the Stage Characteristics

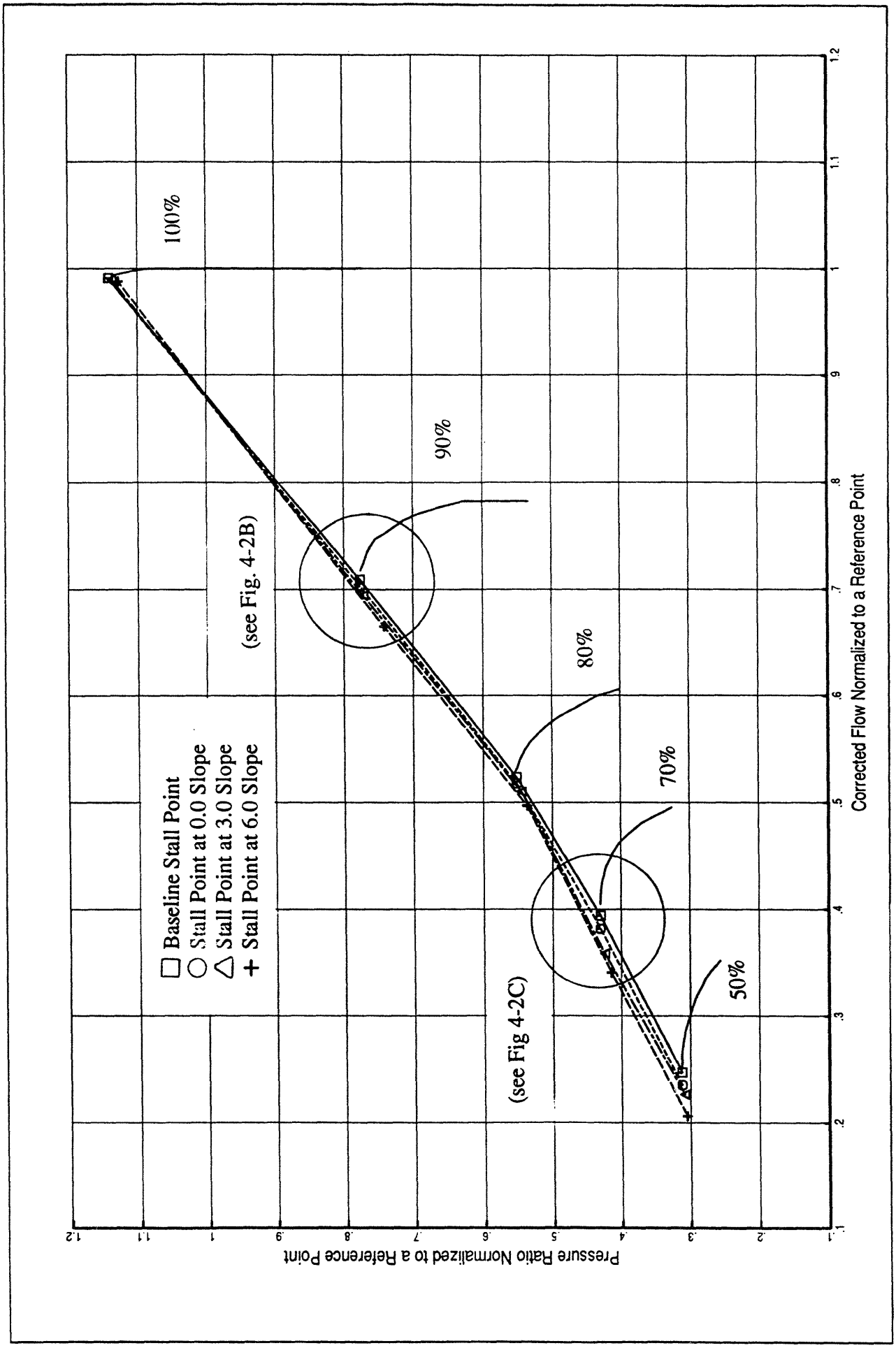

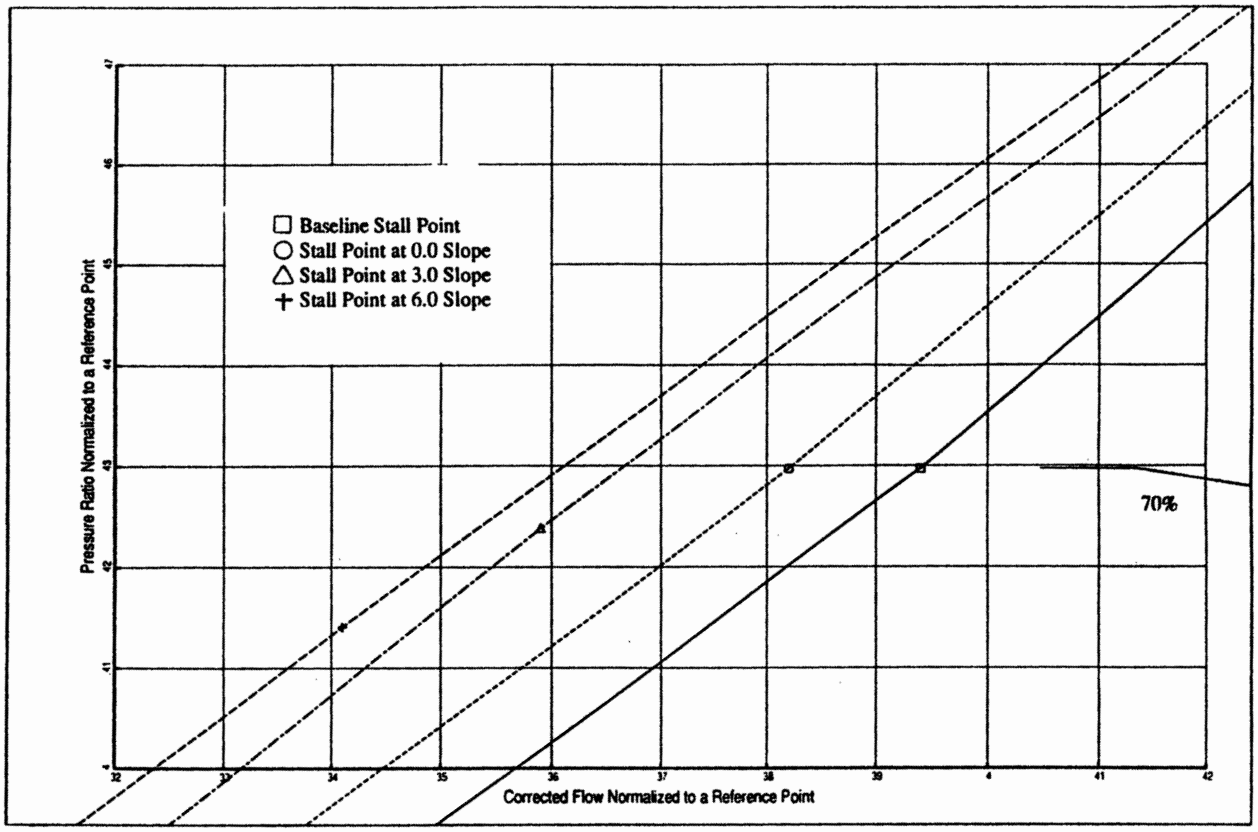

Figure 4-2C: Extrapolated Stall Line at 70% Speed

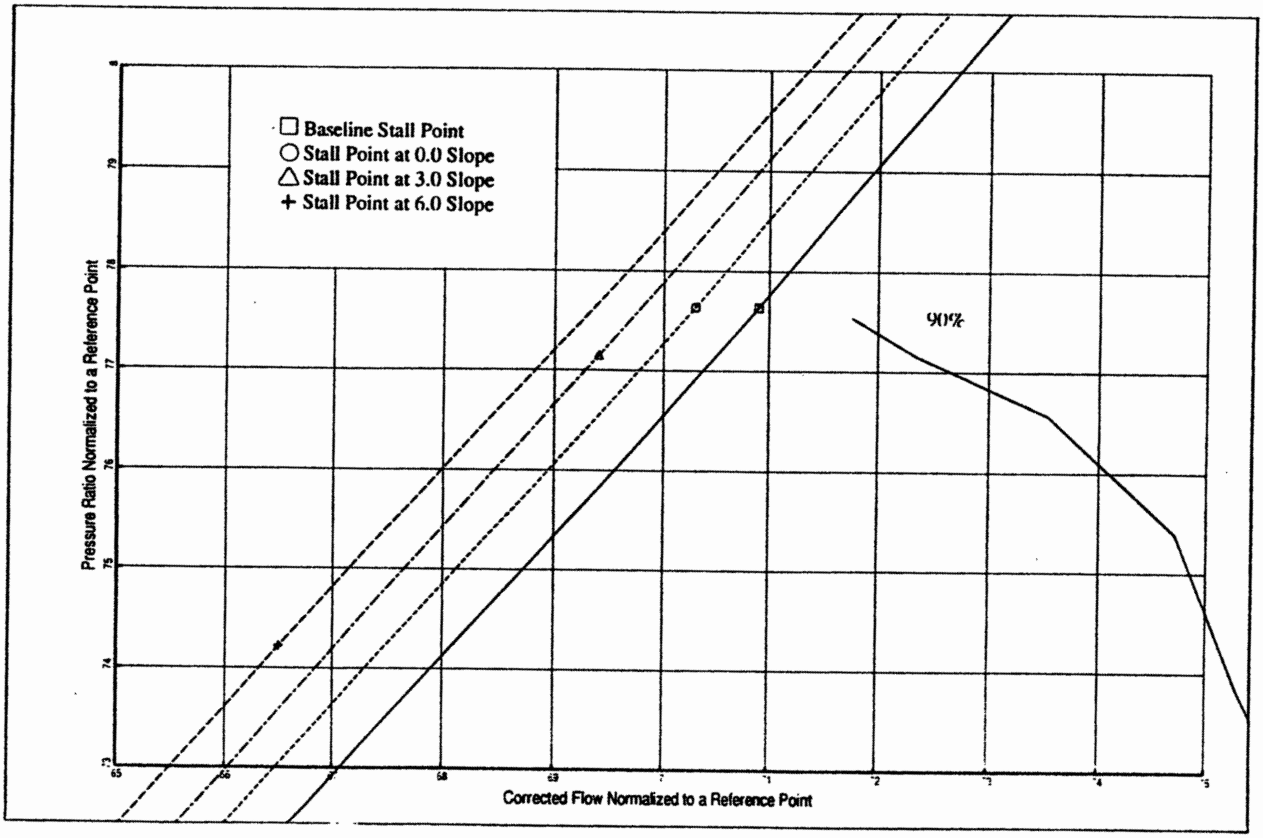

Figure 4-2B: Extrapolated Stall Line at 90% Speed

The extrapolation of the compressor characteristics were done for three cases:

- Extending Φ_{stall} until $d\Psi'/d\Phi$ became greater than 0.0.
- Extending Φ_{stall} until $d\Psi'/d\Phi$ became equal to 3.0.
- Extending Φ_{stall} until $d\Psi'/d\Phi$ became equal to 6.0.

From Figure 4-2A all the cases resulted in approximately the same increase in overall stall margin: 0.0% at 100% speed and 2.5% at 70% speed. Reductions in the stalling flow coefficient as the slope was increased to more positive values was offset by the losses in pressure coefficient.

The magnitudes of the improvement in stability are consistent with reference 2-5 for a well matched multistage compressor. Although relatively small, reference 2-5 predicts that the gain in stall margin should increase as the stages become more mismatched; a situation which would exist if variable stators are adjusted to maximize efficiency.

The magnitude of stall suppression that will ultimately be realized on high speed multistage configurations depends on future development of the technology. For this reason, this study did not directly apply the estimated stall margin gain based on the above calculation. Instead, a range of stall margin was assumed: 5% and 20% levels of control stall margin.

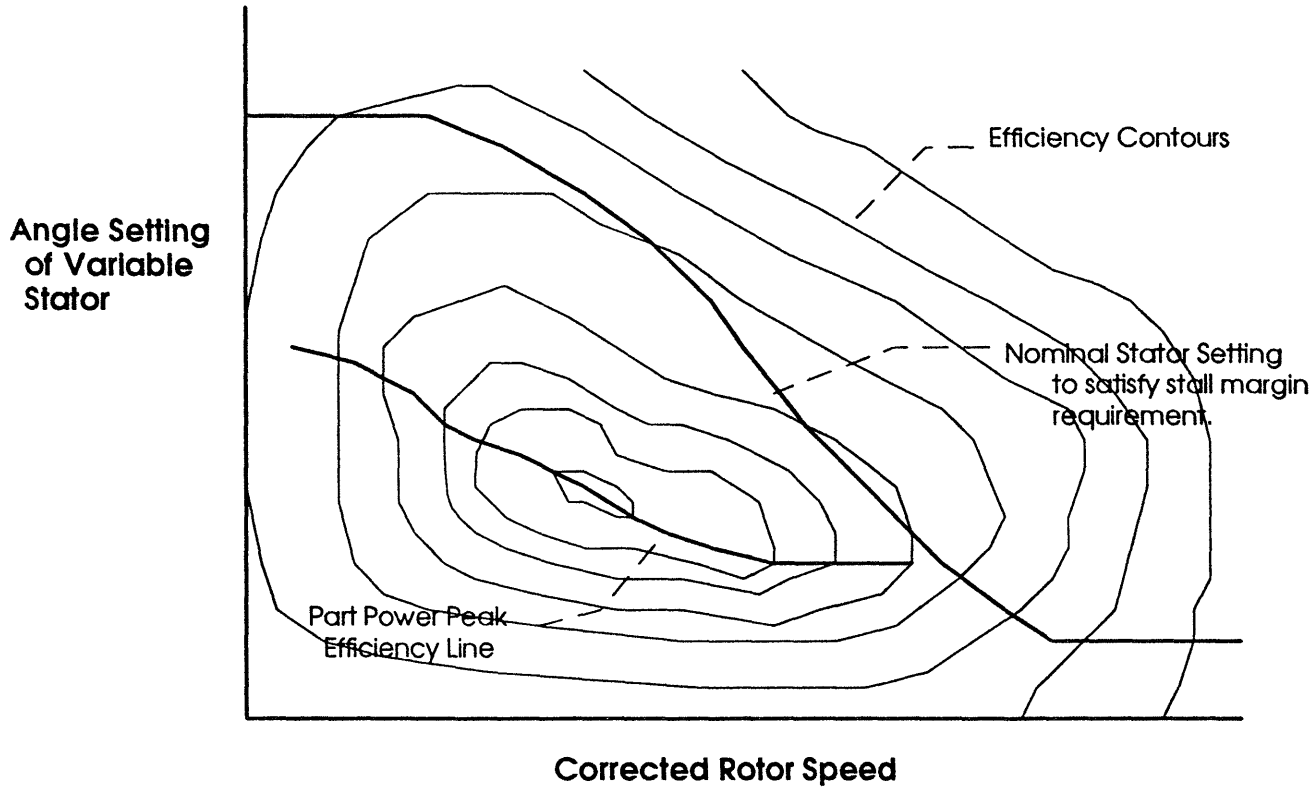

Figure 4-3: Typical Variable Stator vs Corrected Speed Howell Diagram

4.4 Optimizing Core Variable Stators

The potential improvement in efficiency and the influence of variable stator position are demonstrated by a typical Howell compressor diagram (Figure 4-3). Figure 4-3 plots the variable stator angle as a function of corrected rotor speed with efficiency contours superimposed. As illustrated, the nominal stator angle does not coincide with the line of peak efficiency. The deviation is generally greatest at lower speeds. At these operating conditions, the variable stators sacrifice efficiency to alleviate stage mismatch and to provide the required stability margin.

Core compressor efficiency was optimized by applying empirically based variable stator modifiers on the baseline component maps. To cover a range of relevant operating speeds, the optimized variable stator schedule was defined by running a series of cycle points principally along an intermediate rated power (IRP) acceleration at 35,000 ft (MN from .2 to 2.0). For the compressor used in this study, Figure 4-4 compares the location of the peak efficiencies relative to the baseline stator schedule at sea level static (SLS) operation. Note that larger angle adjustments were required at part power operation where the greatest potential efficiency gains may be achieved.

Applying sensitivity factors which degraded the stall line for changes in the stator schedule resulted in a loss in stall margin of 4% to 5%. Although a maximum efficiency improvement of 6% was possible at very low rotor speeds (Figure 4-5), the efficiency increase ($\Delta\eta$) for typical operating speeds ranged from .005 to .01.

The results of this analysis should be a conservative estimate of potential compressor efficiency improvements. Redefining both the stator and blade velocity diagrams during the preliminary design phase, for example, would produce larger gains in efficiency for a given loss in stall margin.

Figure 4-4: Core Compressor Howell Diagram

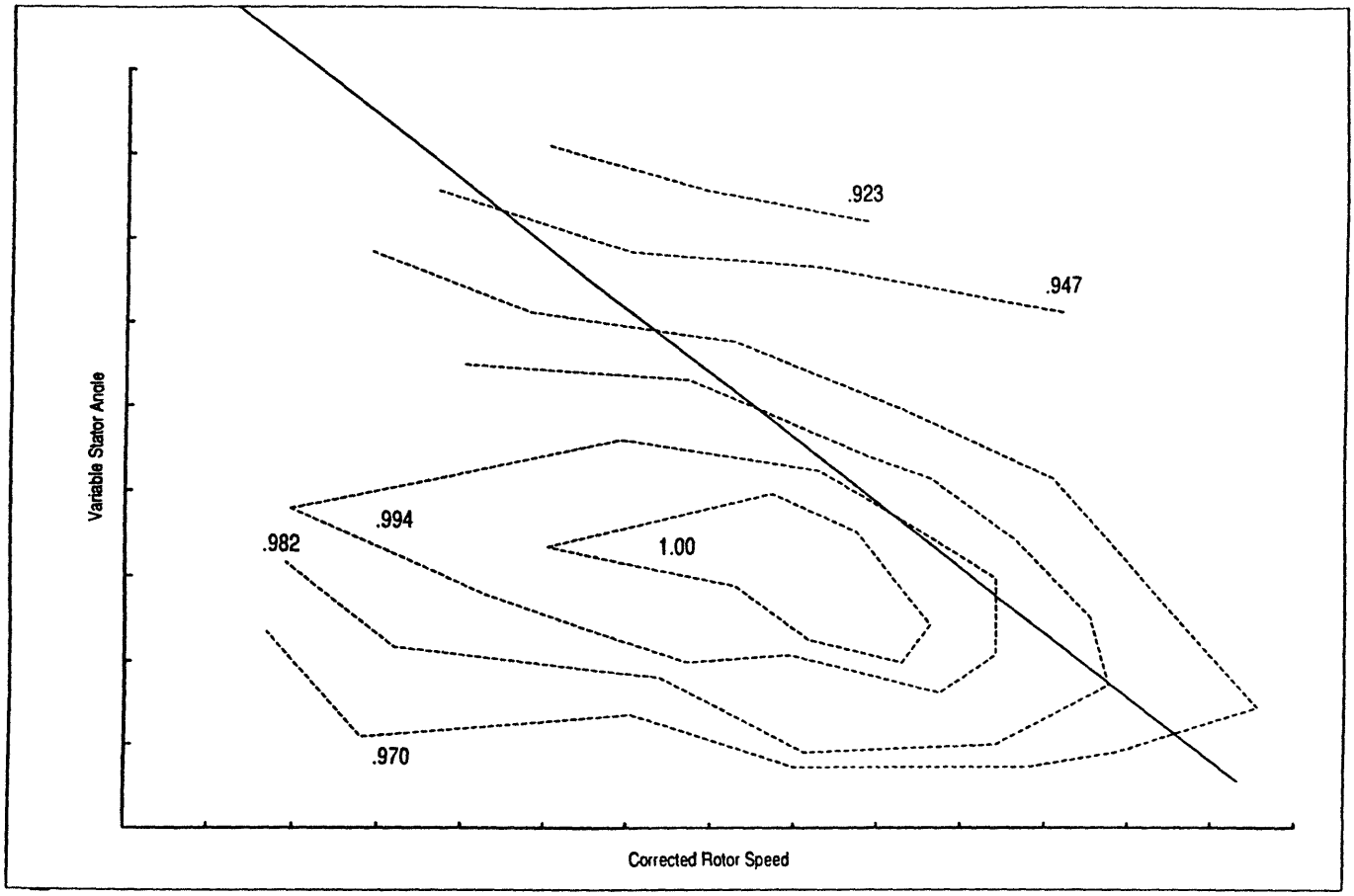

4.5 Comparison to other compressor designs

Data from several compressor designs were collected to quantify the potential efficiency improvements for different designs. These designs include:

- The core compressor used in this study;
- High Pressure Compressor #1: a multistage high pressure compressor for a high bypass ratio turbofan;
- Fan #1: a multistage fan for a medium bypass ratio turbofan;
- Fan #2: a multistage fan for a medium bypass ratio turbofan.

Figure 4-5 summarizes the potential efficiency improvements due to optimizing the variable stators as a function of rotor speed. The potential improvement covers a wide range- 0.0% to 7.6%. As the data suggests, using active control to optimize variable stators depends on the baseline compressor being considered. For some designs, little or no benefit would be achieved and this application of active control would not be appropriate.

However, at the preliminary design level, given the flexibility to optimize not only the variable stator angle but also the basic blade geometry of the rotors and stators, larger efficiency benefits for all compressors are expected.

4.6 Discussion and Conclusions

A consequence of changing the variable geometry schedule was a change in the speed at flow characteristic; i.e., as the variable stators are opened, the swirl angle is reduced and a given flow is achieved at a lower speed. This observation has several implications. First, if the engine is maximum mechanical speed limited, this attribute may allow the compressor to avoid this limitation and operate at the desired higher flow levels. Further, if the design speed and maximum speed are reduced, benefits on mechanical life, stress and weight may be realized.

Figure 4-5: Potential Efficiency Gains for Different Compressors

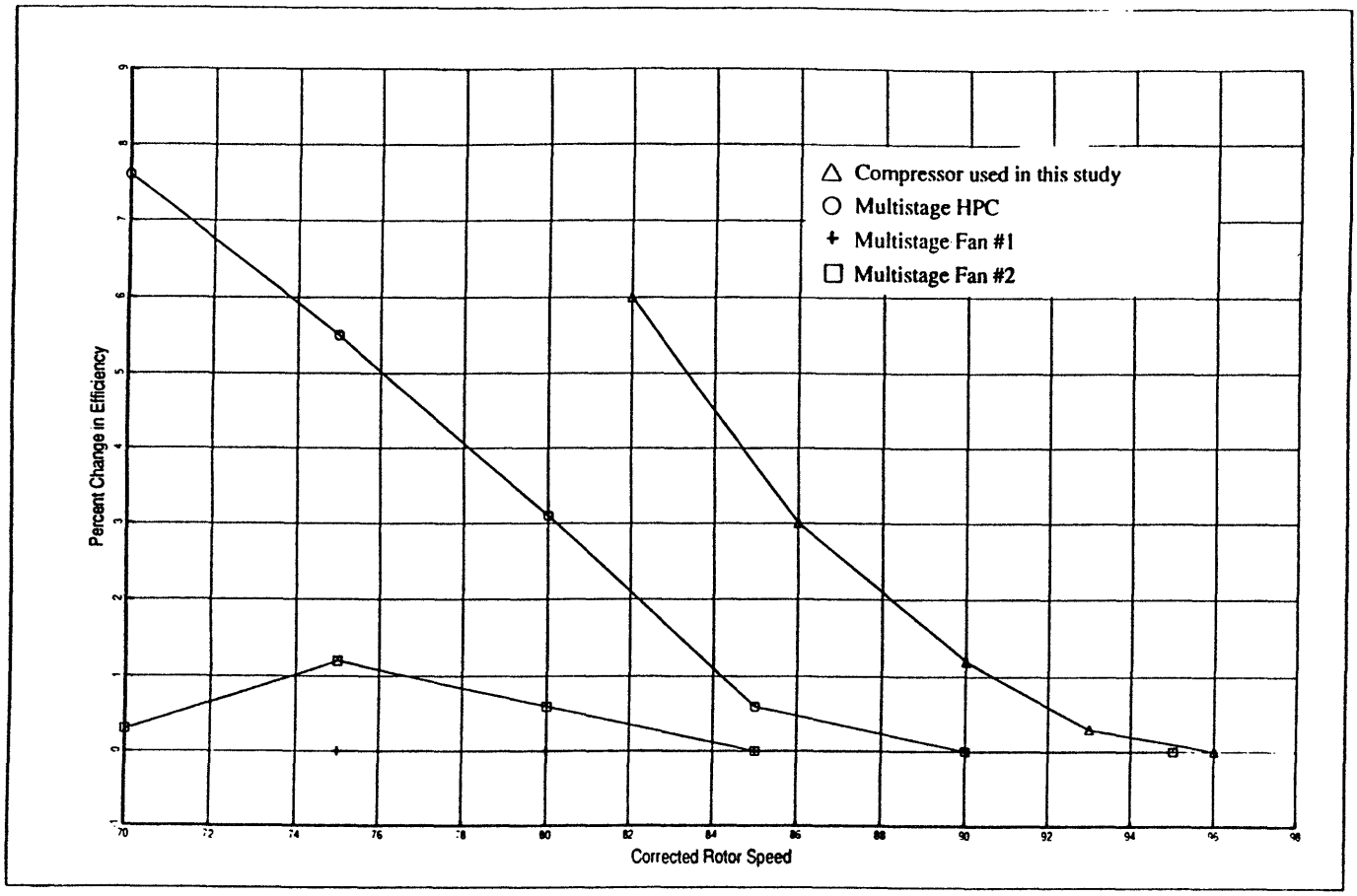

On the other hand, the lower speed negatively impacted the efficiency of the high pressure turbine used in this study. When the optimized variable geometry compressor was coupled to the existing turbine, losses in HPT efficiency offset gains in HPC efficiency. Chapter 7 discusses this in more detail. Because of this mitigating effect and because of potential efficiency improvements from optimizing both the blade and stator aerodynamic velocity diagrams, the greatest performance gains would result if efficiency is optimized during the preliminary design phase of the compressor.

During the developmental phase, additional design steps may be taken to avoid these penalties. For example, because of the loss in HPT efficiency on an existing engine, the optimized compressor may be more appropriate for an entirely new design. In this case, the HPT can be designed to achieve the higher efficiency at the lower speed. Note, however, if the speed decreases significantly, additional turbine stages may be needed to maintain the desired efficiency level. More stages, of course, mean greater weight.

The analysis quantified trading the stall margin provided by variable stators for improved component efficiency. Stability otherwise sacrificed would be provided by active control. An extension of this application uses active control to replace variable stators- an attractive design option if the weight of the active control hardware is less than the variable stator hardware.

The magnitude of stall margin which active control must provide is estimated from data provided in reference 4-1. A 15 stage compressor required IGV and 4 stages of variable stators to move the compressor knee below the normal range of operation. In doing so, the variable stators provided about 25% stall margin. Although this magnitude is well above the estimated 2.5% stall margin which active control would provide for the baseline compressor used in this study, active control may yet provide sufficient stall margin to justify eliminating variable stators. The 2.5% stall margin improvement was for a compressor with variable geometry and hence reasonable stage matching. However, as

discussed in section 4.3, significant stall margin may be gained when active control is applied to a compressor with highly mismatched stages; a scenario which would occur when variable stators are removed. This topic requires further study and is reserved as a topic for future research.

Chapter 5: Cycle Design Point Program Analysis

5.1 Introduction

A design point analysis has been conducted to quantify the thermodynamic cycle trends associated with implementing active control. This design point methodology, as discussed in Chapter 3, isolates the effect of raising compressor pressure ratios. Further, these trends have been used to rationalize the off design results to be discussed in Chapter 6 and Chapter 7. In short, the design point analysis quantified the engine thrust and fuel consumption variation as compressor pressure ratios were increased above the baseline value. For this analysis, the sensitivities were generated for a single reference operating condition subject only to a turbine inlet temperature (T41) limit.

As part of the design point study, this chapter introduces the various cycle properties which directly affect engine thrust. In doing so, the fundamental connection to performance benefits and penalties have been highlighted.

5.2 Method

To ensure that the design point program provided results consistent with the baseline engine configuration, the thermodynamic properties at the design point were

matched to a more sophisticated cycle deck having component off-design capabilities (see section 3.3). Component efficiencies, pressure losses and cooling flows were input into the design point program based on cycle deck data using sea level static (SLS), standard day (STD) temperature as the reference point.

A parametric study was conducted to assess the effects of increased compressor pressure ratio. In this study, core compressor pressure ratio was parametrically modified while holding T41, bypass ratio (BPR), fan pressure ratio, and core duct Mach number constant. In addition, the adiabatic efficiencies in the fan, core compressor, and turbines were held constant. Carpet plots of specific fuel consumption (SFC) vs specific thrust (FN/W2) as functions of pressure ratio were generated to illustrate the results.

To understand the factors which contribute to engine thrust, the gross thrust function has been derived below. This equation expresses gross thrust as a function of exit flow, exit total temperature, nozzle total pressure, exit static pressure, and gas properties. For ideal gross thrust in which the flow fully expands to ambient conditions and the thrust coefficient is unity, the governing equation is:

(5-1) $FG=(W9)(V9)$

where FG is the ideal gross thrust

W9 is the exhaust flow

V9 is the exhaust velocity

Using the isentropic relationships, eq 5-1 may be expressed as:

(5-2a) $V9 = (a9)(MN9)$

$= [\gamma R(TS9)]^{.5}(MN9)$

since $T9/TS9= (1+ (\gamma-1)/2\ (MN9)^2)$

$P9/PS9= [(1+ (\gamma-1)/2\ (MN9)^2)]^{(\gamma/(\gamma-1))}$

$MN9=\{[(P9/PS9)^{((\gamma-1)/\gamma)}-1]*[2/(\gamma-1)]\}^{.5}$

(5-2b) $$V9 = \{(2\gamma R/(\gamma-1))T9\,[1-(P9/PS9)^{(1-\gamma)/\gamma}]\}^{.5}$$

where a9 is the sonic velocity at the exhaust plane

MN9 is the Mach number at the exhaust plane.

T9 is the total temperature at the exhaust plane.

TS9 is the static temperature at the exhaust plane.

P9 is the total pressure at the exhaust plane.

PS9 is the static pressure at the exhaust plane.

(5-3) $$FG/[(W9)(T9)^{.5}] = \{2\gamma R/(\gamma-1)[1-(P9/PS9)^{(1-\gamma)/\gamma}]\}^{.5}$$

Taking the derivative yields:

(5-4) $$\frac{dFG}{FG} = \frac{dW9}{W9} + \frac{dT9}{2T9} - \frac{(1-\gamma)/\gamma\,(PS9/P9)^{(1-\gamma)/\gamma}}{2[1-(PS9/P9)^{(1-\gamma)/\gamma}]}\,\frac{d(PS9/P9)}{(PS9/P9)}$$

Figure 5-1 plots the gross thrust function. From the plot and equation 5-4, several qualitative conclusions can be made :

- a 1% change in mass flow results in a 1% change in gross thrust
- a 1% change in exhaust temperature results in a .5% change in thrust
- at low nozzle pressure ratios, a 1% change in exhaust pressure results in greater than 1% changes in thrust.
- at high nozzle pressure ratios, a 1% change in exhaust pressure results in less than 1% changes in thrust.

Figure 5-1: Ideal Gross Thrust Function

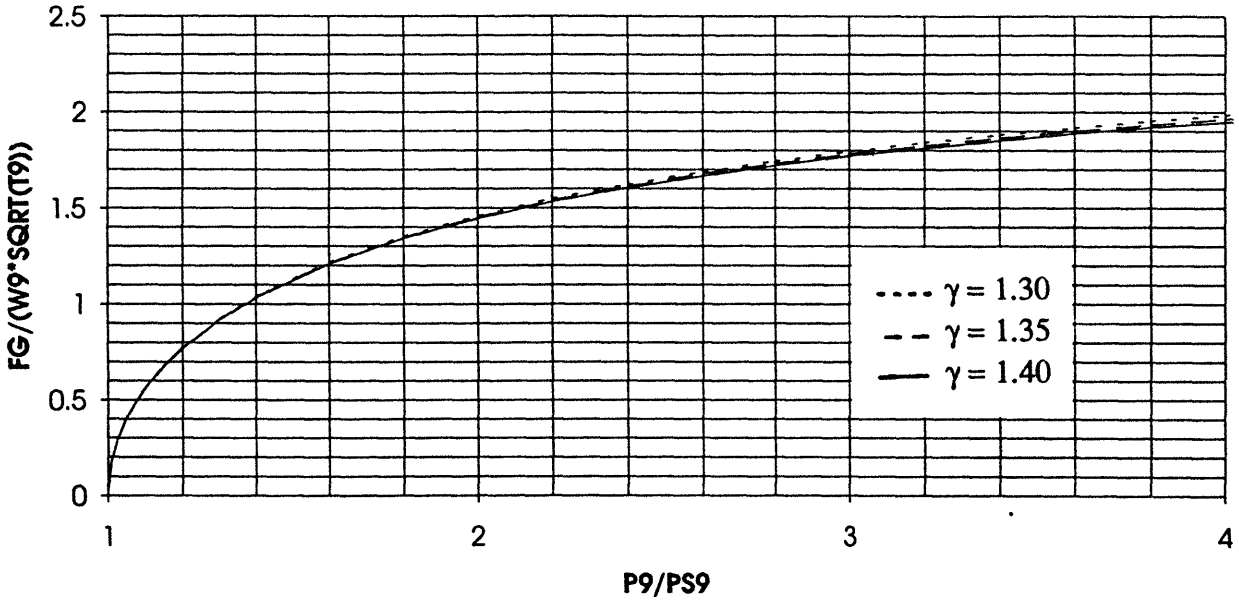

5.3 Higher pressure ratio operation

In general, at a specified turbine inlet temperature and bypass ratio, an optimum compressor pressure ratio exists which maximizes specific thrust. As shown in Figure 5-2, as pressure ratio increases, specific fuel consumption (SFC) decreases and specific thrust (FN/W2) initially increases. At larger pressure ratios, however, additional increases in pressure continue to lower SFC while now acting to lower specific thrust. For most applications, the cycle is designed to operate slightly past the peak thrust level; i.e., some thrust is sacrificed in order to achieve the improved SFC. Small gas turbines are the exception if manufacturing constraints prevent achieving the elevated pressure levels (reference 5-1).

The reference operating point for the baseline engine indeed fell beyond the peak thrust point. As shown in Figure 5-3, further increases in pressure ratio (P3Q25) caused decreases in both SFC and specific thrust: a 5% increase in core pressure ratio improved SFC by -.79%, but decreased specific thrust by -.35%; a 20% pressure ratio increase caused a -2.85% improvement in SFC, but a -1.5% degradation in specific thrust.

In addition to the bypass ratio (BPR) representative of the baseline engine configuration used in this study, the SFC vs specific thrust characteristic was determined for a series of bypass ratios. As indicated by Figure 5-3, higher bypass ratios shifted the characteristic towards lower SFC and lower thrust.

5.4 Design Trades

Several observations are evident from the carpet plot shown in Figure 5-3. First and foremost, higher pressure ratio operation by itself cannot result in both improved SFC and thrust for a given T41 and BPR. Hence, if active control is implemented, other engine configuration changes must also be made to compensate for the lost performance.

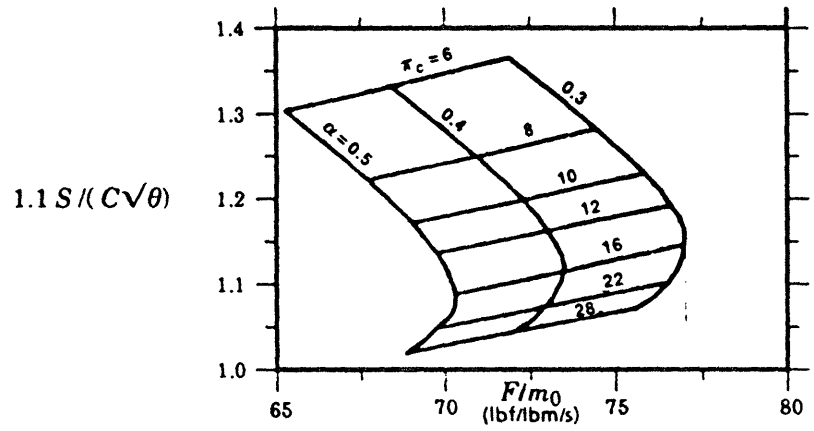

Figure 5-2: Typical Specific Fuel Consumption vs. Specific Thrust Carpet Plot (reference 3-3)

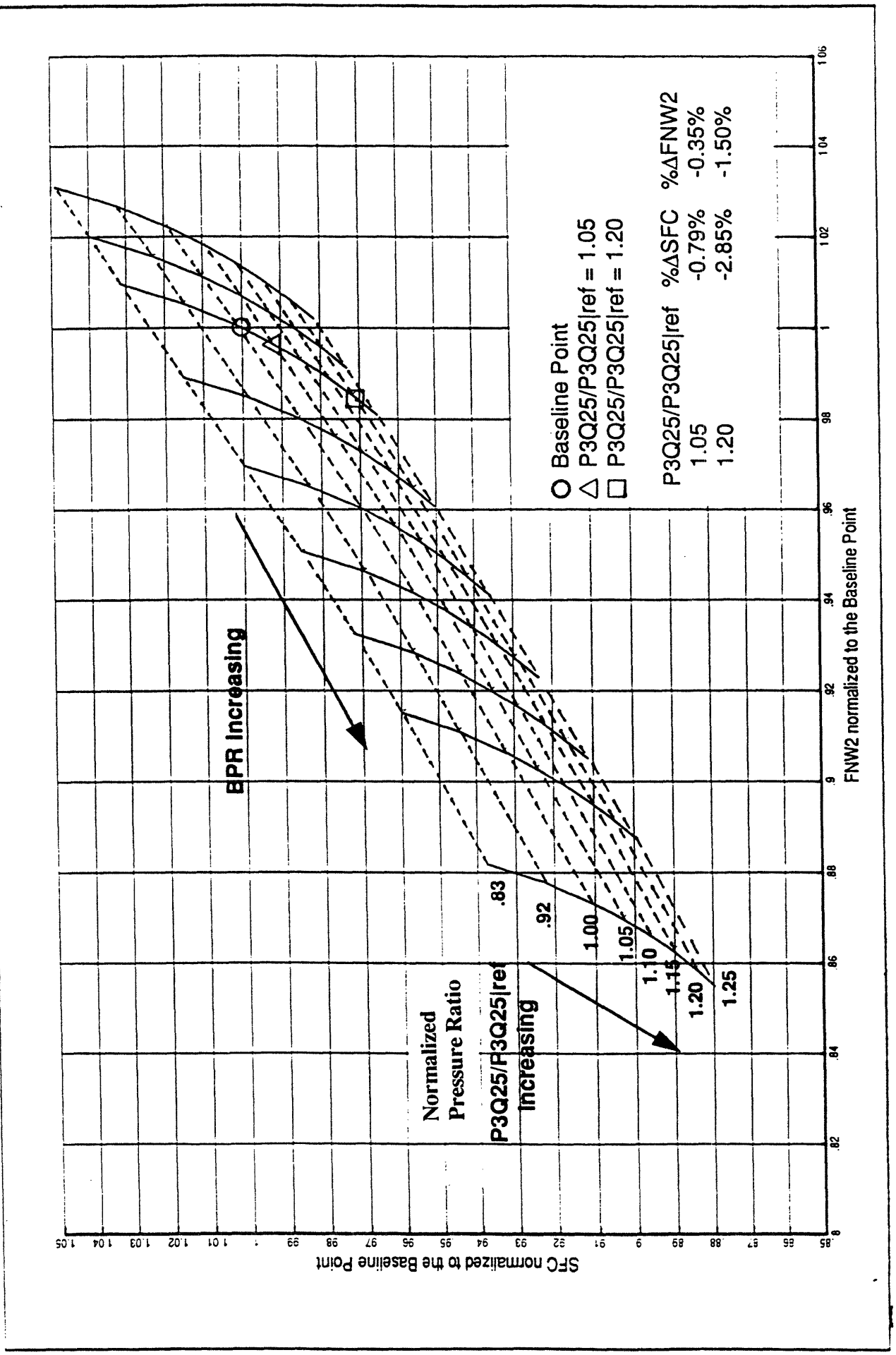

Figure 5-3: SFC vs Specific Thrust at Various Levels of Pressure Ratio and Bypass Ratio

For example, to realize the SFC benefit while maintaining constant thrust, the BPR must be reduced and/or the engine inlet flow must be increased. By reducing the bypass ratio, engine operation would shift as shown in Figure 5-4. For afterburning turbofans, however, the lower thrust may not be feasible if a minimum BPR limit exists.

Alternatively, for a lower specific thrust (FN/W2) , increasing the inlet flow (W2) maintains the absolute level of thrust (FN). However, for turbofans whose maximum flow levels are limited by choking in the fan, increases in inlet flow would require a larger fan and the associated penalty involving greater size and weight.

A potential application of using active control to raise compressor pressure ratios is subsonic non afterburning aircraft such as commercial configurations. Typically, these designs have large bypass ratios due to the desire to achieve exceptional SFC instead of high specific thrust. With active control, however, the benefits of a high bypass ratio engine may be achieved in a low bypass ratio configuration. That is, the aircraft can have the same SFC while having significantly more thrust if operation is shifted as shown in Figure 5-4. With this higher specific thrust, for example, the engine inlet flow may be reduced to yield a decrease in weight.

5.4 Conclusions

The design point program identified thermodynamic trends which were used to explain the results of the off design analysis presented in Chapter 6. Cycle limits, principally maximum T41, caused lower specific thrust when active control was applied to raise operating pressure ratios. The loss in thrust may be attributed to lower exhaust temperatures and pressures per eq 5-2. The fundamental cause for the lower exhaust temperature and potentially lower exhaust pressures is discussed in Appendix A.

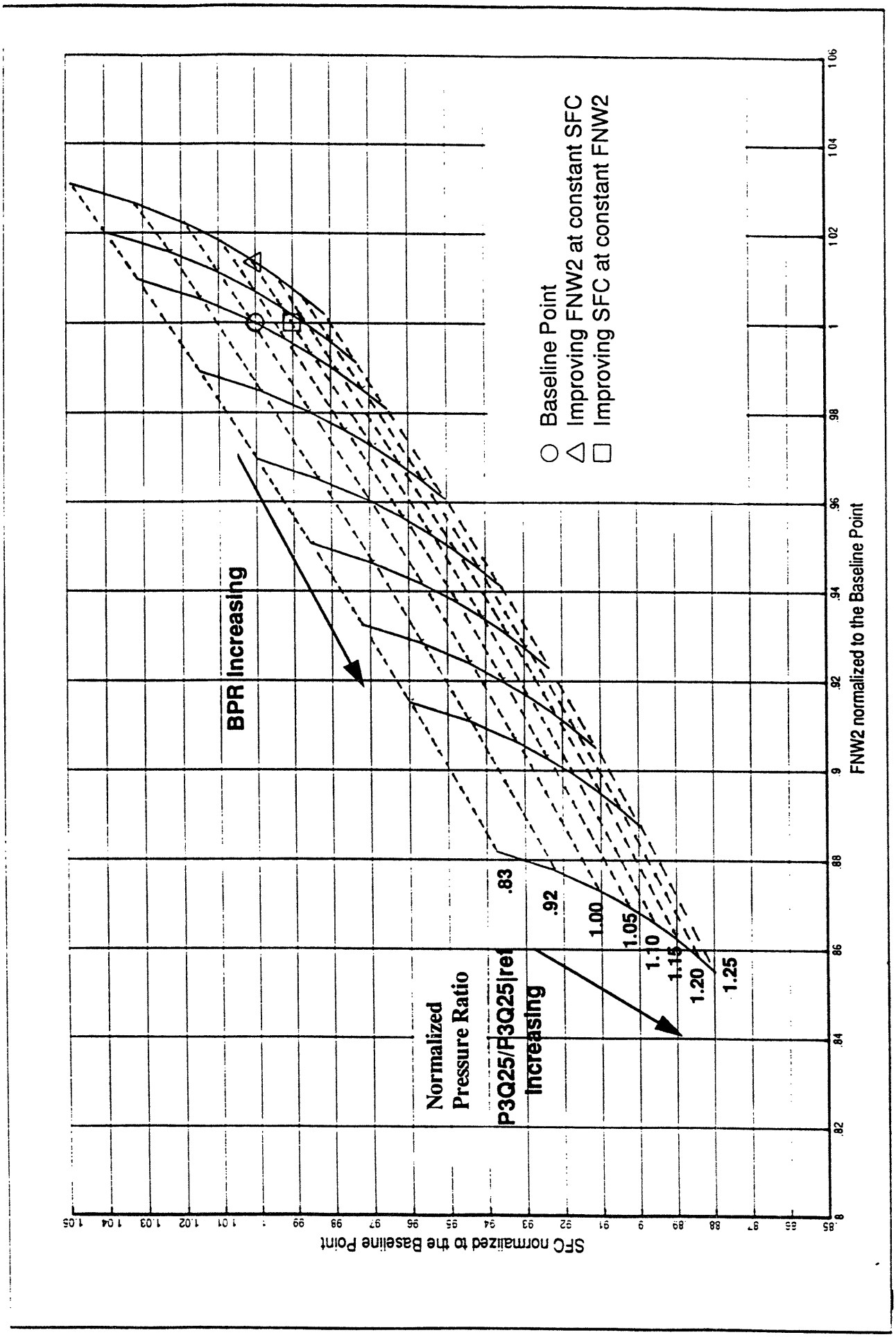

Figure 5-4: Cycle Design Trades: Improved SFC at constant Thrust and Improved Thrust at constant SFC

At high power, an important result is that higher thrust and lower SFC are not feasible without additional cycle changes. Scenarios in which both thrust and SFC improve include:

- Raising T41 which implies improvements in material capability and/or performance trades involving higher turbine cooling flows;
- Lower BPR configurations which allow the same thrust at constant SFC or alternatively the same SFC at constant thrust. A minimum limit on BPR, however, will exist for afterburning operation since bypass flow provides cooling to the afterburner liner. This design trade is further discussed in Chapter 6;
- Increasing inlet flow (W2) in order to compensate for a lower specific thrust (FN/W2). The engine will achieve constant thrust by scaling up the engine size to increase flow. The larger engine size, however, results in a weight penalty.

Chapter 6: Cycle Off Design Analysis: Higher Pressure Ratio Operation

6.1 Introduction

The engine flight envelope is the range of inlet operating conditions within which the engine is designed to operate. Shown in Figure 6-1, the flight envelope is defined in terms of flight Mach number and altitude. Often, the ambient temperature is also included in the definition. Within the envelope, the aircraft application dictates that certain flight conditions take precedence over others. For a commercial aircraft, for example, high altitude subsonic cruise conditions are important to its mission. For military fighters, subsonic cruise and supersonic operation are conditions which are important to the mission.

The design point analysis in the preceding chapter focused on a single, specific flight condition. However, because the cycle must operate throughout the flight envelope, for all practical purposes it always operates "off design". As such, it is appropriate to assess the effects of active control on off design engine performance. A General Electric Aircraft Engines cycle deck containing component performance maps has been used to predict engine performance. This model was discussed in Chapter 3.

An important consequence of assessing off design performance is insight into the effects of cycle limits other than stall margin and T41 discussed earlier. These limits influence and may restrict how additional stall margin may be utilized in the design process. In some cases, these constraints dictate that the benefits of active control can only be implemented if additional, potentially significant, engine redesign is also undertaken. For example, increases to the pressure ratio on the core compressor may be limited by maximum compressor discharge pressure and temperature. These limits are established by the structural integrity capabilities for the given materials; higher pressure and temperature limits would result in cost and/or weight penalties associated with the improved materials. Further, in a turbofan engine, excessively increasing fan pressure ratio may reduce the bypass ratio to levels which provide inadequate cooling flow to the afterburner liner. Hence, by exploring other cycle limits, guidelines will be established which identify additional configuration changes needed to fully realize the benefits of active control.

This chapter outlines how component improvements of actively controlled compressors translate into overall engine system benefits throughout the flight envelope. Further, because of the diverse operational requirements associated with an aircraft mission profile, the performance impact at both high power and low power cruise conditions has been examined. In short, the effect of active stall control on engine performance due to the following factors have been reviewed:

- the effect of using the additional stall margin to operate an existing compressor at higher pressure ratios (discussed in Chapter 6);
- the effect of using the additional stall margin to optimize the variable stator angles to achieve best efficiency (discussed in Chapter 7);
- the effect of increasing the compressor efficiency by improved positioning of the compressor line of peak efficiency (discussed in Chapter 7).

6.2. Figures of Merit

6.2.1 Aircraft Mission Profiles

Two types of engine performance have been assessed. First, the effects on high power performance have been quantified. For military fighter applications, high power, or combat performance, includes maximum nonafterburning operation, or intermediate rated power (IRP), and augmented operation. The effects on combat performance have been quantified in terms of percent changes in engine net thrust (FN) and specific fuel consumption (SFC) at a given flight condition. For commercial applications, high power is indicative of the thrust available at take off conditions.

The second barometer is the impact on aircraft cruise performance. Because the aircraft spends the majority of the mission flight time at cruise conditions, the engine specific fuel consumption is an important measure of performance. From the specific range equation, fuel consumption has a direct relationship to aircraft range. Or, for the same range, better fuel consumption translates into a lower fuel payload and hence a weight reduction.

Specific range equation

(6-1) $SR = [Vk/(FN*SFC)] = [Vk/WFT]$ nautical miles/ lbm

where Vk = aircraft velocity (knots)

FN= net thrust (lbf)

SFC= specific fuel consumption ((lbm/hour)/lbf)

At a given flight condition (Vk=constant), the change in specific range may be expressed as:

(6-2) $\% \Delta SR = [SR|_{final} - SR|_{initial}]/SR|_{initial}$

$= [WFT|_{initial} - WFT|_{final}]/WFT|_{final}$

where $WFT|_{initial}$ = the baseline level of fuel flow

$WFT|_{final}$ = the fuel flow with active control implemented

Important combat and cruise conditions for a military fighter application are superimposed in Figure 6-1. They include (reference 6-1, 6-2):

10K/.4/ 40% IRP thrust: a typical low power loiter condition.

35K/.85/80% IRP thrust: a typical outbound cruise point.

35K/.85/50% IRP thrust: a typical inbound cruise point.

SL/.8/60% IRP thrust

SL/.8/ IRP

30K/.8/IRP

30K/1.5/IRP: supersonic penetration

10K/.9/Max AB: combat maneuvering

20K/.9/Max AB: combat maneuvering

30K/ .8 to 1.6/ (max AB): aircraft acceleration conditions.

SLS operating line: Takeoff, also a typical reference condition since engines most often tested at sea level ambient conditions.

35K/.85 operating line: Cruise

Figure 6-1: Flight Envelope

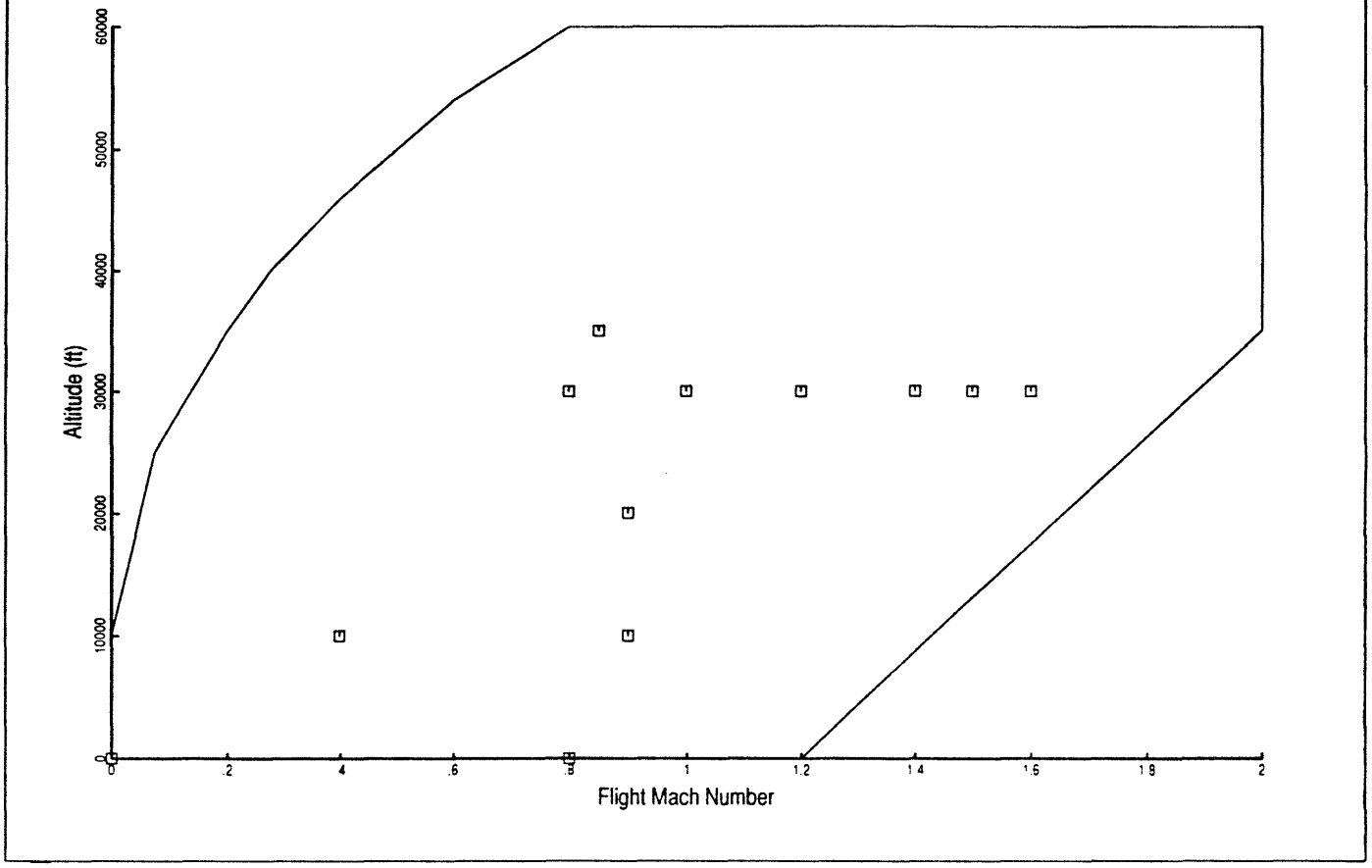

6.2.2 Cycle Limits

The amount of additional stall margin which may be utilized depends on the presence of other cycle limits. Figure 6-2 is a summary of some of the limits which restrict cycle performance. These constraints include:

Fan stall margin: fan stability margin required to prevent stalls based on engine operability requirements;

Core compressor stall margin: compressor stability margin required to prevent stalls based on engine operability requirements;

T41: maximum turbine inlet temperature limit dictated by materials technology, cooling flow, and hardware durability requirements;

T3: maximum compressor discharge temperature limit dictated by materials technology and hardware durability requirements;

P3: maximum compressor discharge pressure limited by mechanical structural integrity requirements;

N2: maximum low pressure spool rotor speed dictated by mechanical stress limitations;

N25: maximum high pressure spool rotor speed dictated by mechanical stress limitations;

A8: minimum and maximum exhaust nozzle area dictated by engine/nacelle installation requirements.

Figure 6-2 Summary of Engine System Design Limits

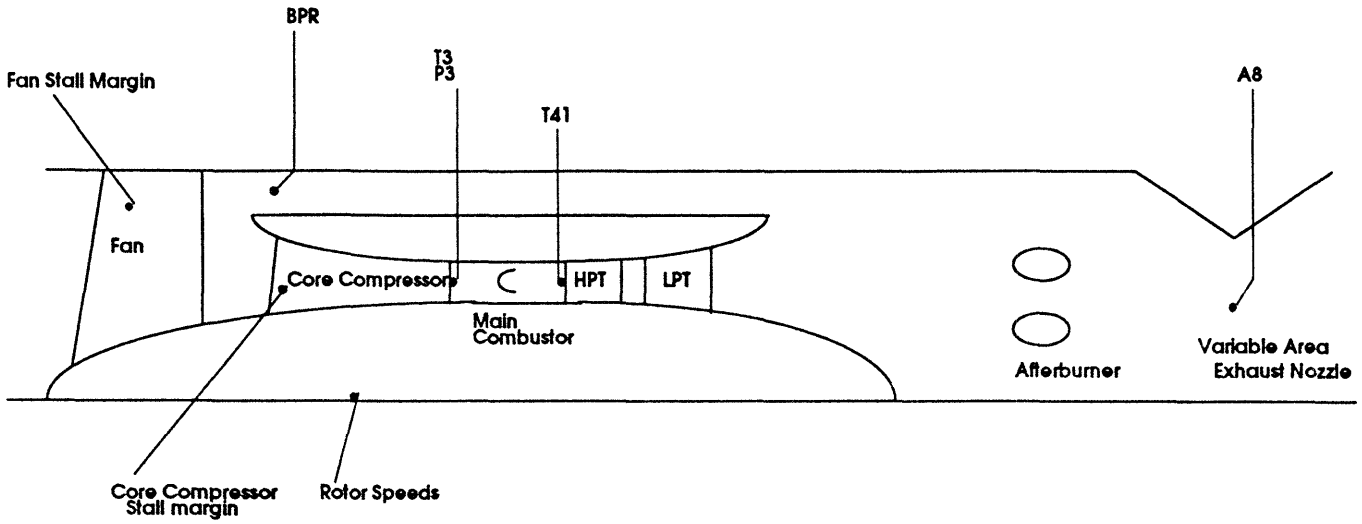

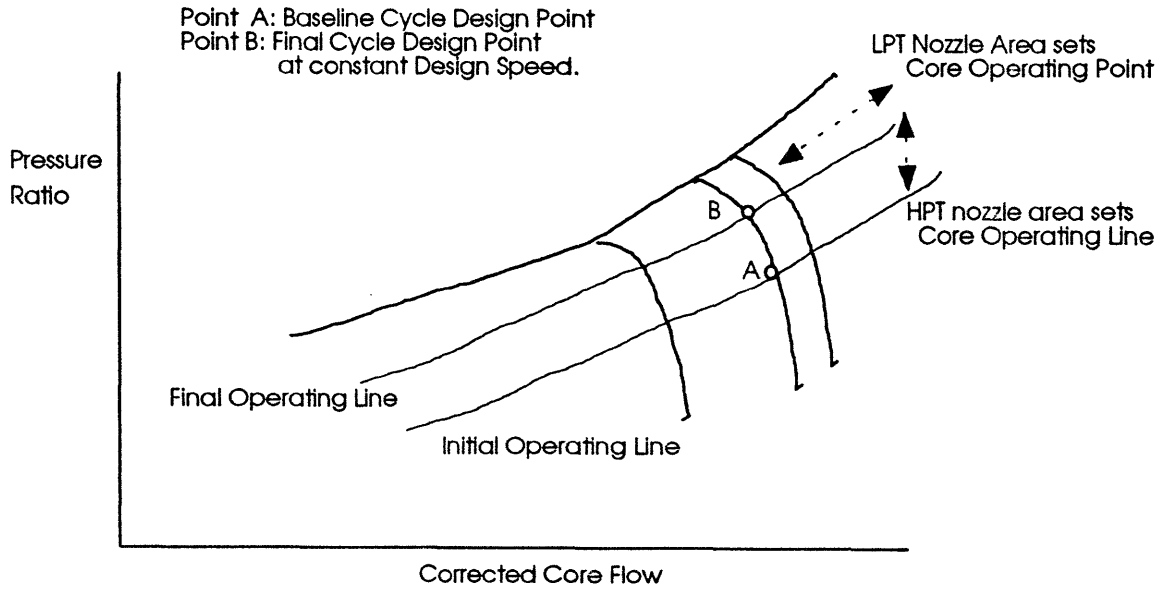

Figure 6-3: Raising HPC Operating Line using HPT and LPT Nozzle Areas

6.3 Method for Achieving Higher Pressure Ratio Operation

To begin with, higher pressure ratio operation was simulated by throttling compressor operation along a constant speed line at constant T41. Using sea level static (SLS) standard day operation as the reference point, the baseline cycle was modified by adjustments to both the HPT and LPT throat areas. Applying the method described below, the core compressor operating line was raised 5% and 20 % above the baseline. These magnitudes were selected to model a range of additional stall margin which ultimately may be provided by active control.

Conceptually, for the core compressor, the decreased HPT nozzle area backpressured the compressor to raise the operating line. To prevent rotor overspeeds, operation along the line was controlled by decreasing the LPT nozzle area until the same speed was achieved at the higher pressure ratio. As shown in Figure 6-3, the HPT nozzle area set the operating line, and the LPT nozzle area defined the operating point along that line. For clarity, any secondary effect of LPT area on compressor operating line has been omitted.

The use of the LPT nozzle area to set the operating line is explained by demonstrating the validity of the following trend: the LPT nozzle area (A49) is reduced to cause compressor pressure ratio (P3Q25) to shift down along its operating line toward the target speed. To a first order, both the HPT and the LPT nozzle areas are assumed choked. For this condition, the corrected flow through each nozzle is a constant:

$$(6\text{-}3)\quad W41R = \frac{W41\ \sqrt{T41}}{P41\ A41} = \text{constant1}$$

$$(6\text{-}4)\quad W49R = \frac{W49\ \sqrt{T49}}{P49\ A49} = \text{constant2}$$

where W41 is the physical flow through the HPT.
W49 is the physical flow through the LPT; assumed equal to the HPT flow.

T41 is the HPT inlet temperature.

T49 is the LPT inlet temperature; approximately equal to the HPT exit temperature.

P41 is the HPT inlet pressure.

P49 is the LPT inlet pressure; approximately equal to the HPT exit pressure.

A41 is the HPT nozzle area.

A49 is the LPT nozzle area.

Combining equations 6-3 and 6-4 and expressing the HPT temperature ratio in terms of its pressure ratio and polytropic efficiency (η_p) yields:

$$(6\text{-}5) \qquad T41/T49 = \{P41/P49\}^{[\eta_p(\gamma-1)/\gamma]}$$

$$(6\text{-}6) \qquad W41R/W49R = (A49/A41)\,(P49/P41)^{[1-\eta_p(\gamma-1)/(2\gamma)]}$$

$$= \text{constant3}$$

For the sample case in which A49 decreases, equation 6-6 dictates that P49/P41 must increase towards unity. This trend implies that the expansion ratio across the turbine decreases. As a result, the lower available turbine work requires lower compressor work. Since the compressor inlet pressure is approximately unaffected by turbine nozzle area adjustments, the compressor pressure ratio must decrease. In summary, as initially stated, reducing the LPT nozzle area moves the compressor down its operating line toward lower pressure ratios and lower rotor speeds.

Increased fan pressure ratios were achieved in a similar manner. The variable exhaust nozzle area was the mechanism which backpressured the fan and raised the fan operating line. Operation at the desired speed was directly maintained by the engine fuel control. As with the core, 5% and 20 % increases in fan operating line position were analyzed.

6.4 Results

Higher pressure ratio operation resulted in both performance benefits and penalties. The impact of the increased pressure rise depended on whether the fan or compressor was actively controlled. Further, the impact was a function of engine power setting and flight condition. In summary,

- At high power, higher core compressor pressure ratios resulted in lower IRP thrust. The high pressure turbine inlet temperature (T41) limit and the compressor discharge temperature limit (T3) were the key factors causing performance penalties. However, for augmented operation, judiciously scheduling of the afterburning fuel flow offset the negative impact of higher pressure ratios on thrust. In fact, during certain conditions thrust increased relative to the baseline.
- For both IRP and augmented operation, higher fan pressure ratios resulted in significantly higher thrust for fan stall margin limited conditions. The benefit was achieved because the stall margin provided by active control permitted the cycle to operate at higher T41 and hence higher exhaust temperatures. However, for the engine configuration studied, the thrust improvements reached a maximum when fan stall margin was no longer the limiting constraint. The factors which became limiting include afterburner cooling flow requirements and exhaust nozzle area geometry limitations.
- At part power, cruise conditions, higher core compressor pressure ratios resulted in significant specific fuel consumption improvements. Unlike high power operation, the benefit resulted because the cycle was well below the T41 or T3 limits.

6.4.1 Higher pressure ratio operation: core compressor

The core compressor operating line was raised 5% and 20%, and cycle data was generated for IRP operation over a range of altitudes and flight Mach numbers. Figure 6-4 illustrates the T41 profile which resulted. In the figure, T41 normalized to a reference value is plotted as a function of fan inlet temperature (T2) normalized to a reference value. The figure demonstrates that for the cycle used in this study, different cycle limits caused three distinct regions of operation: first, at low T2 conditions, fan stall margin was limiting (region 1, Figure 6-4); second, at moderate T2 conditions, turbine inlet temperature was limiting (region 2, Figure 6-4); third, at high T2 conditions, compressor discharge temperature was limiting (region 3, Figure 6-4). Additional limits such as maximum physical rotor speeds would have added additional regions to the plot.

The presence of these regions occur when the cycle is optimized for performance throughout the flight envelope. Specifically, the variable exhaust nozzle is the mechanism used to maximize thrust for a given inlet flow. As the exhaust nozzle area is reduced, the fan pressure ratio increases. As a result, downstream cycle pressures and temperatures (e.g. T3 and T41) also increase. Whether the temperatures or fan stall margin becomes the limiting constraint depends on the engine inlet temperature.

In region 1, for example, the low T2 condition resulted in the cycle temperatures being well below their respective limits. Hence, the fan stall limit was reached first. As shown in Figure 6-4, in region 1, T41 remained relatively unaffected by changes in core operating position. The small variation shown was due to changes in core compressor efficiency as the operating line was raised. The different efficiency resulted in a slightly different T41 for the same fan stall margin.

Figure 6-4: Turbine Temperature Profile vs Inlet Temperature: Higher Core Compressor Pressure Ratios

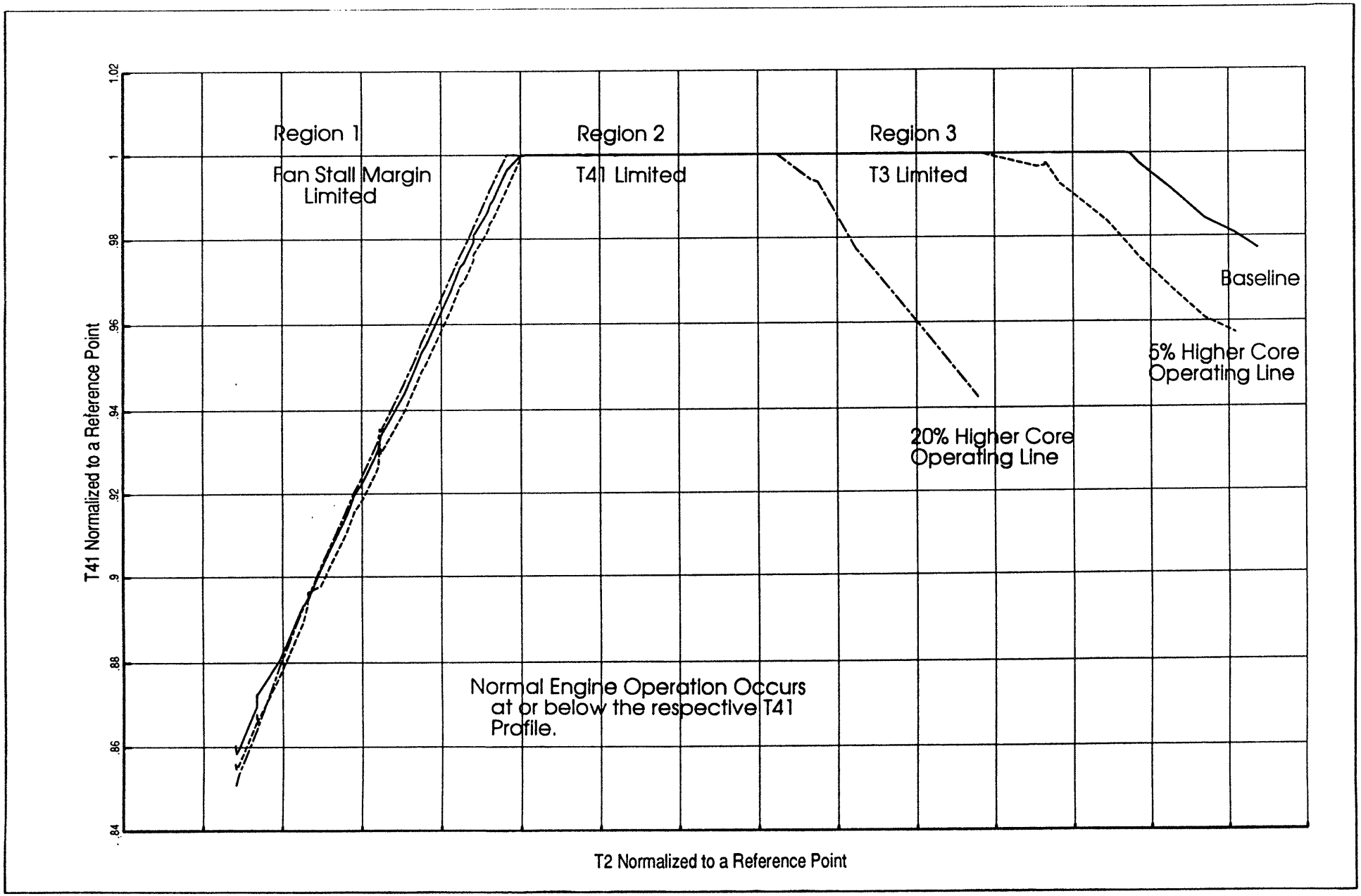

The second and third regions were limited by the turbine inlet temperature (T41) and the compressor discharge temperature (T3), respectively. Unlike the first region, the higher engine inlet temperature resulted in these temperature limits being reached before the fan stall threshold. Further, as shown in Figure 6-4, the T3 limited region was reached at lower engine inlet temperature as the core compressor operating line was raised. Consequently, the engine operated under this constraint over a larger portion of the flight envelope.

The IRP Effect of 5% Increases in Core Operating Line Position

For the 5% increase in core operating line, Figure 6-5 is a contour plot illustrating the effect on IRP thrust throughout the flight envelope. At IRP where the cycle operates at the T41 limit (region 2, Figure 6-4), the off design cycle results are consistent with those obtained from the design point analysis (Chapter 5): if the reference operating line is scaled 5%, reduction in specific fuel consumption ranged from -.5% to -1.4% while net thrust reduction ranged from 0.0 to -.5%. The rationale for these trends are similar to that discussed in Chapter 5 . At constant T41, the decrease in exhaust temperature (T8) offsets the increase, if any, of exhaust pressure (P8) when compressor pressure ratio is increased.

Figure 6-5: Thrust Impact at IRP due to Raising Core Operating Line 5%

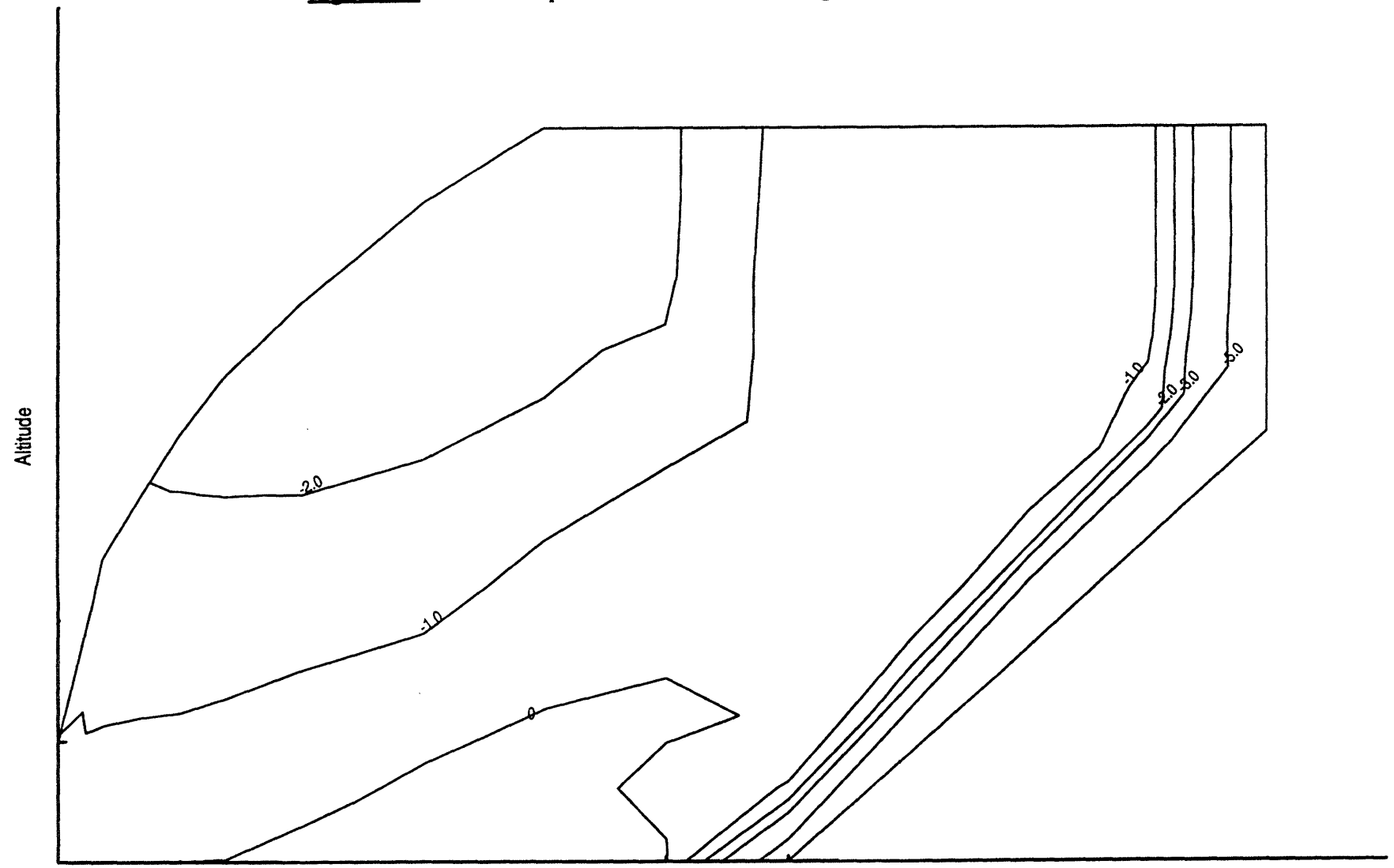

In region 1 (Figure 6-4) where the cycle operates under fan stall margin limited conditions, IRP thrust decreases ranged from -1.5% to -2.5% and the SFC improvement ranged from -.82% to -1.41%. The magnitude of the thrust losses were more severe than in region 2 for two reasons:

- Similar to region 2, the cycle operated at approximately constant T41; hence, the higher pressure ratio in the compressor caused a larger enthalpy drop across the turbine. As a result, the LPT exit temperature decreased based on the arguments presented in Appendix A (Figure 6-6A). This trend is also consistent with observations made during the design point analysis (Chapter 5).

- Unlike region 2, however, as the cycle rebalanced in region 1, an increase in bypass ratio accompanied the higher compressor pressure ratios. Thus, since mass flow through the turbines decreased, the specific enthalpy decreased even more to achieve the specified total enthalpy change. As a result of the lower specific enthalpy, turbine exhaust temperature decreased more in region 1 than in region 2 (Figure 6-6A). Figure 6-6B illustrates the change in bypass ratio for the different operating regions.

In addition to thrust losses when at constant T41 (regions 1 and 2), more significant performance degradations occurred at high Mach flight conditions where T41 was cutback to hold T3 (region 3, Figure 6-4). Increases in core pressure ratio caused the cycle to reach the T3 limit at lower T2 conditions and resulted in more severe reductions in T41. As one would expect, since thrust decreased at constant T41, thrust decreased more significantly when the T41 level was reduced. Raising the core operating line to consume 5% stall margin, for example, reduced thrust between -2.0% and -7.7% depending on the magnitude of the T41 cutback. SFC did improve by -.1% to -1.4%.

Figure 6-6A: Turbine Discharge Temperature Profile: T56 vs T2 for a 5% Higher Core Operating Line at IRP

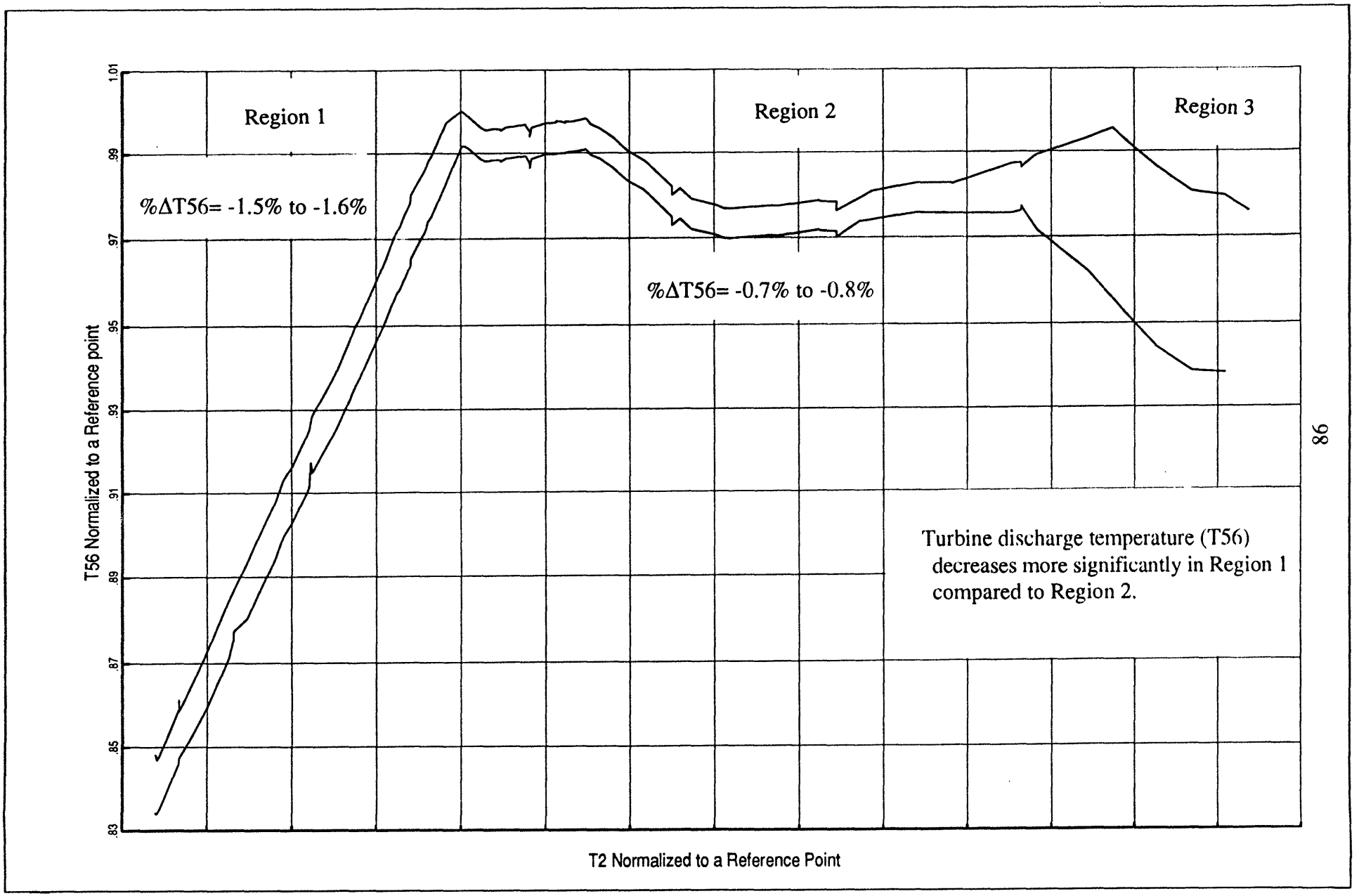

Figure 6-6B: Turbine Discharge Temperature Profile: BPR vs T2 for a 5% Higher Core Operating Line at IRP

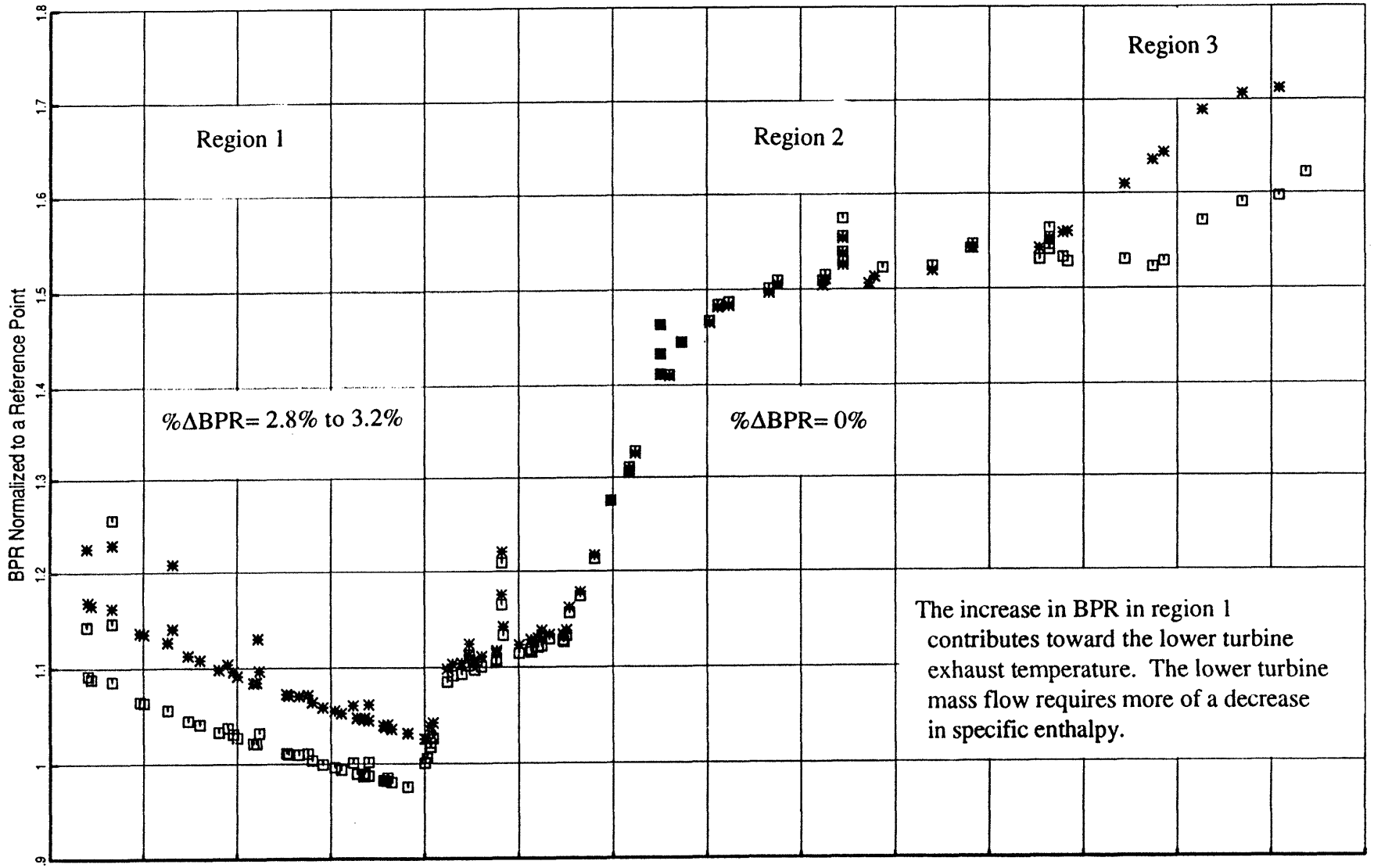

Figure 6-7 illustrates the extent to which the flight envelope is affected by the T3 limit. Note that for a five percent operating line increase, only the extreme right hand side of the envelope was affected. Although the design compromises between higher pressure ratio operation and high T2 operation depends on the specific application, the preceding results qualitatively indicate that configurations emphasizing SFC over high Mach number operation are potentially attractive candidates for using active control to raise the core operating line. For the military mission, for example, none of the key mission points described in section 6.2.1 occur in the T3 limited region for a 5% increase in core operating line. Hence, the thrust penalty during T3 limited operation is acceptable for a 5% increase in core pressure ratio.

The Afterburning Effect of a 5% Increase in Core Operating Line Position

In addition to the effect on IRP performance, a 5% higher core operating line affected afterburning performance. Similar to IRP, the higher core pressure ratio caused a decrease in the gas generator discharge temperature (T56). However, unlike IRP, the augmentor may increase fuel flow to minimize or negate any decrease in the exhaust temperature caused by the higher pressure ratio operation.

If the cycle is designed to run to the same total fuel flow, for example, during higher pressure ratio operation, fuel not burned in the main combustor is burned in the augmentor. For a 5% increase in core operating line, the following occurred:

- In region 1, the decrease in thrust ranged from -0.6% to -1.55%. This performance loss was less severe than IRP operation because of the increase in afterburner enthalpy rise.
- In region 2, the thrust increase ranged from 0.1% to 0.8%.
- In region 3, the thrust decreased from -1.2% to -4.3%. Again, the loss was less severe than at IRP.

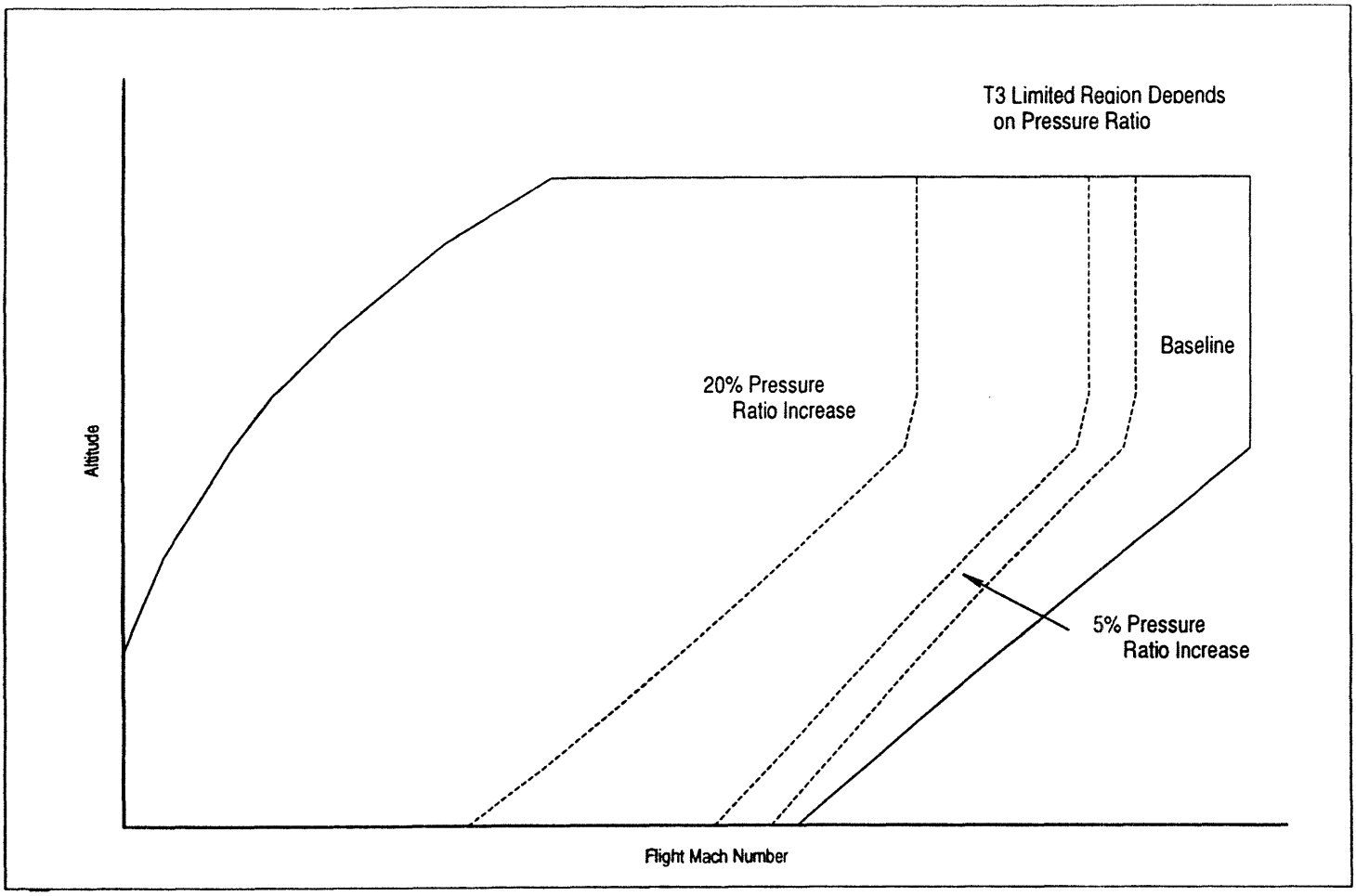

Figure 6-7: T3 Limited Operation Covers a Larger Portion of the Flight Envelope as Core Pressure Ratio is Raised

The Effect of a 20% Increase in Operating Line Position

A 20% higher core operating line results in more significant thrust degradations. The worse case point (sea level/ 1.0 MN) resulted in thrust decreasing by 23% while SFC increased by 3.9%. The loss in thrust was caused by significant reductions in T41. The degradation in SFC was due to the lower cycle efficiency (% $\Delta\eta$=-3.8%).

Unlike the 5% increase in operating line, the 20% operating line increase significantly affected the operating envelope (Figure 6-7). The key mission points which were affected include SL/.8/IRP; 30K/1.5/IRP; 10K/.9/MAX AB; and 30K/1.35 to 1.6/ MAX AB. Because the T3 limited region consumes such a large portion of the flight envelope, a 20% pressure ratio increase would be cause unacceptable penalties for the fighter aircraft application. Better use of the additional 20% stall margin that is available should be considered.

The magnitude of the performance degradations for a 20% operating line increase indicates that the engine configuration studied was not designed for such a high compressor pressure ratio. An additional consequence of maintaining the T3 limit at high T2 conditions is choking of the core stream duct at the matching plane; i.e., the duct is undersized and cannot maintain subsonic flow. Choked flow at this location is not desirable for several reasons. First, the high Mach number entering the afterburner would prevent light off. Second, higher duct pressure losses would result.

The Effect of Increasing the Core Operating Line on Part Power Cruise Performance

At part power conditions, the engine was able to provide the same level of thrust at lower levels of SFC. The SFC benefit was achieved without the thrust penalty because the engine was not T41 or T3 limited at part power. As a result, the pilot could set the throttle to increase inlet flow to achieve the desired thrust level. The thrust otherwise lost

due to running to a higher pressure ratio was offset by running to a higher corrected inlet flow (W2R).

Figure 6-8 shows a SLS operating line from flight idle (FI) power to IRP. The plot compares the baseline case against the 5% higher compressor operating line. For typical cruise conditions, the engine operates between 50% and 80% of IRP thrust. At 80% of the reference IRP thrust, SFC decreased by -1.13% while W2R increased by .57%; at 50% thrust, SFC decreased by -1.26% and W2R increased by .58% (see Table 6-1).

Besides the improvement in SFC, an additional benefit is gained by increasing the inlet flow. Although the engine net thrust is constant, the aircraft installed net thrust will increase due to a reduction in the spillage drag. The higher inlet flow approaches the design flow of the inlet; hence, less spillage drag would result. This increase in installed thrust translates into further improvements in installed SFC by an equal percentage.

Figure 6-9 shows a 35,000 ft/.85 MN operating line. As summarized in Table 6-1, a decreases in SFC of -.74% and -.84% were achieved at 50% thrust and at 80% thrust, respectively. These fuel consumption benefits may be interpreted as improved aircraft specific range. With the improved specific range (eq 6-1A), at 35,000ft/ .85 MN, the aircraft can achieve either:

- Increased range for the same fuel weight and payload weight. Although other flight conditions besides altitude cruise comprise the full aircraft mission (such as take off, climb, descent, etc.), the majority of the flight time is spent at cruise. Hence, up to .73% -.84% increased range would be expected. For an initial range of 1000 nautical miles, for example, an increase by 7 to 8 nautical miles would be achieved.
- Decreased aircraft takeoff weight (by -.73% to -.84% of the fuel weight) for the same range and payload weight.
- Increased payload capacity for the same range and aircraft takeoff weight.

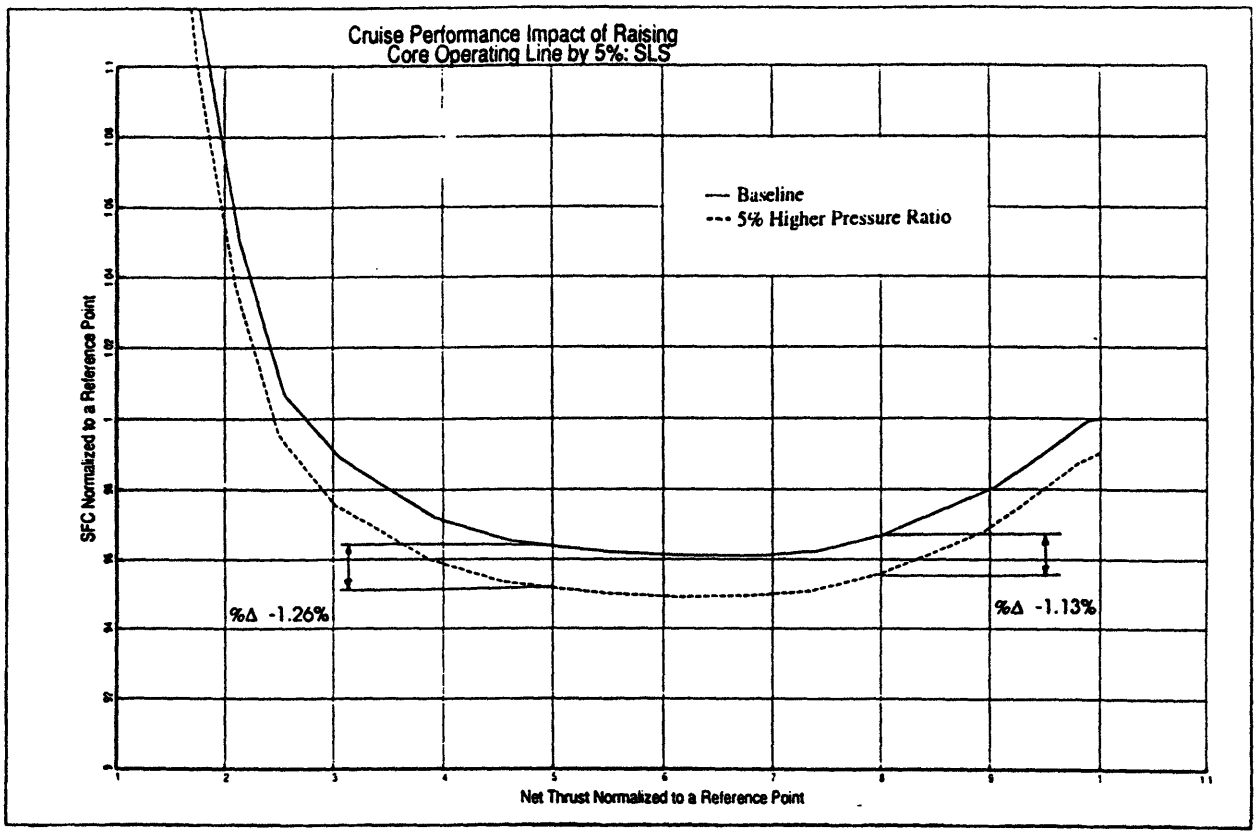

Figure 6-8: Raising Core Pressure Ratio by 5%: Part Power Benefit at SLS

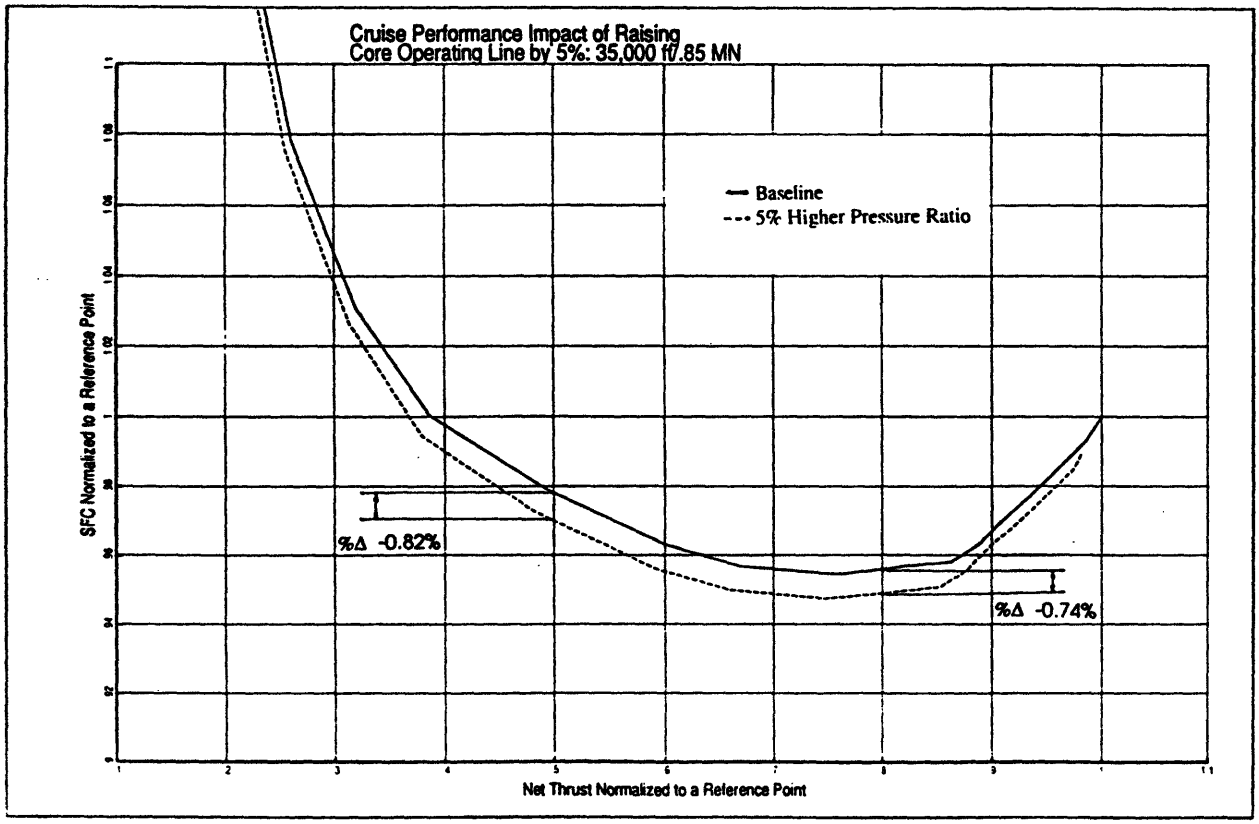

Figure 6-9: Raising Core Pressure Ratio by 5%: Part Power Benefit at 35,000 ft/ .85 MN

Table 6-1: Part Power Performance Improvements for a 5% Higher Core Compressor Operating Line

	50% Thrust			80% Thrust		
Condition	%ΔSFC	%ΔW2R	%ΔSR	%ΔSFC	%ΔW2R	%ΔSR
SLS	-1.26%	0.58%	1.27%	-1.13%	0.57%	1.13%
35K/.85	-.82%	0.71%	0.84%	-.74%	0.67%	0.73%

6.4.2 Higher pressure ratio operation: Fan

Whereas raising core pressure ratio negatively impacts thrust at high T2 conditions, raising fan pressure ratio at low T2 conditions offered significant benefits. At the low T2 conditions (region 1, Figure 6-10), the additional stall margin provided by active control allowed further increases in fan operating line by closing the variable exhaust nozzle. The result was the cycle reaching its fan stall margin limit at higher levels of T41. Following the arguments discussed earlier, the higher T41 contributed toward a higher exhaust temperature (T8) and pressure (P8) which resulted in more gross thrust. The change in IRP exhaust temperature (T8) as fan pressure ratio is increased in the low T2 region is shown in Figure 6-11.

The region in the flight envelope where a benefit was obtained is shown in Figure 6-12. This is consistent with the results of the HIDEC program (reference 2-13) and the results demonstrated by Seymour (reference 2-22). The extent of this region will vary from application to application depending on the inlet temperature at which the engine transitions from fan stall limited operation (region 1, Figure 6-10) to T41 limited operation (region 2, Figure 6-10). In addition, recall that the performance benefits of the HIDEC program required the absence of inlet distortion whereas no such restriction is required to achieve the active control benefit.

Figure 6-10: Raising Fan Pressure Ratio: T41 vs T2 Profile at IRP

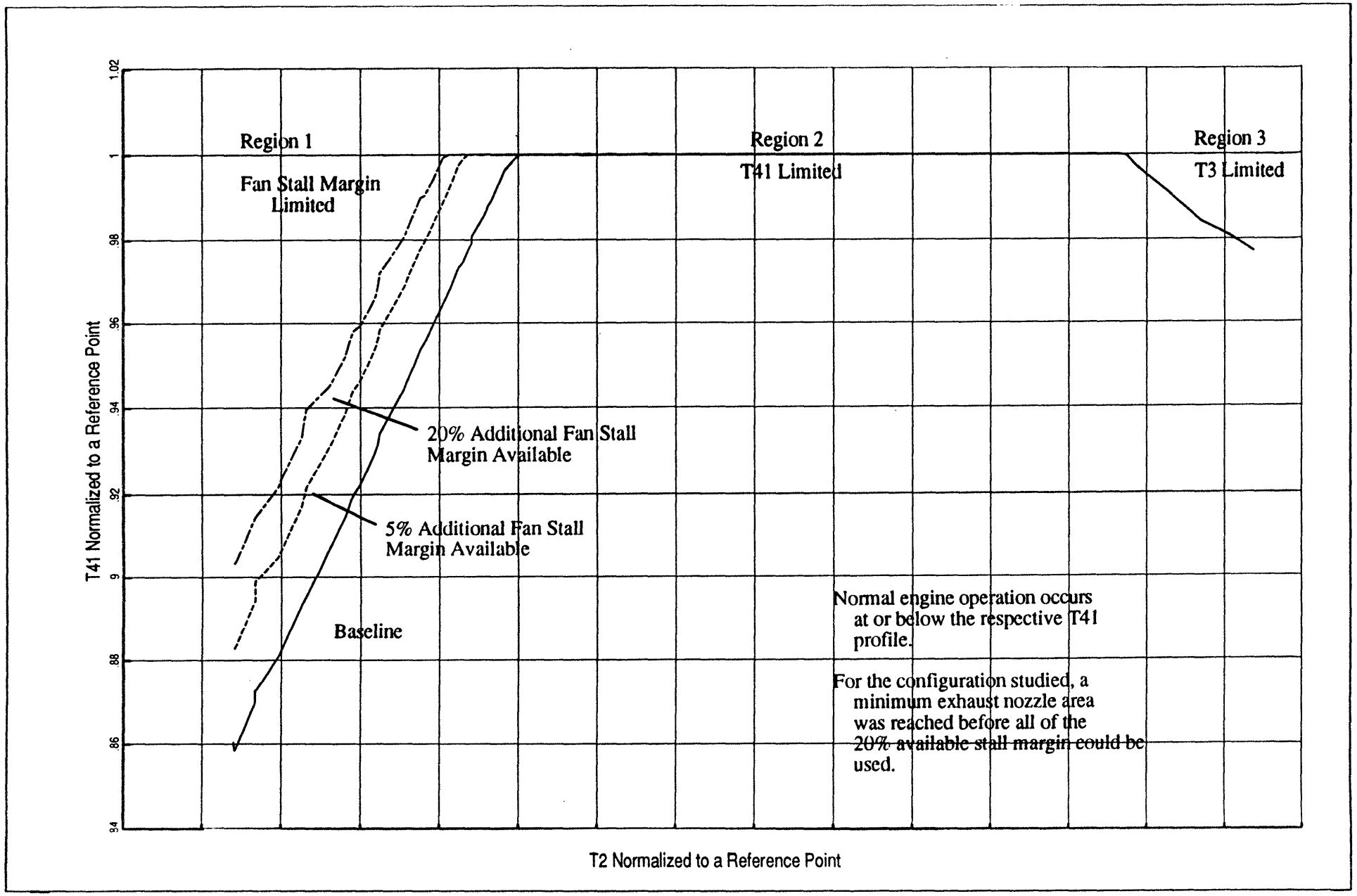

Figure 6-11: Raising Fan Pressure Ratio by 5%: Change in Exhaust Temperature

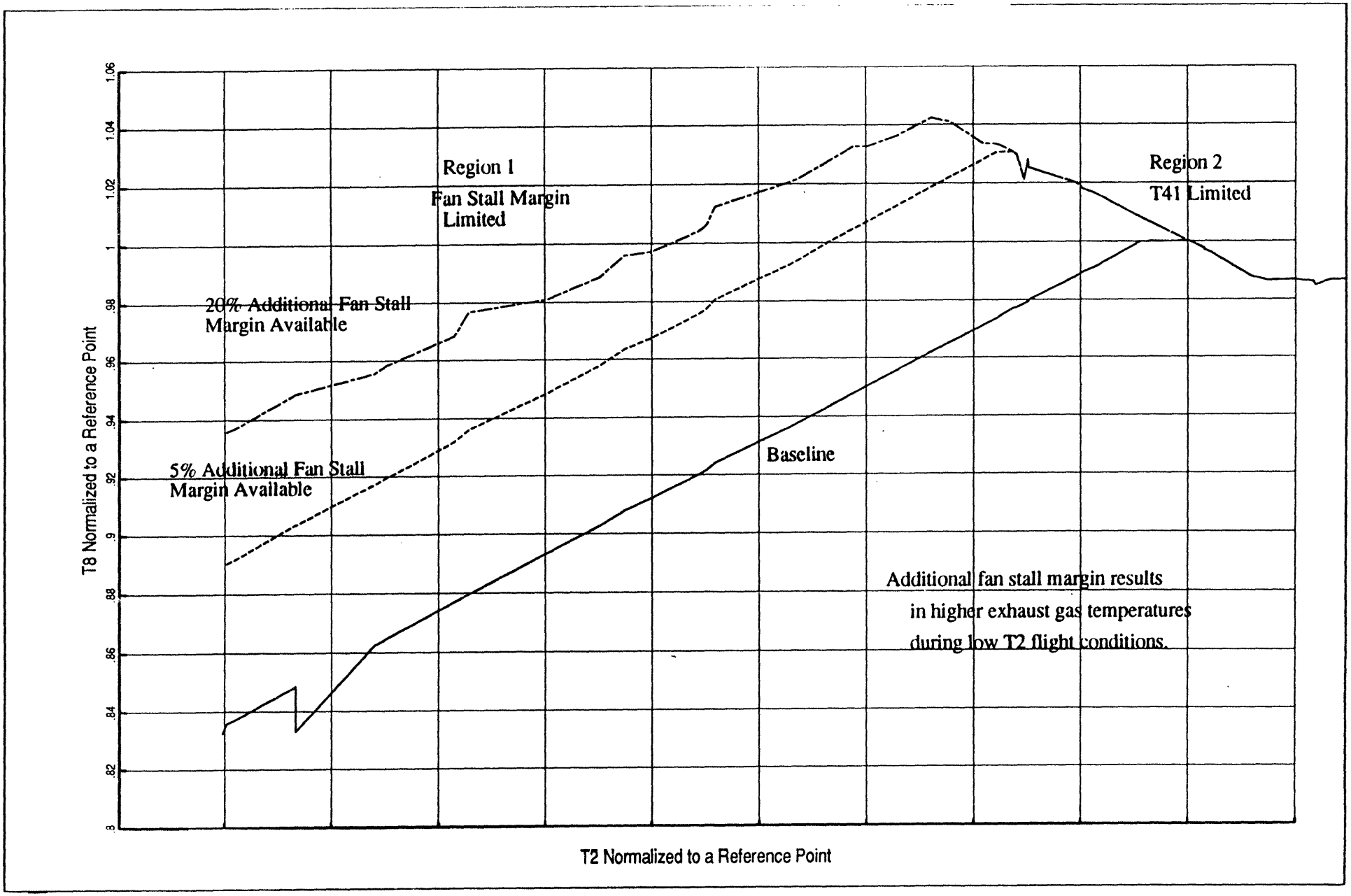

In region 2 and 3 (Figure 6-10) where the engine is either T41 or T3 limited, the additional fan stall margin cannot be traded to improve performance. Any increases in fan pressure ratio would require reductions in inlet flow in order to hold T41. Since the baseline cycle's combination of inlet flow and fan pressure ratio already optimized thrust (per eq. 5-4), no improvement potential exists.

The Effect of Higher Fan Operating Lines on High Power Performance

As fan operating line is raised in region 1 (Figure 6-10), the engine provides both higher IRP and afterburning thrust. Figures 6-12 and 6-13 illustrate the IRP thrust increases throughout the envelope for potential fan operating line increases of 5% and 20% respectively. Consuming an additional 5% fan stall margin resulted in thrust increases ranging from 0.0 (high T2, regions 2 and 3) to 8.0% (41,400 ft/.4 MN). Specific fuel consumption increases ranged from 0.0% (high T2) to 2.8% (16,000 ft/0.0 MN).

The 20% additional stall margin provided by active control allowed increases in thrust between 0.0% (high T2) and 12.5% (36,000ft/.4 MN). The degradation in fuel consumption ranged from 0.0% to 4.7% (35,000 ft/.2 MN). However, at IRP, the configuration studied could not utilize all of the available stall margin. Instead, the cycle became limited by the minimum exhaust nozzle area. If this limit could be avoided, however, such as during the preliminary design phase of the engine, higher thrust increases could be realized.

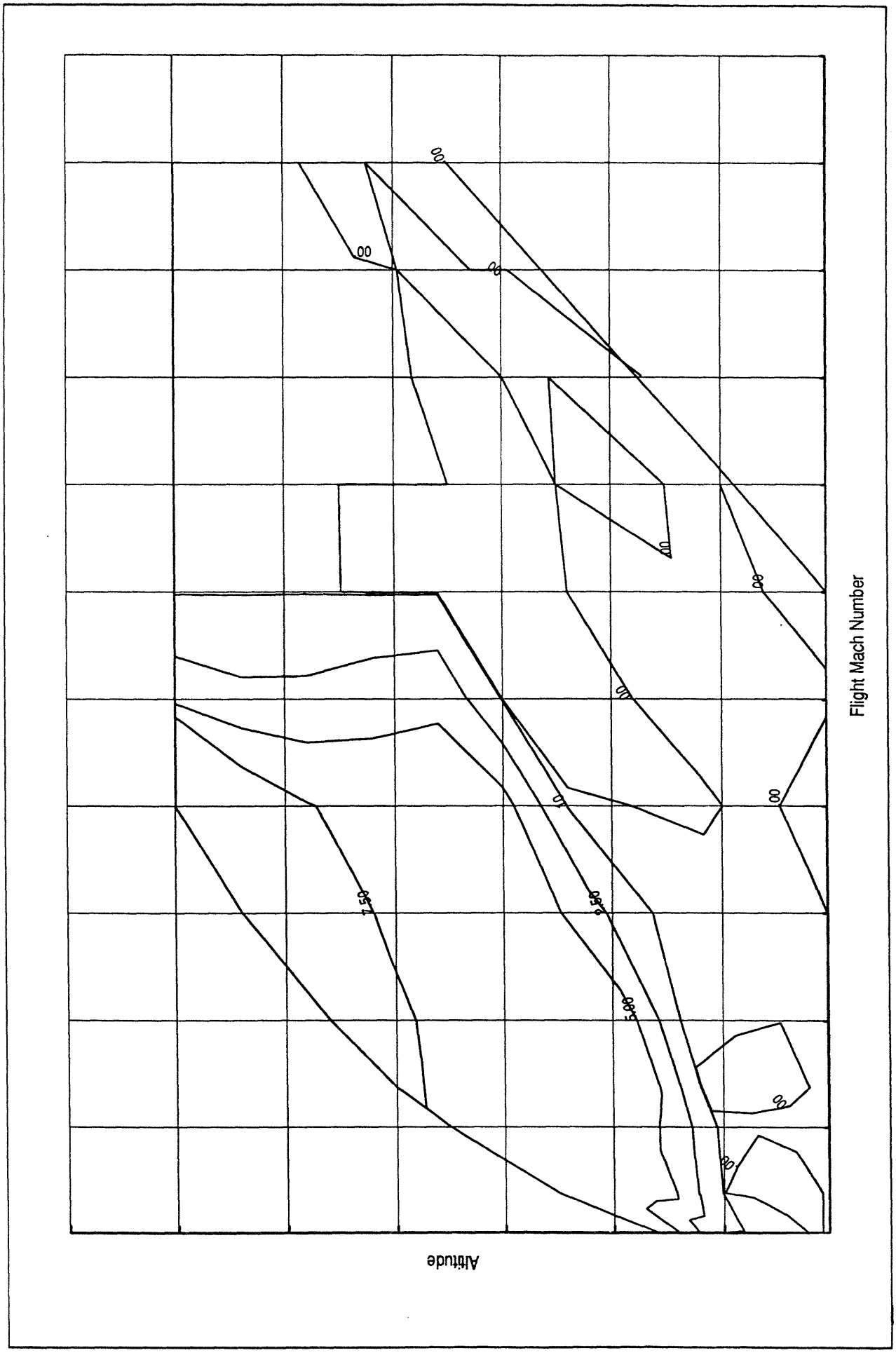

Figure 6-12: Raising Fan Pressure Ratio by 5%: Thrust Contour Plot

Figure 6-13: Raising Fan Pressure Ratio by 20%: Thrust Contour Plot

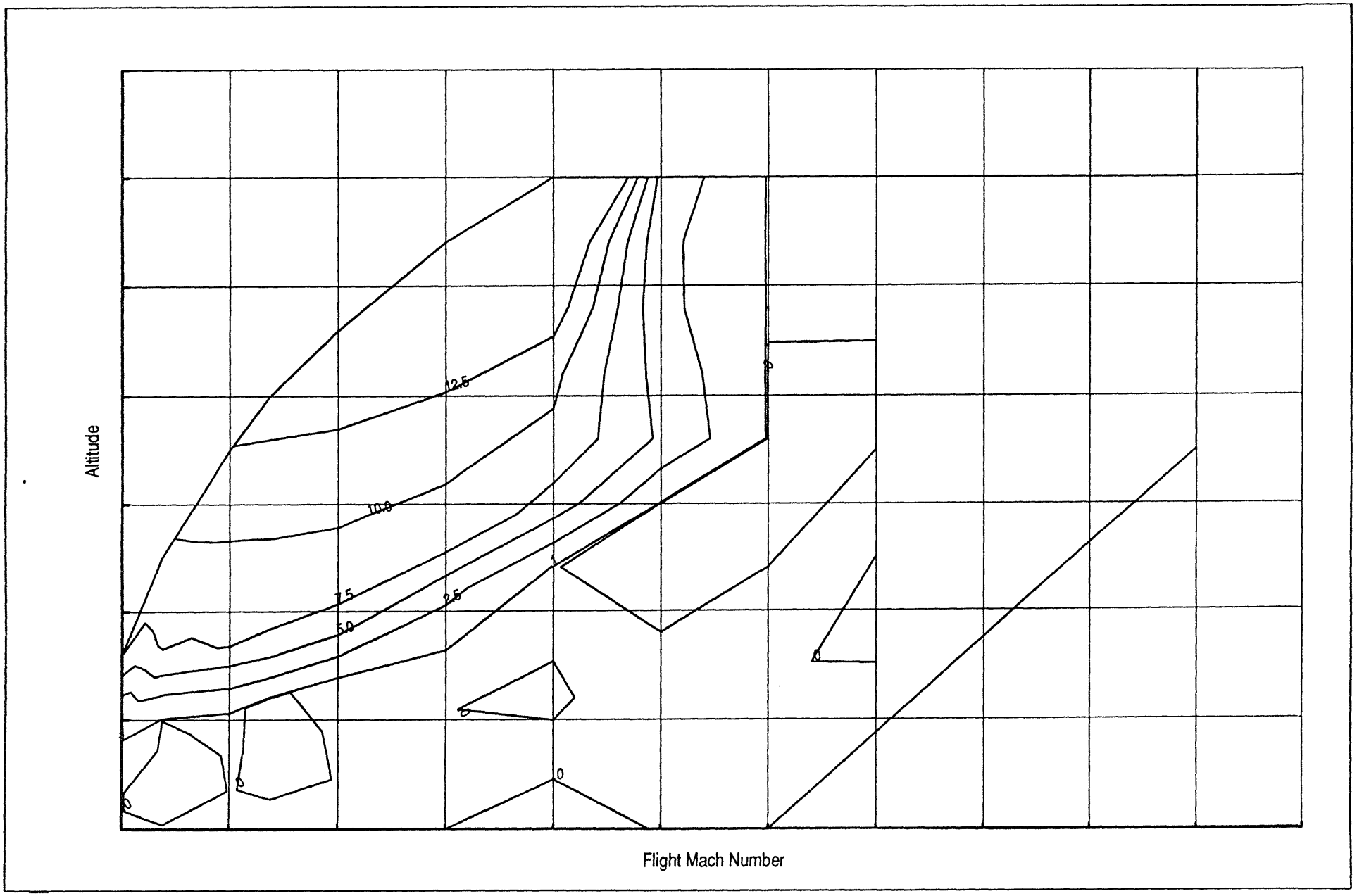

In addition to the stall margin and temperature limits which restricted IRP operation, afterburner operation requires other design challenges. Adequate cooling of the afterburner hardware is required. For the engine configuration studied, a minimum bypass ratio constraint limited low T2 flight conditions (region 1, Figure 6-10).

This limit became important in the low T2 region as fan operating line was throttled higher because BPR decreased as exhaust nozzle area was reduced. For the configuration studied, minimum BPR became the limiting constraint after the fan operating line was raised to consume approximately 5% stall margin. Any additional stall margin available through active control above 5% could not be utilized due to the BPR constraint. Figure 6-14 is a T41 vs T2 plot for 5% and 20% available stall margin. Note that the change in T41 for the 20% case results in essentially the same temperature as the 5% case. Figure 6-15 shows an envelope of the thrust increase during afterburning operation. The region which becomes BPR limiting is highlighted in Figure 6-16. The maximum thrust increase was 5.4% (36,000 ft/ .275 MN).

The minimum BPR constraint became limiting for the engine configuration studied. However, engines with higher design bypass ratios would be able to use more of the available stall margin and improve thrust by a greater amount.

Figure 6-14: Raising Fan pressure Ratio: T41 vs T2 profile during Afterburning Operation (with BPR limit)

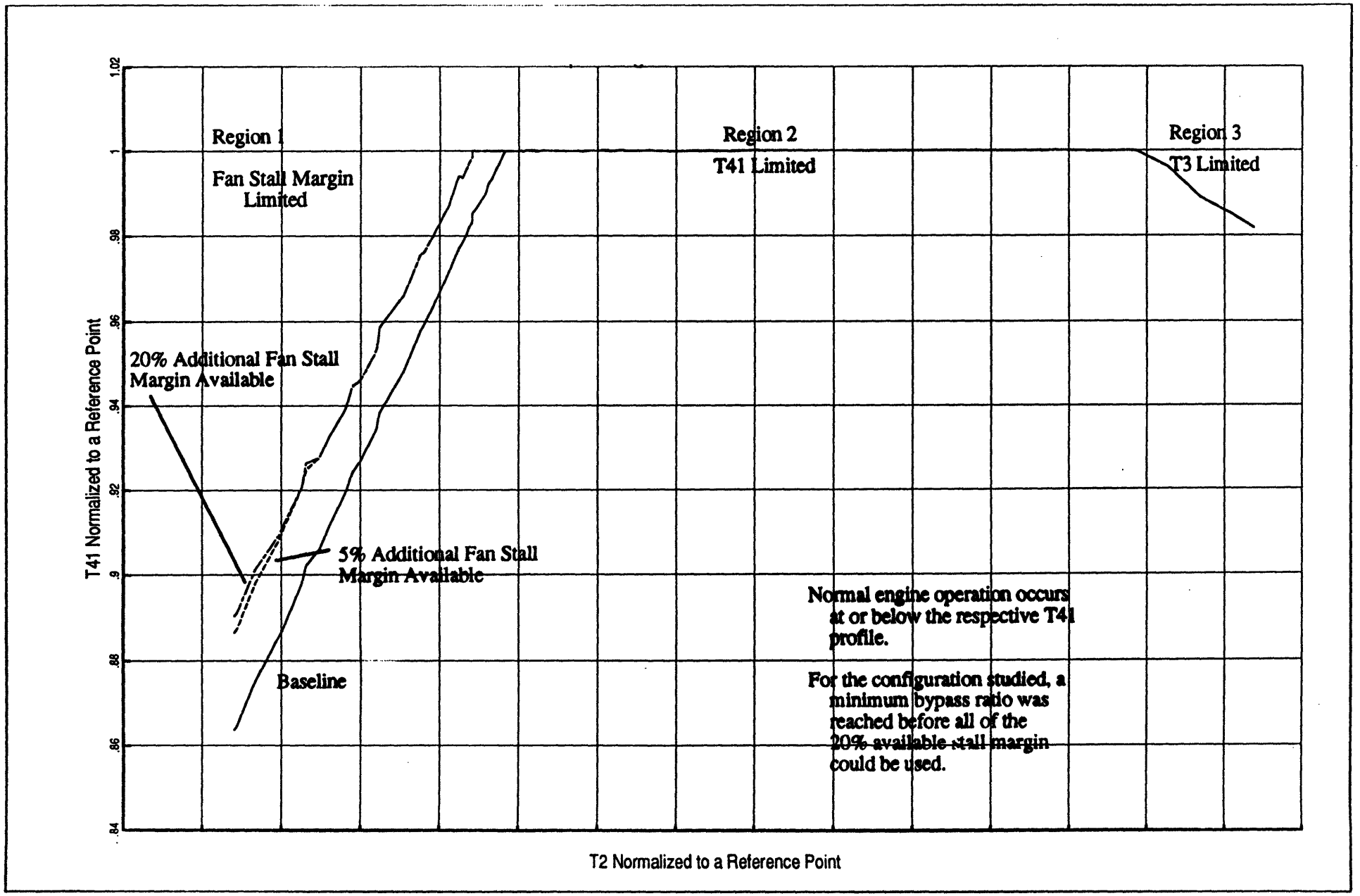

Figure 6-15: Raising Fan Pressure Ratio: Thrust Contour Plot with the Region that is BPR Limiting

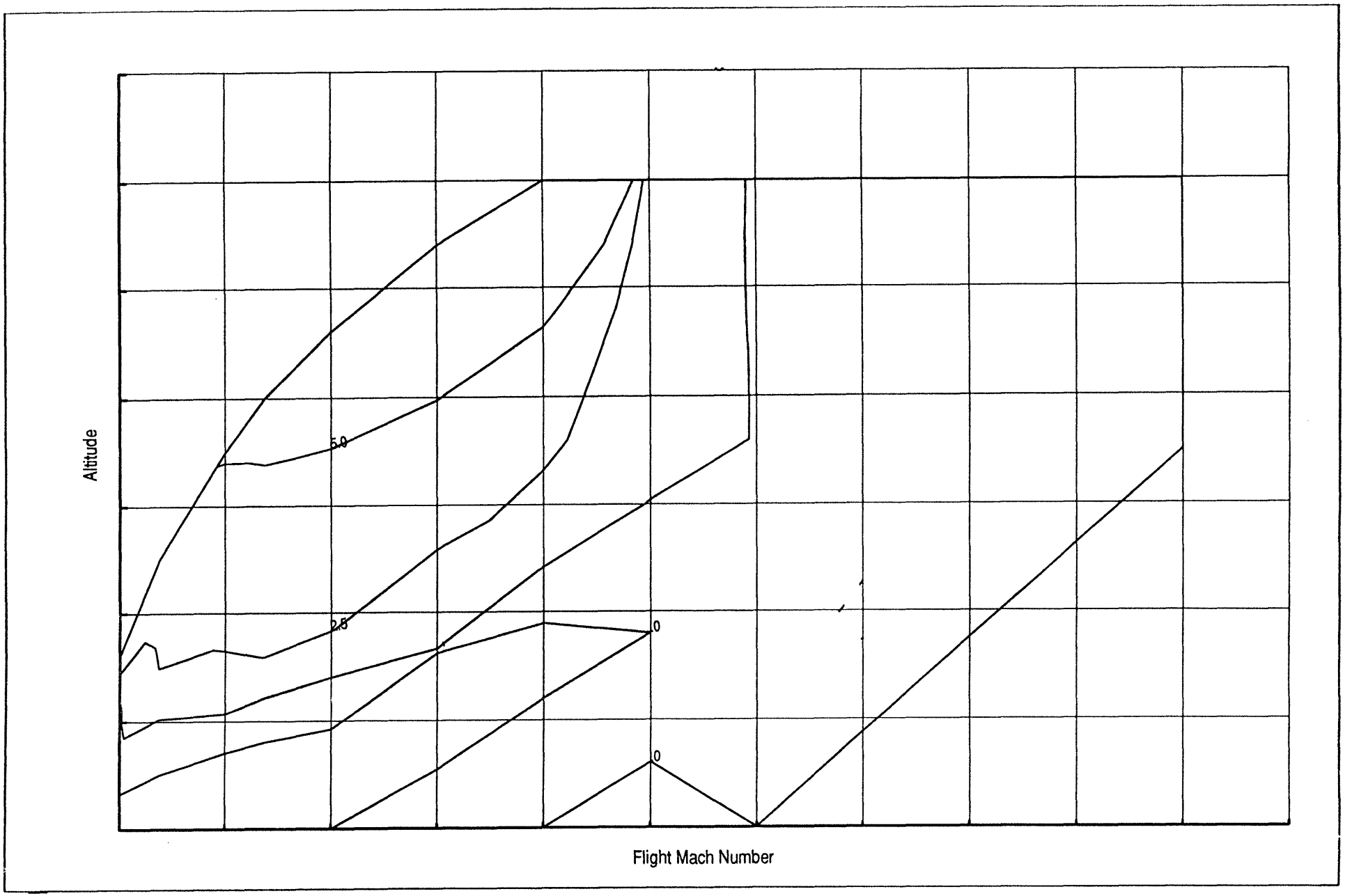

Figure 6-16: Region of Envelope in which Minimum BPR Eventually Supersedes Minimum Fan Stall Margin as the Limiting Cycle Constraint.

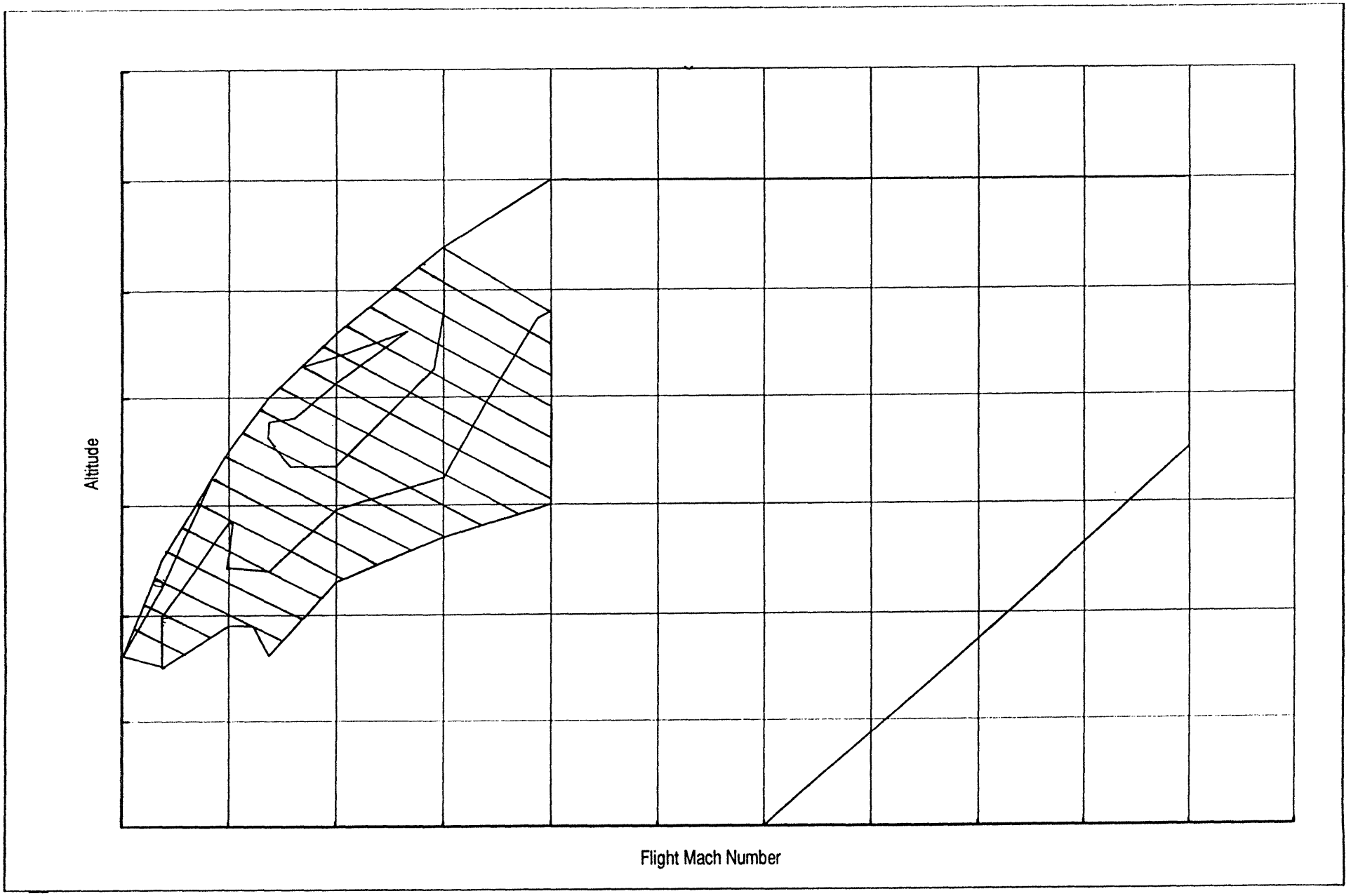

The Effect on Key Mission Operating Conditions

Of the key high power tracking points (section 6.2.1), 35,000 ft/.85 MN/ IRP and 30,000 ft/.8 MN/Max AB fall within the region of the envelope where higher fan pressure ratio is beneficial. Tables 6-2 and 6-3 quantify the changes in performance for these 2 points. The data for these operating conditions, as noted below, indicate that the baseline cycle could not fully utilize the 20% available stall margin.

At 35,000 ft /.85 MN /IRP, a significant improvement in thrust occurred which was accompanied by a degradation in SFC. The data in Table 6-2 indicates that:

- Thrust increased 6.1% if active control provided 5% additional stall margin; 9.1% if 20% stall margin was available. For the latter case, as discussed below, the baseline engine could not use all of the available 20% control stability margin due to a minimum exhaust nozzle area restriction.
- SFC was penalized at this flight condition from 2.7% to 4.3 % for the cases in which active control provided stall margin levels of 5% and 20%, respectively. This penalty occurred due to the decrease in overall cycle efficiency (Table 6-2); i.e., the higher thermal efficiency which resulted from the higher compressor pressure ratio was offset by a greater loss in propulsive efficiency caused by the higher exhaust flow velocity.

thrust increased 6.1% if active control provides 5% stall margin; 9.1% if 20% stall margin is provided. Accompanying these thrust increases, however, was a degradation in fuel consumption (SFC increase) ; that is, the increase in fuel flow needed to raise T41 offsets the thrust increase. This effect occurs due to the decrease in overall cycle efficiency (-2.6% for the 5% pressure ratio increase and -4.1% for the 20% case). The improvement in cycle thermal efficiency due to higher pressure ratio operation is less than the decrease in propulsive efficiency caused by the higher exhaust velocity (Table 6-2).

For this 35,000 ft/ .85 MN operating condition, the limit on minimum exhaust nozzle area (A8) prevented the cycle from using more than 7.7 % additional stall margin on the baseline engine configuration used in this study. Decreases in area to further backpressure the fan would require redesign of the exhaust nozzle hardware. Further, all points in the low T2 region reached the minimum exhaust area limit before the assumed 20% stall margin improvement was reached. Hence, better implementation of the 20% stall margin improvement during the preliminary design phase of an engine would optimize the system and further improve performance.

At 30,000 ft/.80/Max AB, the cycle was initially stall margin limited. When the fan operating line was raised 4.7%, the engine reached its maximum T41 and a maximum thrust improvement of 2.6% was achieved (Table 6-3). Any additional active control stall margin could not be used at this key flight condition. Only conditions at lower inlet temperatures, conditions not necessarily critical to the mission, could have used the additional margin. Hence, if active control provides up to 20% stall margin , the excess stability range should be applied toward optimizing other design factors such as efficiency or weight. Further, the fact that the baseline engine configuration could not use the available margin implies that larger benefits would result if active control could be applied during the preliminary design phase.

Table 6-2: Performance Improvements at 35K/.85 MN/IRP

$\%\Delta SM_{avail}$	5%	20%
$\%\Delta SM_{realized}$	5%	7.7%
%ΔFN	6.1%	9.1%
%ΔSFC	2.7%	4.3%
$\%\Delta\eta_{ov}$	-2.6%	-4.1%
$\%\Delta\eta_{prop}$	-3.3%	-4.9%
$\%\Delta\eta_{therm}$	0.7%	0.8%

Table 6-3: Performance Improvements at 30K/.8/Max AB

$\%\Delta SM_{avail}$	5%	20%
$\%\Delta SM_{realized}$	4.7%	4.7%
%ΔFN	2.6%	2.6%
%ΔSFC	-2.6%	-2.6%
$\%\Delta\eta_{ov}$	2.8%	2.8%
$\%\Delta\eta_{prop}$	-2.0%	-2.0%
$\%\Delta\eta_{therm}$	4.8%	4.8%

6.4 Conclusions

Depending on the region of the flight envelope, both performance benefits and penalties resulted when the additional stall margin provided by active control was used to raise fan or compressor pressure ratios. Raising fan pressure ratios during low T2 conditions caused significant high power thrust improvements. Increasing the core operating line resulted in thrust penalties when the cycle was T3 limited. When T41 limited, thrust increased during afterburner operation but decreased during IRP operation. Accompanying this penalty, however, were significant specific fuel consumption benefits at cruise conditions.

The thrust penalty during higher core pressure ratio operation in region 2 (during IRP) and region 3 (during IRP and MAX AB; Figure 6-4) cannot be offset by higher fan pressure ratios. As shown in Figure 6-10, higher fan pressure ratios only provided thrust in region 1. Hence, to maintain constant thrust at the higher core pressure ratios, the only alternative is to increase the flow capability of the engine as discussed in Chapter 5; i.e., to increase the engine size and weight.

The higher pressure ratio application of active control is particularly appropriate for aircraft configurations which emphasize cruise performance over high power operation. These applications include commercial and military aircraft in which range is prioritized over maximum thrust. A different implementation of the control stall margin should be considered, however, for aircraft which frequently operate in the high Mach number environment. Such applications include high speed civil transports and supercruising fighters which frequently operate in the T3 limited region.

This chapter reviewed using the additional stall margin provided by active control to increase the operating pressure ratio. For both the fan and the compressor, the maximum useful amount of stall margin that the configuration could meaningfully use was approximately 5%. Additional stall margin above this level could not be utilized due to other design constraints. These constraints included minimum BPR, minimum exhaust

nozzle area, and more severe T3 limiting effects. Hence, additional stall margin above 5% would be better implemented during the preliminary design phase of the engine. Alternatively, instead of raising pressure ratios, use active control to optimize efficiency and eliminate the compromise with the conventional stall line. This topic is addressed in Chapter 7.

Chapter 7: The Effect of Compressor Efficiency Improvements on Cycle Off Design Performance

7.1 Introduction

As discussed in chapter 4, potential compressor efficiency improvements are possible if the compressor is designed to a lower stall line. Stall margin otherwise sacrificed would be provided by active control. In this chapter, the efficiency gains quantified in Chapter 4 are applied to the engine cycle to determine the benefit in terms of thrust and fuel consumption.

Two applications in which active control improves compressor efficiency have been quantified. Both involve modifying the aerodynamic velocity triangles to achieve better efficiency at the expense of stall margin. Conceptually, both effects have been quantified by applying appropriate modifiers to the component maps. The difference lies in the manner which each model affects the performance of other engine components.

The first model was a straightforward efficiency derivative of the compressor. In this case, an adjustment on the compressor map efficiency was made with no adjustments to other map parameters such as flow or pressure ratio. This simplified model represented the presence of active control stall margin being incorporated during the preliminary design phase of the engine. The model reflected situations which include positioning the

design point such that the line of peak efficiencies coincides with the normal operating line.

The second model applied the optimized variable stator schedule on the baseline engine configuration. The model included the secondary effects associated with the new variable stator settings. One which became important was the loss in HPT efficiency which acted to offset gains in compressor efficiency.

7.2 Method

The first model assumed that the additional stall margin provided by active control was included in the initial design of the compressor. Under these conditions, blade and/or stator flow angles are assumed to achieve the target efficiency without affecting the performance of other components.

To quantify this effect, a sensitivity analysis was conducted. This back to back cycle calculation modified a single design input variable (such as efficiency) above its baseline value. By holding all other design parameters constant, the change in engine performance due to only changing the single input parameter was calculated. The sensitivity is basically a derivative of the cycle's set of governing equations.

For example, the change in thrust as a function of fan efficiency :

(7-1) $$\frac{d(FN)}{d\eta_f} = \frac{\Delta FN}{\Delta \eta_f}$$

(7-2) $$\frac{\Delta(FN)/FN}{\Delta \eta_f} = \frac{(FN' - FN|_i)/FN|_i}{\eta_f' - \eta_f|_i}$$

where $\eta_f|_i$ is the baseline efficiency
η_f' is the new efficiency
$FN|_i$ is the baseline thrust
FN' is the new thrust due to the change in efficiency

The second model, however, quantified the performance impact on an existing compressor. That is, the model calculated the net performance benefit due to the various offsetting effects as variable stators are adjusted. Variable stators were first adjusted to maximize efficiency at the expense of stall margin. To model this change, modifiers were applied to the reference map values at a given corrected rotor speed. In addition to efficiency, adjustments to pressure ratio, flow, and the stall line were required to simulate the shift in the compressor stage characteristic.

Additional effects on the engine system occurred for this second model. As the stator was opened to reduce the stage inlet swirl angles, the compressor achieved the same flow at a lower rotor speed. This effect has several potential consequences beyond its impact on compressor efficiency. First, on the positive side, the lower speed may allow a lower maximum physical speed to achieve desired flow levels and hence a reduction in rotor stress and/or weight. Or, for engines limited by maximum rotor speeds, the lower speed will allow the compressor to realize its maximum flow capability without hitting the maximum speed limit. For engines in which these speed restrictions are alleviated, potentially large IRP and afterburning performance benefits would result.

Conversely, the new variable stator settings included penalties when applied to the baseline engine configuration. For the turbine used in this study, the lower rotor speeds caused migration of the turbine operating point away from its peak efficiency. Hence, a turbine efficiency penalty resulted which tended to offset the compressor efficiency improvements.

An additional effect which occurred was a nominal shift in the compressor operating line. Because of the shift in the compressor characteristic as the stators were changed, the operating line moved slightly lower. Hence, the lower part power pressure ratios also trended toward offsetting the SFC improvements gained from the higher efficiency.

7.3 Results

7.3.1 Cycle Sensitivity Factors

Tables 7-1, 7-2 and 7-3 summarize the results of the sensitivity analysis for three different flight conditions: SLS/IRP, SLS Max AB, and 35,000 ft/ .85 MN/80% IRP thrust. The effect of both a positive and negative efficiency change is used to demonstrates that the derivative is approximately linear for the level of efficiency changes of interest.

Improvements in fan and compressor efficiencies resulted in significant high power thrust improvements (Table 7-1 and 7-2). This data was generated at constant inlet flow and T41. For fan efficiency changes of .01 (~ 1%), thrust increased more than 1% for both IRP and maximum AB conditions. A .01 core efficiency improvement resulted in over 1.5% improvement in thrust at these high power conditions.

At high power, the increase in core efficiency resulted in counterintuitive increases in SFC. The effect was due to the decrease in propulsive efficiency which exceeded and offset the increase in thermal efficiency. Specifically, compressor discharge temperature (T3) became lower due to the improved efficiency. However, since the sensitivity was calculated at a constant T41, more fuel was added to compensate for the larger enthalpy rise across the combustor. For this particular flight condition, the increase in fuel flow was greater than the thrust improvement.

Table 7-3 summarizes the performance sensitivity at 35,000 ft/ .85 MN. The data was generated at constant thrust and fan operating line position to simulate a typical cruise condition. At 80% of IRP thrust, specific fuel consumption improved by -.52% for a .01 fan efficiency increase and -.42% for a .01 core efficiency increase. These magnitudes represent significant improvements.

In addition to representing performance gains due to better positioning of the peak efficiency line, Table 7-3 represents the upper bound for performance gains due to optimizing variable stators for efficiency. For instance, if the cycle is in the preliminary

design phase, the designer has the flexibility to compensate for the potential mitigating factors (such as lower HPT efficiency discussed in Chapter 4). However, in the results that follow, the tuned variable stator schedule has been implemented on an existing engine configuration. The net performance benefit of improved core efficiency along with the secondary effects which lower HPT efficiency and core operating line have been quantified.

Table 7-1: Engine Performance Sensitivities to Component Efficiencies

SLS/STD/IRP at constant inlet flow and T41

	Δ	%ΔFN	%ΔSFC	%ΔWFT	$\%\Delta\eta_{prop}$	$\%\Delta\eta_{therm}$
ηf	0.01	1.40%	-0.16%	1.24%	-1.39%	1.58%
	-0.01	-1.49%	0.28%	-1.22%	1.53%	-1.78%
ηc	0.01	1.87%	0.07%	1.95%	-1.85%	1.82%
	-0.01	-1.94%	0.10%	-1.84%	1.99%	-2.05%

Table 7-2: Engine Performance Sensitivities to Component Efficiencies

SLS/STD/MAX AB at constant inlet flow, T41, and afterburner fuel flow

	Δ	%ΔFN	%ΔSFC	%ΔWFT	$\%\Delta\eta_{prop}$	$\%\Delta\eta_{therm}$
ηf	0.01	1.25%	-1.26%	-0.04%	-1.26%	2.57%
	-0.01	-1.28%	1.34%	0.04%	1.32%	2.61%
ηc	0.01	1.64%	-1.67%	-0.06%	-1.67%	3.42%
	-0.01	-1.63%	1.72%	0.05%	1.70%	-3.34%

Table 7-3: Engine Performance Sensitivities to Component Efficiencies

35,000ft/.85 MN/80% thrust at constant FN and exhaust nozzle area

	Δ	%ΔFN	%ΔSFC	%ΔWFT	$\%\Delta\eta_{prop}$	$\%\Delta\eta_{therm}$
ηf	0.01	0.00%	-0.52%	-0.53%	0.23%	0.29%
	-0.01	0.00%	0.54%	0.54%	-0.23%	-0.31%
ηc	0.01	0.00%	-0.42%	-0.42%	0.21%	0.21%
	-0.01	0.00%	0.46%	0.46%	-0.20%	-0.26%

7.3.2 Optimizing Core Variable Stators

The improved compressor described in Chapter 5 was incorporated into the cycle deck to assess the effect on overall engine performance. Three sets of flight conditions were analyzed: high power operation throughout the flight envelope; discreet mission points per section 6.2.1; and two operating lines indicative of subsonic cruise performance.

In general, the data resulted in the following observations:

- Up to 1% improvement in efficiency was realized at the expense of 4% in stall margin;
- The largest efficiency and SFC benefits occurred at part power conditions- conditions at which compressor stage mismatch is most severe and hence the largest design trades between efficiency and stall margin may be made;
- At high power, decreases in HPT efficiency offset the HPC efficiency improvement leaving little or no increase in overall engine performance.

The following discussion elaborates on these conclusions.

Key Mission points

Table 7-4 summarizes the improvement in thrust and/or SFC due to higher compressor efficiency. In general, about a 10 degree adjustment in the variable stator setting improved efficiency up to 1% while sacrificing about 4% in stall margin. The decrease in turbine efficiency due to the lower rotor speed was approximately .5%.

Table 7-4A: Effect of Tuned Variable Stators at Key Mission High Power Operating Conditions

Operating Condition		SL/.8/IRP	30K/.8/IRP	30K/1.5/IRP	20K/.9/MAX
%ΔFN	%	0.93	-0.04	0.52	0.20
%ΔSFC	%	-0.39	-0.01	0.02	-0.21
ΔT41	deg R	0.0	-2.0	0.0	-.1
$\%\Delta\eta_{ov}$	%	0.39	0.01	-0.02	0.21
$\%\Delta\eta_{p}$	%	-0.46	0.02	-0.18	-0.14
$\%\Delta\eta_{th}$	%	0.85	-0.01	0.17	0.35
$\Delta\eta_{fan}$	-	0.000	0.000	0.000	0.000
$\Delta\eta_{core}$	-	0.008	0.006	0.008	0.006
$\Delta\eta_{HPT}$	-	-0.003	-0.005	-0.003	-0.004
$\Delta\eta_{LPT}$	-	0.001	0.000	0.001	0.000
ΔSMcore	%	-3.5	-4.4	-3.6	-4.1
ΔPCN25R	%	-1.73	-2.08	-1.73	-1.95
ΔVG	deg	10.08	9.51	10.16	9.69

Table 7-4B: Effect of Tuned Variable Stators at Key Mission Part Power Operating Conditions

Operating Condition		SL/.8/60% IRP	10K/.4/40% IRP	35K/.85/50% IRP	35K/.85/80% IRP
%ΔFN	%	0.93	0.14	0.00	0.00
%ΔSFC	%	-0.42	-0.55	-0.44	-0.17
ΔT41	deg R	-5.1	-15.5	-15.7	-8.1
$\%\Delta\eta_{ov}$	%	0.42	0.55	0.43	0.17
$\%\Delta\eta_{p}$	%	-0.16	0.14	0.15	-.08
$\%\Delta\eta_{th}$	%	0.58	0.42	0.28	0.25
$\Delta\eta_{fan}$	-	0.000	0.001	0.001	0.000
$\Delta\eta_{core}$	-	.008	.010	.010	.008
$\Delta\eta_{HPT}$	-	-0.003	-0.002	-0.003	-0.004
$\Delta\eta_{LPT}$	-	0.000	0.000	0.001	0.000
ΔSMcore	%	-3.7	-3.8	-3.4	-3.4
ΔPCN25R	%	-1.77	-1.78	-1.77	-1.81
ΔVG	deg	10.59	10.93	10.44	9.92

Operating lines

To further illustrate the impact on cruise performance, operating lines at sea level static and 35,000 ft/ .85 MN were analyzed. Figure 7-1 (SLS) and Figure 7-2 (35,000 ft/ .85 MN) illustrate the change in SFC as a function of thrust characteristic. The improvement in cruise SFC ranged from -.21% to -.41% for SLS operation and -.25% to -.41% for 35,000 ft/.85 MN operation.

The overall engine performance on an existing cycle did not improve as much as the sensitivity factor derived in section 7.3.1. As noted previously, a primary cause was the degradation in HPT efficiency as the variable stators were adjusted. As the variable stators were positioned to improve compressor efficiency, a specified flow was achieved at a lower rotor speed. The lower speed negatively impacted the HPT efficiency for the configuration studied.

7.4 Conclusions

This chapter explored incorporating a compressor with optimized efficiency into an engine cycle. Stall margin otherwise sacrificed when optimizing the efficiency was provided by active control. Based on the performance sensitivity factors, significant improvements in both thrust and fuel consumption can be achieved if this application of active control is done during the preliminary design phase of the engine.

When applied to the existing baseline engine configuration, however, less impressive performance gains resulted. Losses in HPT efficiency which accompanied the change in rotor speed when the variable stators were adjusted caused only nominal net cruise SFC improvements. However, for other engines, the HPT efficiency may or may not decrease as the rotor speed is reduced.

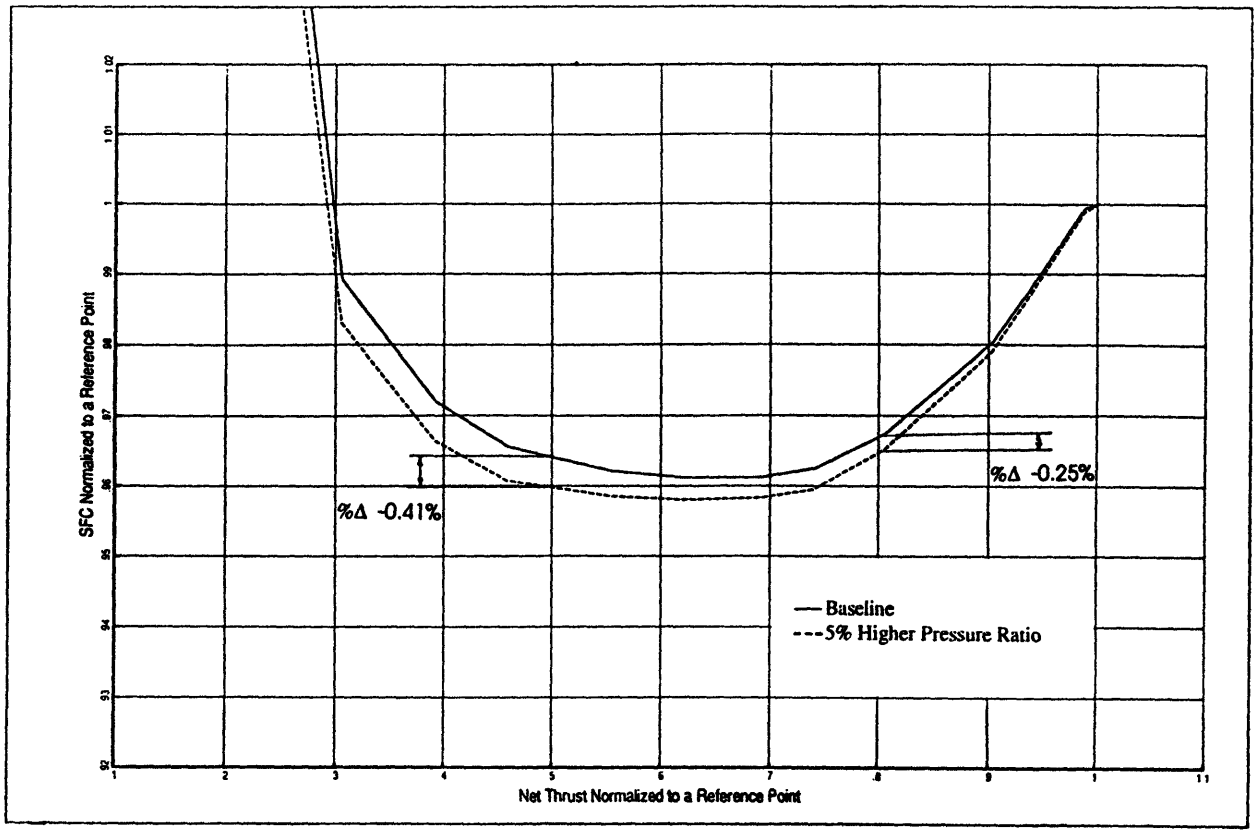

Figure 7-1: SLS Operating Line: SFC vs FN with Optimized Core Variable Stators

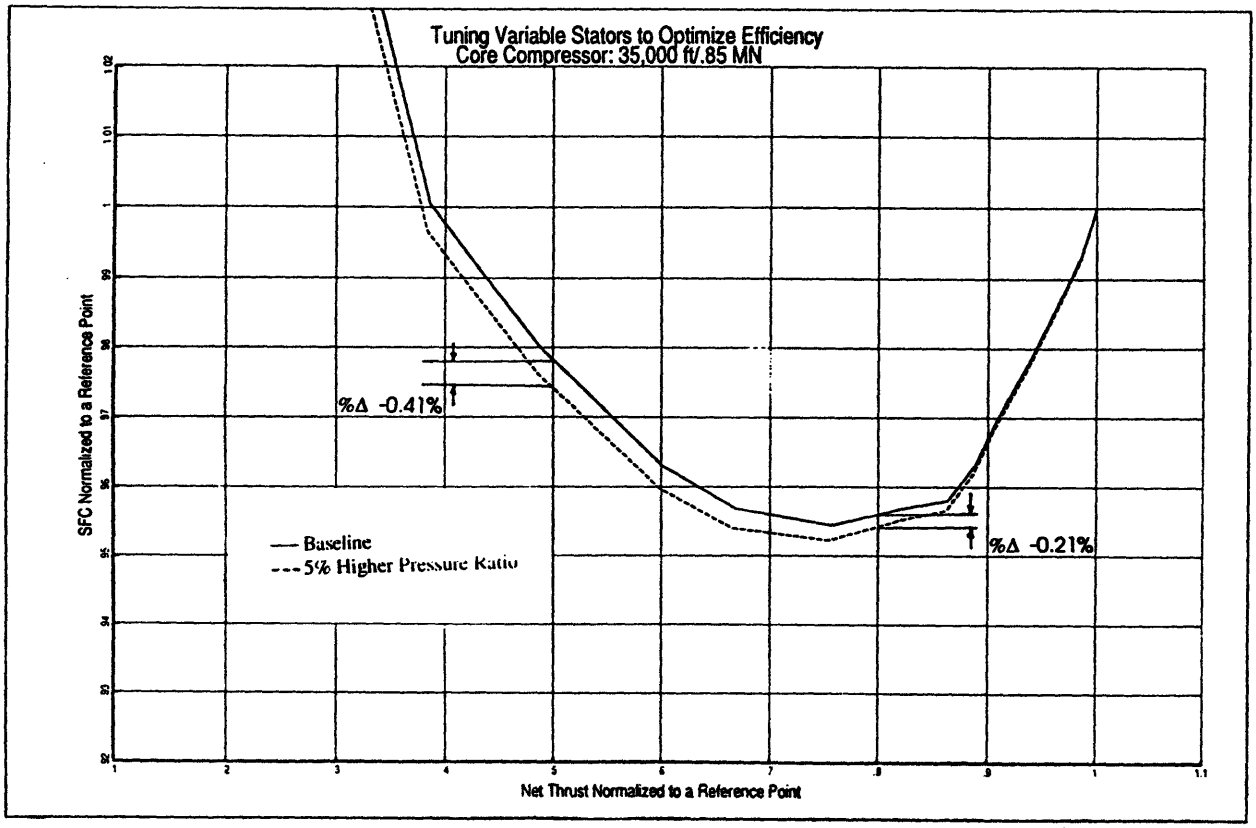

Figure 7-2: 35,000 ft/.85 MN Operating Line: SFC vs FN with Optimized Core Variable Stators

This benefit would further decrease if the presence of active control hardware in the flow path degraded efficiency; a scenario not accounted for in this study.

If implemented during the preliminary design phase, compressor design optimization above and beyond tuned stator settings could be conducted. Optimizing both the stator and blade aerodynamics would lead to larger compressor efficiency gains. Further, during the preliminary design phase, the opportunity would exist to mitigate potential losses in HPT efficiency.

Using active control to only optimize the variable stators is not worthwhile for the baseline engine configuration used in this study. However, coupling this method with raising the compressor pressure ratio is a viable option. This application would be especially appropriate if active control improved stall margin by more than 5%. As stated in Chapter 6, other cycle limits prevented raising pressure ratios more than 5%. Hence, otherwise unusable stall margin above this level could be applied toward optimizing compressor efficiency.

The improvement in compressor efficiency also extends the T41 limited operating region at the expanse of the T3 limited operating region (Chapter 6). Because an increase in T41 may be achieved, significant IRP and afterburning thrust increases would result for the affected flight conditions.

This benefit would be achieved if the absolute level of compressor efficiency is improved such as during the preliminary design phase scenario discussed in section 7.3.1. For the configuration studied, however, optimizing the variable stators did not yield this benefit. The efficiency benefit of the optimized stators occurred at lower rotor speeds typical of cruise operation rather than high power. Hence, the T41 limited region was not extended.

Chapter 8: Recommendations for Future Work

8.1 Introduction

The potential of active control challenges the traditional design philosophy toward achieving stable compressor operation. In this study, active control was used to raise compressor pressure ratios and to optimize compressor efficiency on a baseline, low BPR afterburning turbofan. In quantifying the effects, thrust and specific fuel consumption were used as the primary figures of merit. However, other factors associated with applying active control on a baseline engine configuration merit additional study. Further, there are other applications of active control which may result in even greater benefits.

This chapter summarizes topics which are recommended for further study. In general, these topics address various elements regarding active control which remain unresolved. They include:

- Additional benefits of applying active control on existing engine configurations; and
- Benefits of using active stall control on developmental engines at the preliminary design level;

8.2 Additional benefits of applying active control on existing engine configurations

8.2.1 Reduced rotor speeds

This study demonstrated that a specified flow was achieved at lower rotor speeds as the variable stators were adjusted to optimize efficiency (Chapter 5). This characteristic has several potential benefits. First, performance compromises for cycles which are limited by rotor speed can be minimized and/or eliminated. Second, improved hardware durability would result as mechanical stress decreased for the same turbomachinery weight. Alternatively, for the same mechanical stresses, a weight savings may be achieved (see section 8.2.2). Other benefits include improved compressor foreign object damage (FOD) capability as rotor speeds decrease (for example, bird and ice ingestion).

8.2.2 Lower LPT Temperatures

Higher core compressor pressure ratios indirectly affect the mechanical integrity of the LPT hardware. As described in Appendix A, at constant T41, HPT exit temperature (T42) must decrease as compressor pressure ratio is raised. Hence, temperature at the LPT inlet becomes lower. One potential benefit is improved durability of the hardware operating in the less severe temperature environment. Alternatively, for the same mechanical life, a weight savings may be achieved.

For configurations with cooled turbine blades, the cooling flow may be reduced or eliminated to maintain the same mechanical life. The lower cooling flow would improve engine system performance.

8.2.3 Transient Performance

As indicated by the stability audit (Figure 2-3), the stall line position affects transient as well as steady state performance. If the stall margin provided by active control is allocated toward transient operation, engine configurations whose accelerations are stall margin limited would achieve faster transient accelerations.

8.3 Benefits of using active control on developmental engines at the preliminary design level

In addition to studying active control on a baseline configuration, incorporating active control early in the design process is a topic recommended for further study. As discussed in Chapters 5,6, and 7, potentially larger benefits would result if active control could be applied during the preliminary design phase.

8.3.1 Design new compressors to maximize efficiency

This research reviewed adjustments to variable stators to improve efficiency on a baseline engine. The magnitude of this benefit, however, was limited because angle adjustments were subject to the restrictions set by the existing baseline hardware. However, during the preliminary design phase, the designer is not subject to this constraint. Instead, the aerodynamics of both the variable stators, fixed stators and blades could be optimized for efficiency. The stability margin traditionally achieved by the aerodynamic design of the compressor would be provided by active control.

In addition, active stall control potentially would allow improved design point efficiency. Traditionally, the efficiency at the design point is compromised to minimize the stall line knee. With active stall control to compensate for the stall line knee at lower speeds, improved efficiency at higher speeds may be achieved.

An additional factor which should be included in future studies is the potential loss in efficiency due to active control. The use of high frequency guide vanes, for example,

may contribute additional profile losses which would offset any increase in design point efficiency.

8.3.2 Design compressors to minimize weight

Additional stall margin could also be used to reduce the weight of the compressor. If a stage could operate at higher loads, fewer stages would be required to achieve the same overall pressure ratio. This option may be especially attractive to high pressure ratio compressors from which one or more stages could be removed.

Compressor weight may also be decreased by using higher blade aspect ratios. Traditionally, low aspect ratios are used due to their beneficial influence on the stall line (reference 2-10). The higher aspect ratios would decrease the overall length while degrading stall margin. Stall margin otherwise sacrificed would be provided by active control.

For the baseline engine configuration, adjustments to the variable stators improved efficiency, lowered stall margin and required lower wheel speeds (U). For an existing compressor, the radius (r_t) is fixed and the wheel speed reduction can only be achieved by a lower rotor physical speed (ω).

(8-1) $U_t = \omega r_t$

where U_t is the design wheel speed (ft/sec)

ω is the design rotor speed (rad/sec)

r_t is the design reference radius (ft)

However, at the preliminary design level, the designer has the option of reducing the compressor tip radius to lower the wheel speed. Hence, at constant rotor speed (ω), the compressor is scaled down in radius and the overall size and weight of the compressor is reduced. One additional advantage to maintain rotor speed (ω) is the elimination of the potential HPT efficiency losses associated with optimizing the variable stators (Chapter 7).

8.3.3 Active control as an alternative to variable stators.

Currently, variable stators provide additional stall margin and potentially higher low speed efficiency at the expense of engine weight. One possible application of active control is to replace variable stators all together. Among the issues which would need to be studied include the magnitude of stall margin improvement which active control would have to provide; the weight trade between active control hardware and variable stator hardware; potential efficiency losses if variable stators are eliminated; and whether active control is suitable toward alleviating stall caused by high incidence angles.

Chapter 9: Summary of Conclusions

9.1 Introduction

The primary focus of this analysis was to implement active stability control as a retrofit or upgrade to an existing engine configuration. The study applied the additional stall margin available from active control toward optimizing compressor efficiency and raising cycle pressure ratios. The effects on thrust and specific fuel consumption were quantified for several conditions. These conditions represented high power combat operation (IRP and Max AB) and part power cruise operation throughout the flight envelope. The results and conclusions from the data are summarized below. Table 9-1 summarizes a configuration which maximizes the performance benefits from active stall control.

9.2 Compressor Analysis

- Based on the extended stable operating range demonstrated by active control experiments, the fan characteristic used in this study was extrapolated accordingly. Nominal increases in stall margin were achieved: 0.0% at 100% speed and 2.5% at 70% speed.
- Optimizing the core compressor variable stators resulted in efficiency increasing by .5% to 1.0% at the expense of -4.0 to -5.0% in stall margin.

- The potential efficiency benefit by adjusting variable stators (0.0% to 7.6%) varies widely depending on the compressor.

9.3 Design Point Cycle Analysis

- At constant T41 and BPR, higher fan or core compressor pressure ratios resulted in improved SFC but lower thrust.
- To achieve a performance benefit without the associated penalty, engine configuration changes would be required. Improving SFC at constant thrust or improving thrust at constant SFC, for example, would require lower levels of design BPR.
- At constant T41 and BPR, higher cycle pressures decreased thrust due to the decrease in exhaust gas temperature. For very high increases in compressor pressure ratio, exhaust pressure also decreased.

9.4 Off Design Cycle Analysis: Higher pressure ratio operation

- The engine cycle analyses indicates that if active control can provide up to 5% additional stall margin, significant performance benefits (particularly SFC) can be achieved. Above 5% available stall margin, other cycle constraints become limiting (BPR and A8) and any additional control stall margin could not be used.
- For active control stall margin contributions above 5%, preliminary design applications would achieve larger benefits than existing configurations. During the developmental phase, the design may be tailored to maximize the benefits of the available stall margin.
- At high power, the effect of higher pressure ratios depended on the region of the flight envelope in which the baseline engine operated under fan stall margin limited conditions (region 1); T41 limited conditions (region 2); or T3 limited conditions (region 3) (see Figure 6-4).

9.4.1 Higher core compressor pressure ratios

- At IRP, thrust decreased throughout the flight envelope as core pressure ratios was increased. The thrust degradations occurred for reasons similar to the design point analysis; namely, lower exhaust temperatures. However, during off design operation, thrust decreased more due to the cutback in T41 (T3 limited operation) and the increase in bypass ratio (fan stall margin limited operation).
- At Max AB, the loss in thrust due to the higher core pressure ratio may be minimized (T3 limited and fan stall margin limited operation) or eliminated (T41 limited operation) if total engine fuel flow is held constant. At constant total fuel flow, the fuel not used in the main combustor at the higher pressure ratio was burned in the afterburner. Hence, the larger enthalpy rise in the afterburner compensated for the lower turbine exhaust temperature caused by the higher pressure ratios.
- If 20% additional stall margin is available, raising core pressure ratio by 20% is not a desirable option for the configuration studied. The region of T3 limited operation increased significantly and resulted in unacceptable thrust losses.
- At cruise, a higher core pressure ratio resulted in significant SFC improvements:

Condition	50% IRP Thrust	80% IRP Thrust
SLS	-1.26%	-1.13%
35,000 ft /.85 MN	-0.82%	-0.74%

9.4.2 Higher fan pressure ratios

- Raising fan pressure ratio improved high power thrust during fan stall margin limited conditions. For this configuration, available stall margin above 5% could not be used because minimum A8 (for IRP) and minimum BPR (for Max AB) became limiting. Larger performance improvements could be achieved if the engine studied had a higher

design bypass ratio. Under this scenario, more of the available stall margin could have been used.

- The use of higher fan pressure ratios may be used to offset the thrust losses of higher core pressure ratios during fan stall margin limited conditions. In this case, both the fan and core compressor would have to be actively controlled. The net result would be eliminating the penalty of higher core pressure ratio operation (low T2 thrust) while achieving the cruise SFC benefit.

9.5 Efficiency

- Improvements in fan or compressor efficiency would improve combat thrust and part power SFC. The benefits would be largest if incorporated during the preliminary design phase in which potential mitigating effects could be avoided.
- The optimized variable stators provided nominal improvements in SFC. Optimizing variable stators for efficiency on an existing configuration resulted in penalties which offset the benefit of the improved efficiency. For the configuration studied, the potential SFC improvement due to the improved compressor efficiency was reduced approximately by 50% when the loss in HPT efficiency was included.
- Given the relative magnitude of the benefit, and potential efficiency losses due to the presence of active control hardware, using active control to optimize variable stators is not recommended.
- The best option for the engine configuration studied is to use active control to raise cycle pressure ratios until other cycle limits prevent further increases. Any additional stall margin, otherwise unusable, should be used to optimize efficiency with the variable stators.

Table 9-1: Active Stall Control on both the Fan and Core Compressor

Active Control Application	Effect	Comment
Raise Fan Pressure Ratio	• Increases thrust at both IRP and Max AB during fan stall margin limited operation (region 1, Figure 6-10)	• For the configuration studied, 5% was the maximum acceptable increase in fan pressure ratio. • If more stall margin is available, higher performance benefits could be achieved if the cycle had not become BPR or A8 limited • Larger benefits would result on medium bypass engines.
Raise core pressure ratio	Effect on Combat Performance (5% Higher Core Pressure Ratio) Region 1 %ΔFN -1.5 to -2.5 (IRP) -.6 to -1.55 (Max AB) %ΔSFC -.82 to -1.41 .6 to 1.55 Region 2 %ΔFN 0.0 to -.5 0.1 to 0.8 %ΔSFC -.5 to -1.4 -0.1 to -0.8 Region 3 %ΔFN -2.0 to -7.7 -1.2 to -4.3 %ΔSFC -.1 to -1.4 1.2 to 4.3	• In region 1, the increase in thrust with the higher fan pressure ratio may be used to offset the thrust loss due to the higher core pressure ratio. • The loss in thrust in region 3 is acceptable if T3 limited operation represents an acceptable portion of the flight envelope.
Raise core pressure ratio	• Cruise Performance improves significantly 35,000 ft/ .85 MN: Power Level %ΔSFC 50% IRP -0.82% 80% IRP -0.74%	
Optimize compressor variable stators	• Nominal improvements in cruise performance 35,000 ft/ .85 MN: Power Level %ΔSFC 50% IRP -0.41% 80% IRP -0.21%	• More significant benefits would be realized if the HPC efficiency improvement was not accompanied by a HPT efficiency loss.

10. References

Chapter 1

1-1.) Epstein, A.H., Ffowcs Williams, J.E., and Greitzer, E.M.,
"Active Suppression of Compressor Instabilities", AIAA/ 10th Aeroacoustics Conference AIAA Paper No. 86-1994, July 1986.

1-2.) Greitzer E.M., Epstein, A.H., Guenette, G.R., Gysling, D.L., Haynes, J., Hendricks, G.J., Paduano, J., Simon, J.S., Valavani, L.,
"Dynamic Control of Aerodynamic Instabilities in Gas Turbine Engines" AGARD Lecture series 183.

1-3) Simon, J.S., Valavani, L., Epstein, A.H., Greitzer, E.M.,
"Evaluation of Approaches to Active Compressor Stabilization"
ASME Paper 92-GT-182.

Chapter 2

2-1) Greitzer, E.M.,
"Surge and Rotating Stall in Axial Flow Compressors, Part I: Theoretical Compression System Model," *Journal of Engineering for Power*, Vol. 98, No 2, April 1976.

2-2) Lieblein, S.
"Loss and Stall Analysis of Compressor Cascades," *Journal of Basic Engineering*, September, 1959.

2-3) Koch, C.C.
"Stalling Pressure Rise Capability of Axial Flow Compressor Stages,"
Journal of Engineering for Power, Vol. 103, October 1981.

2-4) Cumpsty, N.A.
Compressor Aerodynamics, John Wiley & Sons, 1989.

2-5) Hosny,W.M., Levanthal, L., Steenken, W.G.,
"Active Stabilization of Multistage Axial-Compressor Aerodynamic System Instabilities," ASME paper 91-GT-403.

2-6) Epstein, A.H., Private Communication, 1993.

2-7) Stone, A.
"Effects of Stage Characteristics and Matching on Axial-Flow Compressor Performance," Transactions of the ASME, August 1958.

2-8.) Greitzer, E.M.
"Review- Axial Compressor Stall Phenomena," Transactions of the ASME Volume 102, June 1980.

2-9) Prell, M., Private Communication, 1993.

2-10) Wennerstrom, A.J.,
"Low Aspect Ratio Axial Flow Compressors: Why and What it Means," The Third Cliff Garrett Turbomachinery Award Lecture, October 14, 1986.

2-11) Wilson, D.G.,
The Design of High Efficiency Turbomachinery and Gas Turbines,
MIT Press, 1984.

2-12) Moore, R.D. and Reid, L.
"Experimental Study of Low Aspect Ratio Compressor Blading," *Journal of Engineering for Power*, Vol. 102, October 1980.

2-13) Yonke, W.A. , Landy, R.J., and Stewart, J.F.,
"HIDEC Adaptive Engine Control System Flight Evaluation Results.," ASME Paper 87-GT-257.

2-14) Tich, E.J., Shaw, P.D., Berg, D.F., Adibhatla, S., and Swan, J.A.,
"Performance Seeking Control for Cruise Optimization in Fighter Aircraft," AIAA-87-1929. AIAA/SAE/ASME/ASEE 23rd Joint Propulsion Conference, June 29- July 2, 1987.

2-15) Shaw, P., Foxgrover, J., Berg, D.F., Swan, J., Adibhatla, S., Skira, C.A.,
"A Design Approach to a Performance Seeking Control," AIAA Papre 86-1674, AIAA/SAE/ASME/ASEE 22nd Joint Propulsion Conference, June 16-18, 1986.

2-16) Gilyard, G. and Orme, J.
"Subsonic Flight Test Evaluation of a Performance Seeking control Algorithm on an F-15 Airplane," AIAA Paper 92-3743. AIAA/SAE/ASME/ASEE 28th Joint Propulsion Conference and Exhibit, July 6-6, 1992.

2-17) Ludwig, G.R.
"Tests of an Improved Rotating Stall Control System on a J-85 Turbojet Engine," Transactions of the ASME, *Journal of Engineering for Power*, 80-GT-17.

2-18) Ffowcs Williams, J.E., Harper, M.F.L., Allwright, D.J.,
"Active Stabilization of Compressor Instability and Surge in a Working Engine", ASME paper 92-GT-88.

2-19) Paduano, J.,
"Active Control of Rotating Stall in a Low Speed Axial Compressor", ASME paper 91-GT-88.

2-20) Haynes, J. M., Hendricks, G. J., Epstein, A.H.,
"Active Stabilization of Rotating Stall in a Three-Stage Axial Compressor," ASME Paper 93-GT-346.

2-21) Adibhatla, S., Brown, H., Gastineau, Z.,
"Intelligent Engine Control (IEC)", AIAA Paper 92-3484.

2-22) Seymour, J.A.,
"Aircraft Performance Enhancement with Active Compressor Stabilization," Masters Thesis, 1988.

2-23) Ziegler, H.,
"Effect of Active Compressor Stabilization on Inlet Sizing and Aircraft Performance,"Northrop Memo T234-92-108, September, 14, 1992.

2-24) Chen, G.T., Greitzer, E.M., Epstein, A.H.,
"Enhancing Compressor Distortion Tolerance by Asymmetric Stator Control." AIAA Paper 87-2093, AIAA/SAE/ASME/ASEE 23rd Joint Propulsion Conference, June 29- July 2, 1987.

Chapter 3

3-1) Oates, G.,
Aircraft Propulsion Systems Technology and Design, AIAA Educational Series, AIAA 1989.

3-2) Davis, R. and Vinson, P.
"Cycles Design Point Program," General Electric Aircraft Engines.

3-3) Mattingly, J., Heiser, W.H. and Daley, D. H.
Aircraft Engine Design, AIAA Education Series, AIAA 1987.

3-4) Davidson, T. L.,
"Engine Cycle Models," General Electric Company, 1991.

3-5) Davis, R. H.,
Advanced Course in Engineering Cycle Design Lecture Notes, General Electric Aircraft Engines, 1990.

3-6) Kerrebrock, J.L.,
Aircraft Engines and Gas Turbines, The MIT Press, 1977.

3-7) Christopherson, C.K. "Performance Studies of Split Compression Differentially Geared Aircraft Gas Turbines," Masters Thesis, 1987.

Chapter 4

4-1) Carchedi, F., Wood, G.R.,
"Design and Development of a 12:1 Pressure Ratio Compressor for the Ruston 6-MW Gas Turbine," *Journal of Engineering for Power*, Vol 104, October 1982.

4-2) Hendricks, G., Bonnaure, L.P., Longley, J.P., Greitzer, E.M., Epstein, A.H.,
"Analysis of Rotating Stall Onset in High Speed Axial Flow Compressors," AIAA Paper 93-2233, AIAA/SAE/ASME/ASEE 29th Joint Propulsion Conference and Exhibit, June 28-30, 1993.

4-3) Fink, D., Private Communication, 1993.

Chapter 5

5-1) Davis, R.H. private communication, 1993.

Chapter 6

6-1) Mattingly, J., Heiser, W.H. and Daley, D. H.,
Aircraft Engine Design, AIAA Education Series, 1987.

6-2) Geiger, J. Private Communication, 1993.

Appendix A1

A1-1) Davis, R.H. private communication, 1993.

Appendix A1: The Effect of Higher Cycle Pressure Ratios on Exhaust Temperature and Pressure

A1.1 The effect of higher pressure ratio operation on exhaust temperature

As outlined by the gross thrust equation (eq 5-3, Figure 5-1), ideal specific thrust is a function of the flow, exhaust total temperatur, and total pressure. Because the thermodynamic trends are not necessarily intuitive, the effect of changes to compressor pressure ratio on the exhaust properties is examined below. To illustrate the effects conceptually, let us discuss a simplified turbofan cycle. For this cycle, core compressor pressure ratio is increased at constant T41, fan pressure ratio, and bypass ratio. Such a scenario can easily be modelled in the design point program (Chapter 5).

The effect on exhaust gas temperature is straightforward and demonstrated conceptually on the temperature entropy diagrams shown in Figure A1-1 and Figure A1-2. At constant turbine inlet temperature (T41), the turbine discharge temperature (T42) must decrease to satisfy the energy balance as the compressor pressure ratio is raised. Because compressor pressure ratio increases, the compressor work (Δh_c) increases; consequently, the turbine work (Δh_t) also must increase. Since work is proportional to the temperature difference between T41 and T42, T42 must decrease as compressor pressure ratio increases at constant T41 and flow.

Figure A1-1: Temperature vs Entropy Diagram Indicating Excess Cycle Exhaust Pressure and Temperature

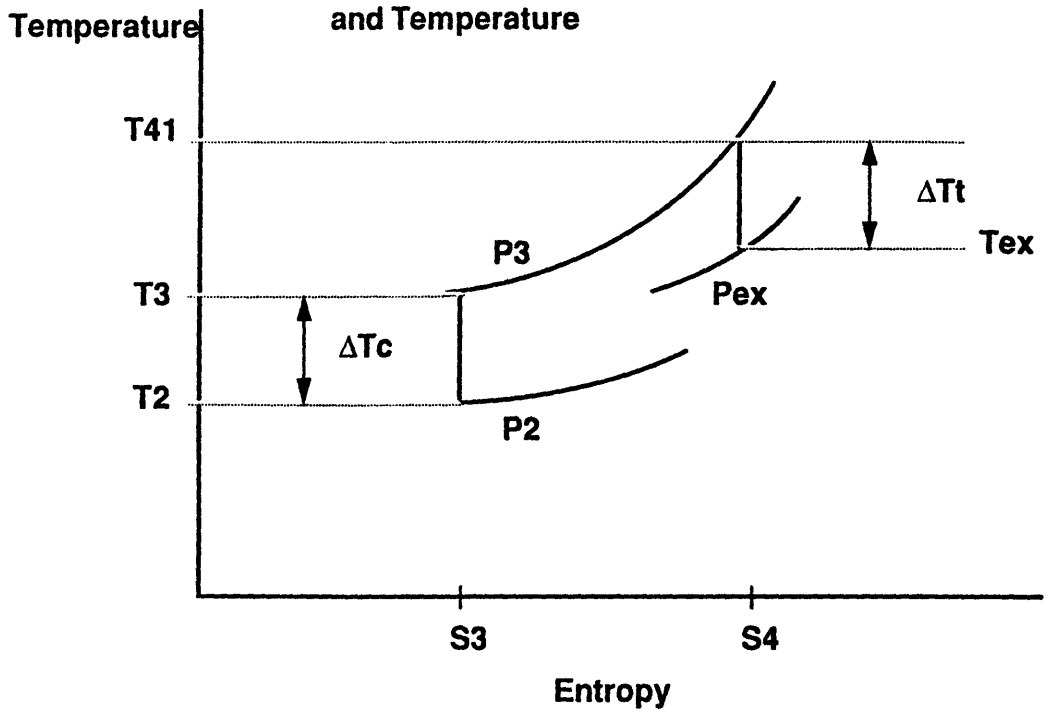

Figure A1-2: Turbine Exhaust Temperature and Pressure After an Increase in Compressor Pressure Ratio at Constant T41 and BPR

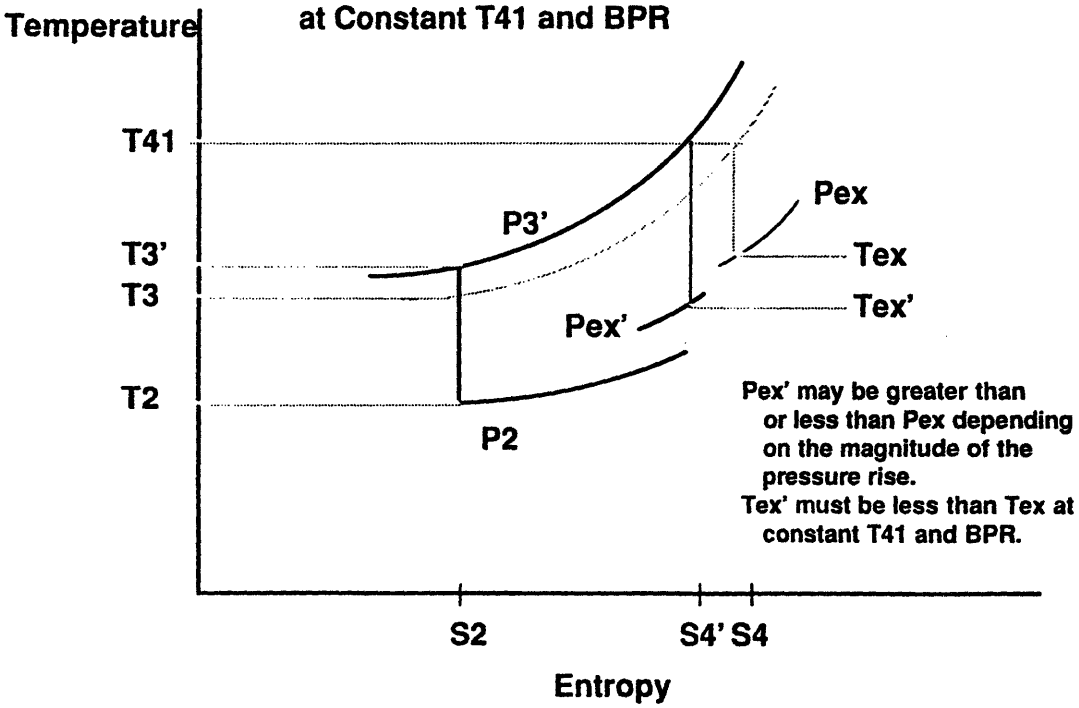

To summarize: At constant T41, for increases in core pressure ratio (P3Q25):

(eq. A1-1) 1) Compressor work increases: $\Delta h_c = h3 - h25$

$= h25(h3/h25 - 1)$

$= C_p(T3/T25 - 1)$ (for perfect gas)

$= C_p[(P3/P25)^{C_p/(R\eta_p)} - 1]$

2) Turbine -compressor steady state work balance $\Delta h_t = -\Delta h_c$

(eq. A1-2) 3) Turbine work $\Delta h_t = C_p(T42 - T41)$

(eq. A1-3) 4) Discharge temp T42 decreases at constant T41 and increasing $|\Delta hc|$ ($\Delta hc < 0$) $T42 = T41 + C_p/\Delta h_t$

$= T41 - C_p/\Delta h_c$

For this example, the enthalpy drop across the LPT is constant since fan pressure ratio and BPR have been unchanged. As a result, the drop in temperature is also achieved at all downstream locations. Hence, one concludes that as compressor pressure ratio increases, the exhaust gas temperature must decrease. Based on eq 5-3, lower exhaust temperature causes thrust to decrease.

A1.2 The effect of higher pressure ratio operation on exhaust pressure

Intuitively, one may be apt to believe that running to higher compressor pressure ratios necessarily results in higher discharge pressures. Hence, based on the gross thrust function, thrust must increase. However, depending on the magnitude of the increase in compressor pressure ratio, exhaust pressure may increase or decrease. The effect on pressure is more subtle due to the fact that T41 is held constant. Fundamentally, the phenomena is based on the fact that isobars diverge as entropy is increased on a

temperature entropy diagram. Combining the perfect gas law with Gibbs equation yields (reference 2-11):

(eq. A1-3) $\delta T/\delta s = T/Cp$ at constant pressure

That is, the slope of a constant pressure line increases with temperature.

The following illustrates how the pressure discharged from the turbines is modified for changes in cycle pressure ratio. Again, for simplicity, the example models increases in core compressor pressure ratio at constant fan pressure ratio, bypass ratio, and T41. These assumptions imply that the expansion ratio across the LPT is constant and work can be expressed in terms of the specific enthalpies.

For large pressure increases, the turbine exhaust pressure will decrease. For example, if the pressure ratio is increased to the point in which T3 equals T41, no fuel can be added because the T41 limit must be observed. Since entropy was not increased, the cycle could not utilize the characteristic that isobars diverge. Hence, the turbines must expand back to the compressor inlet pressure. For this case, there is no excess exhaust pressure; the exhaust pressure is clearly lower than the baseline case (reference A1-1).

The sample above was relatively straightforward and was presented first for simplicity. However, to explain why pressure may increase, the phenomena must first be explained in more general terms. The net effect on exhaust pressure is determined by the offsetting impact of two effects, both of which are governed by the characteristic of diverging isobars on a T-S diagram:

- For the turbine to provide the baseline level of compressor work at a lower entropy and constant T41, a higher expansion ratio is required. This contributes toward reducing the exhaust pressure as in the example above (Figure A1-3).
- For the turbine to provide the portion of work above the baseline level, higher exhaust pressure will occur due to the diverging isobars (Figure A1-4).

Figure A1-3: The Lower Turbine Inlet Entropy Tends to Lower the Turbine Exhaust Pressure

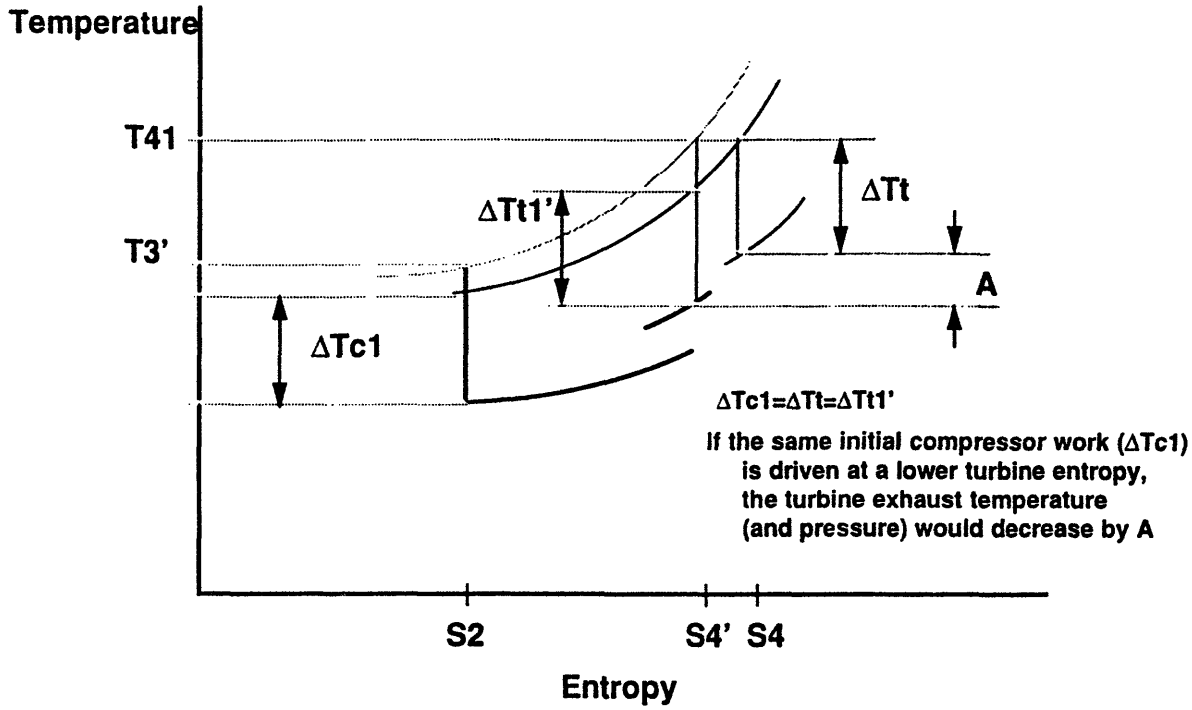

Figure A1-4: The Higher Turbine Inlet Pressure Tends to Increase the Exhaust Pressure

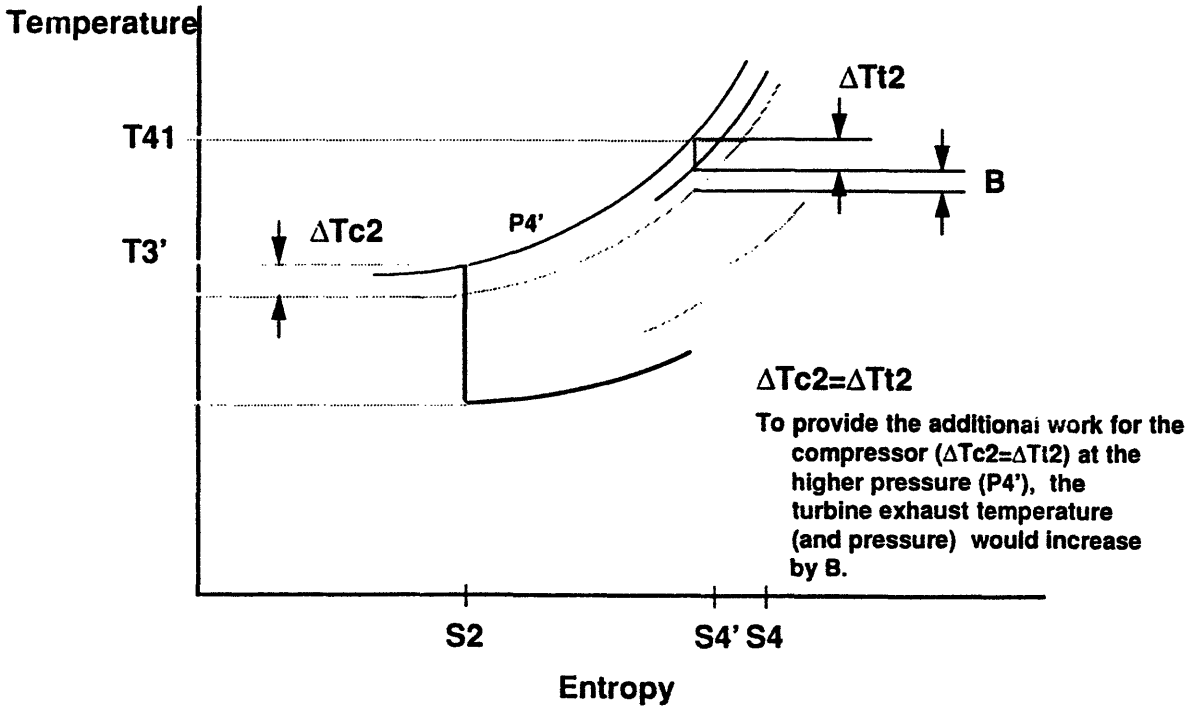

The principle is shown graphically in Figure A1-3 assuming ideal efficiencies and perfect gas properties. At constant T41, as compressor discharge pressure increases, the entropy at the turbine inlet is lower. Hence, the isobars diverge over a shorter change in entropy. As a result, to do the original compressor work (ΔTc) at the lower entropy, the turbine expansion ratio would increase and the cycle would suffer a decrease in exhaust pressure. The decrease in exhaust pressure becomes magnified as the turbine inlet entropy decreases.

On the contrary, for the additional compressor work demanded, the diverging isobars contribute to increasing the exhaust pressure (Figure A1-4).

The net result depends on which effect dominates. In general, for large increases in compressor pressure rise, the decrease in entropy is large and the former effect described above dominates (Figure A1-5). For small increases, the latter affect dominates and exhaust pressure will increase.

Note that in this simplified design point analysis, bypass ratio was held constant. If bypass ratio increased such as in off design simulations, the LPT expansion ratio would increase. That is, to compensate for the lower mass flow passing through the LPT, the change in specific energy across the LPT would increase to maintain the same level of absolute work. This exacerbates the situation and contributes toward lower exhaust pressures and temperatures (see Chapter 6).

Figure A1-5: Exhaust Pressure will Increase or Decrease Depending on the Magnitude of the Increase in Compressor Pressure Ratio